Towards a hybrid density functional theory and molecular mechanics model for large transition metal systems

Sheen, Paul David

Award date:
1995

Awarding institution:
University of Bath

Towards a Hybrid Density Functional Theory and Molecular Mechanics Model For Large Transition Metal Systems

submitted by Paul David Sheen
for the degree of PhD
of the University of Bath
1995

ProQuest LLC
789 East Eisenhower Parkway
P.O. Box 1346
Ann Arbor, MI 48106-1346

Summary

This thesis attempts to evaluate the effectiveness of Density Functional Theory (DFT) for treating transition metal complexes theoretically.

Investigation of various molecular properties shows that an accurate characterisation of the features on the Potential Energy Surface is possible for various ionic species. A range of chlorocuprate complexes are investigated and geometries are seen to be extremely sensitive to choice of basis set, frozen cores and polarisation functions. Accurate transition energies are calculated with the DVXα, but ligand field and charge transfer transitions cannot be calculated simultaneously without the inclusion of lattice effects.

The Local Density Approximation (LDA) gives accurate geometries for the tetrachlorides of the first row transition series whereas the inclusion of gradient corrected functionals leads to overestimated bond lengths. Good Δ_{tet} values are calculated, atomic charges and d-orbital populations provide an insight into the bonding in these complexes.

Vibrational frequencies of three tetra-oxo complexes are calculated and are shown to be in excellent agreement with experimental values.

However, despite the accuracy that is shown for a range of properties, DFT is still incapable of performing calculations on large systems. Hence, in order to investigate the properties of large complexes a combined DFT and Molecular Mechanics (MM) model is developed.

Geometry optimisations are performed on transition metal complexes with one and two simple ligands(H_2O, NH_3, H_2S and PH_3), ligand geometries are varied in

Geometry optimisations are performed on transition metal complexes with one and two simple ligands(H_2O, NH_3, H_2S and PH_3), ligand geometries are varied in order to reproduce the calculated bond lengths found for the larger methyl derivatives. Calculations on real complexes with these truncated derivatives are reasonably accurate considering the inherent approximations. The neglect of steric effects is shown to be important. Finally a combined DFT and MM method is developed and initial results suggest that the inclusion of MM to treat steric effects will give accurate geometries and this can be developed into a computationally useful method.

Acknowledgements

At last it's all finished, and some of you might say about time too, and is always the case with tasks of this magnitude a lot of thanks is due to other people who made everything possible. In the seven years I've been at Bath there have been quite a few of those I'm sorry I can't mention you all but awards are for meritous conduct only.

Firstly, on the academic front, the members of the Inorganic Computational Chemistry Group. To Dr. Robert "I'm not in Tomorrow" Deeth, my supervisor and supplier of advice and ideas (not always good!!) and the occasional beer (likewise), and without whom I would not have got as far as writing this. Also, in no particular order, Mrs Veronica "For the Good of the Group" Paget (née Burton), Miss Sarah "Only Four More Calculations Left" Langford and Mr Mark "Nearly Gone Off the Boil" Bray. I guess we all helped each other out in times of need/stress and who could forget Prague, Newcastle and those lunchtimes/evenings spent in the bar. I wish them all the best in Warwick.

On a non-academic front, I should like to thank the various members of the Rowing club. Such is the case with rowing that I probably spent too much time on it and not enough working, but I wouldn't have missed it. I shared some great times with a great bunch of people, shed sweat and blood and yet still managed to enjoy it all immensely. I guess one day I might even get to win something!!

Various other people don't really come under any heading except friends, a list unfortunately too long to mention names. These people have come and gone but some will always remain. Thanks to you all whoever and wherever you are.

My final thanks are to my family who have supported me always, and never doubted that I was right and never tried to sway me from my chosen course.

To all those that I have mentioned and those that I have not, thank you one and all it wouldn't have been the same without you.

Table of Contents

To all my Grandparents

to whom it would have meant so much to have seen this day.

Chapter 1

Introduction

1.1 Introduction

The use of theoretical methods to study atomic and molecular properties is well established. Systems that have been studied range from the simplest of all, the hydrogen atom, to extremely large biological enzymes. The reason why these studies are so widespread can be explained from a number of considerations. Firstly, computational methods can investigate many atomic and molecular properties including geometries, bond energies, electronic transition energies and nmr spectra. These properties may be impossible or very difficult to measure for some systems. Secondly, toxic and harmful materials can be investigated without risk. Finally, calculations can be used to screen a large number of similar compounds before they are synthesised to see whether they have the necessary properties. This is especially important for systems that are either expensive or extremely difficult and time consuming to produce.

Transition metal complexes are of particular interest to the theoretician because of their widespread use in nature as enzymes. Their catalytic nature is also shown in a wide variety of industrial processes, particularly with respect to organic synthesis. Furthermore, the pharmaceutical industry makes an ever expanding use of drugs containing transition metals. The fact that transition metal complexes are involved in a large number of reactions makes them ideal for computational study in order to understand and improve their properties within a reasonable time frame, at reduced

cost and in complete safety.

However, the nature of these transition metal species is that many of them are quite large and calculations using *ab initio* methods would be extremely time consuming and computationally expensive. In order to reduce the cost of such calculations, a number of groups have developed combined Quantum Mechanical and Molecular Mechanical (QM/MM) methods. The advantage of such methods is that whilst the metal centre or active site is treated accurately using a computationally expensive QM, the remainder of the complex is treated by the less expensive MM method. This enables large systems to be investigated accurately and quickly.

The work presented here centres around the development of a combined Density Functional Theory (DFT) and MM method. Chapter 1 provides an outline of the computational methods used and also a comparison with other techniques. Chapters 2-4 investigate the accuracy of DFT as applied to various transition metal systems and a range of molecular properties. Having shown that DFT is a capable method for transition metal complexes, a combined approach is developed. Chapter 5 gives a review of other work in this field and the way in which this method will be developed. In Chapter 6 the electronic properties of ligands bound to transition metals are investigated to see whether simple ligand mimics, AH_n, can replace alkylated ligands, AR_n. Chapter 7 extends this work to calculations on real complexes. Chapter 8 details the development of the combined method and a sample calculation. Finally Chapter 9 provides conclusions drawn from this work and some suggestions for future work.

1.2 Computational Methods

1.2.1 Introduction

A variety of techniques exist within the scope of computational chemistry, ranging from completely empirical to semi-empirical right through to *ab initio*. For the study of the energetics of organic molecules, sufficient experimental data exists to parameterise a semi-empirical model. By contrast, due to the vast variety of bonding, co-ordination numbers and geometries that are found, using such an approach for the study of transition metals will be, at best, limited. In addition, in order to investigate bond making/breaking processes a quantum mechanical method will be required.

In order to model accurately the properties of transition metal complexes it is necessary to look towards more *ab initio* type methods that have little or no recourse to experiment. A completely rigorous *ab initio* theory would involve no assumptions or approximations and would be able to characterise a system completely. This would correspond to solving the complete Schrödinger equation, but this is not possible for a many-electron system so approximations have to be introduced. The first such approximation is the Born-Oppenheimer approximation[1], in which the more massive nuclei are assumed to be stationary as the electrons move about them. Further, it can be assumed that relativistic effects are negligible, leaving the non-relativistic many-electron Schrödinger equation within the Born-Oppenheimer approximation[1]. This still remains a difficult problem and so a further assumption is made by treating the system as a one-electron problem. This is achieved by considering each electron as moving in a potential field generated by

the remaining electrons and nuclei. This leads to the non-relativistic, Born-Oppenheimer, one-electron Schrödinger equation (1.1).

$$h\phi = \varepsilon\phi \qquad (1.1)$$

where h is the Hamiltonian operator, ϕ is a wavefunction and ε is the energy.

This provides a starting point for the implementation of *ab initio* methods that are within the scope of today's computational power. However, care must be taken so that when these approximations are applied, such as the one-electron treatment, that the treatment of many-body effects such as electron correlation (see 1.2.2) are included. The electron correlation energy is explicitly ignored by Hartree Fock (HF) theory and this is particularly serious for transition metal systems. The large number of electrons in these systems leads to a relatively large correlation energy and so some improved treatment is necessary. Density Functional Theory (DFT) has a much improved treatment of correlation energy. The one-electron Hamiltonian, h, comprises essentially two terms (1.2).

$$h = KE + V \qquad (1.2)$$

where KE describes the kinetic energy of the system and V the potential energy. The potential energy consists of three parts (1.3)

$$V = V_{ne} + V_{ee} + V_{xc} \qquad (1.3)$$

where V_{ne} is the nucleus-electron interaction energy, V_{ee} is the electron-electron interaction energy and V_{xc} is the exchange-correlation energy.

It is the treatment of the third term, V_{xc}, that essentially differentiates one *ab initio* method from another and largely determines how good an approximation that method is. Prominent among such methods are the Hartree-Fock (HF) method, together with the various post Hartree-Fock (PHF) methods, which have been developed to increase the accuracy of the former both in terms of a more rigorous methodology and the quality of calculated results, and Density Functional Theory (DFT). This latter method has emerged recently as an accurate and reliable method for the treatment of transition metal complexes.

A further important point to consider is that of scaling,. This is the time taken by various methods to complete a task of a given size. HF formally scales as n^4 where n is the number of electrons in the system. Therefore a doubling in the number of electrons leads to an approximate 16 fold increase in the time required for the calculation. The various PHF methods scale formally as at least n^5 whereas DFT formally scales only as n^3. Although there are methods available that are capable of reducing these formal scaling factors, they are generally applicable to all methods and so the relative difference in scaling is still the same. In addition to this, results of calculations on transition metal systems suggest[2] that DFT is more accurate than HF and comparable to PHF methods. When the significant reduction in computational cost is considered DFT is seen to be an extremely attractive method for the study of transition metal systems.

1.2.2 Density Functional Theory (DFT)

1.2.2.1 Introduction

DFT has as its basis the notion that the energy of an electronic system can be expressed as a functional of its electronic density. This idea goes back to early work by Thomas,[3a] Fermi,[3b] Dirac,[3c] and Wigner[3d] (see Equation 1.4). This simple but enormously powerful result means that it is possible, in principle, to provide an exact description of all correlation effects within a one-electron (i.e. orbital based) scheme.

$$E = E_K + E_N + E_C + E_{XC} \qquad (1.4)$$

where E is the total energy of the system, E_K is the kinetic energy, E_N is the electron-nucleus attraction and the nucleus-nucleus repulsion, E_C is the Coulombic interaction between two charge clouds and E_{XC} is the exchange-correlation energy. The first three terms are commonly encountered and are conceptually simple. However, the exchange-correlation term is a quantum mechanical expression and has no counterpart in classical theory. In essence, there are two separate terms contained within this expression, exchange, or spin-correlation, and correlation, or charge correlation. The first term measures the lowering of the energy resulting from the tendency for electrons having the same spin to keep apart from one another. The second term measures the lowering of energy due to the fact that orbitals are modified by the repulsion between electrons. It is vital for a full and accurate treatment to include these effects. Neglecting, for example, the effects of

correlation, as in the HF approach, leads to significant errors in the calculation of molecular properties.

The fundamental expression of DFT by (1.4) allows the calculation of the true ground state energy as long as one knows the true electron density and the functional dependence of the above terms on that density. The derivation in 1964 by Kohn and Sham[4] of a set of one-electron equations (1.5) that could, in principle, be used to calculate the exact electron density, freed the way towards a more exact theory.

They have an identical form to the one-electron HF equations, the difference being that the exchange-correlation term, V_{XC}, is not the same. The functional dependence of the various energetic terms on the electronic density is well described for the kinetic, electron-nucleus/nucleus-nucleus and Coulombic terms. However, the functional dependence of the exchange-correlation term has yet to be ascertained. In fact knowledge of the exact functional form requires solving the many-electron Schrödinger equation. This is of course an impossible task and so the best treatment that is possible is to constantly refine a set of approximate functionals that are limited by certain boundary conditions until calculated values of suitable accuracy are obtained. The total energy of an n-electron system can be written[5], without approximation as:

$$E_{el} = -\tfrac{1}{2}\Sigma\int\phi_i(r_1)\nabla^2\phi_i(r_1) + \Sigma\int Z_A(|R_A - r_1|)^{-1}\rho(r_1)dr_1$$
$$+ 1/2\int\rho(r_1)\rho(r_2)(|r_1 - r_2|)^{-1}dr_1dr_2 + E_{XC} \qquad (1.5)$$

where ϕ_i is the ith orbital, r_n is the position of the nth electron, ρ is the electron density, Z_A is the nuclear charge, ∇^2 is the Laplacian operator ($\nabla^2 = \delta^2/\delta x^2 + \delta^2/\delta y^2 + \delta^2/\delta z^2$) and R_A is the nuclear position.

This is in fact Equation 1.4 restated with each of the first three terms being exact. The final term can only be expressed correctly if, as stated above, the functional dependence of this term on the electronic density can be determined. The exchange-correlation energy can be expressed in terms of spherically averaged exchange-correlation hole functions[6]. The hole function $\rho_X^{\gamma\gamma'}(r_1,s)$ contains all information about exchange and correlation between the interacting electrons as well as the influence of correlation on the kinetic energy. The interpretation of this hole function is that an electron at r_1, to a larger or smaller extent, will exclude other electrons from approaching within a distance s. The extent of exclusion, or screening, increases with the magnitude of this function. The exact nature of the function can only be obtained, as stated above, from an exact solution of the Schrödinger equation of the n-electron system. Despite the fact that the one-electron Kohn-Sham equations are of limited value for exact[7] solutions of many-electron systems, they form the starting point for approximate treatments where the exact hole function is replaced by model hole functions. The form of the exact hole function is not known in detail, but a number of its properties can be deduced from general considerations. The model hole functions are, in general[8] constructed in such a way that the general constraints are obeyed.

1.2.2.2 The Local Density Approximation (LDA)

The LDA has developed from the theory of the homogenous electron gas as a way to treat the exchange-correlation problem. The approximation is that the electron density of the system remains constant over all space i.e. the electronic density gradient is always zero. This of course, is not true for most real systems but it serves as a first approximation. The exchange-correlation energy for the homogenous electron gas can be written as:

$$E_{XC}^{LDA} = E_X^{LDA} + E_C^{LDA} \qquad (1.6)$$

The first term, representing the exchange energy, has the form

$$E_X^{LDA} = -9/4\alpha_{ex}[3/4\pi]^{1/3}\Sigma\int[\rho_1^{\gamma}(r_1)]^{4/3}dr1 \qquad (1.7)$$

where the electron gas value for the exchange scale factor, α_{ex}, is 2/3 and ρ_1^{γ} is the electron density for electrons of spin γ.

The exact exchange energy in the Kohn-Sham theory is simply E_{XC} corresponding to a single determinantal wave function constructed from the exact Kohn-Sham orbitals. The second term, representing the correlation energy, has the form:

$$E_C^{LDA} = \int\rho_1(r_1)\varepsilon_c[\rho_1^{\alpha}(r_1)\rho_1^{\beta}(r_1)]dr_1 \qquad (1.8)$$

where $\varepsilon_c[\rho_1^{\alpha},\rho_1^{\beta}]$ represents the correlation energy per electron in a gas with the spin densities ρ_1^{α} and ρ_1^{β}.

As one can see, both the exchange and correlation terms have a dependence on the electron density, and in contrast to HF, this only involves the local value and not a non-local integration over all space. Hence, using the homogeneous electron gas approximation is often referred to as the Local Density Approximation (LDA). The specific correlation energy, $\varepsilon_c[\rho_1^{\alpha},\rho_1^{\beta}]$, is not known analytically. However, approximations of increasing accuracy have been developed. Vosko, Wilk and Nussair[9] have used Padé interpolations to fit $\varepsilon_c[\rho_1^{\alpha},\rho_1^{\beta}]$ from accurate calculations on the homogeneous electron gas due to Ceperley and Alder[10]. A method known as the Hartree-Fock-Slater (HFS), or Xα (see 1.2.3), method developed by Slater and others[11] is a simplified version of LDA which was developed long before any formal development of DFT. The main difference here is that only the exchange part of the exchange-correlation energy (see Equation. 1.10) is retained from Equation 1.9 and in many cases, a value of the exchange scaling factor, α, that is somewhat different from the electron gas value of 2/3. The treatment of exchange-correlation by the LDA, as stated above, relies on more and more accurate models for the exchange-correlation hole functions. The accuracy of such models can be readily compared with exact values for both the exchange and correlation energies. LDA calculations of atomic exchange and correlation energies have been shown[2] to be in error from the exact values by ca. 10% and ca. 100% respectively. This represents a significant error although one must take into account that in absolute terms, due to the difference in magnitude of the exchange and correlation energies,

the exchange energy error is greater than the correlation energy error by approximately an order of magnitude. In order to progress it is necessary to improve the description of the exchange-correlation energy. One way to improve this description is the inclusion of gradient corrections to the LDA.

1.2.2.3 Gradient Corrected Functionals

In the last few years, considerable progress has been achieved within density functional theory in the calculation of molecular properties by the use of gradient corrected functionals. It has been shown above that the LDA is only a first approximation to the picture of electron density distribution in real molecules. The use of these gradient corrected functionals gives a general overall improvement of the results obtained with the LDA. This is especially true for energy quantities such as binding energies in molecules. Gradient corrected functionals have been proposed by Becke[12] for exchange, and by Perdew[13], for correlation, amongst others.

The Becke correction to the exchange energy is defined as

$$E_X^{GC}[\rho] = \sum_{\sigma} \int \rho_\sigma^{4/3} f(x_\sigma) dr \qquad (1.9)$$

where σ is a spin index and $x_\sigma = |\nabla\rho_\sigma|/\rho_\sigma^{4/3}$. The function f is defined as

$$f(x) = -\beta x^2 [1 + 6\beta x \sinh^{-1} x]^{-1} \qquad (1.10)$$

The constant β has the value 0.0042, and has been chosen so as to satisfy some scaling, asymptotic and weak inhomogeneity properties. Hence, the value of the correction to the LDA exchange energy is dependent on the how the electron density gradient changes as a function of the electron density. Therefore there is a measure of the inhomogeneity of the system included although the empirical nature of the constant, β, is such that this cannot (in addition to the LDA treatment) be an exact representation of the exchange energy.

The correlation energy correction of Perdew is defined by

$$E_C^{GC}[\rho] = \int [d(\zeta)]^{-1} C(\rho) \rho^{4/3} x^2 e^{-\Phi(\rho,|\nabla\rho|)} dr \qquad (1.11)$$

where $\zeta = (\rho_\sigma - \rho_\sigma`)/\rho$ is the spin polarisation and

$$d(\xi) = 2^{1/3}[(1/2(1+\zeta))^{5/3} + (1/2(1-\zeta))^{5/3}]^{1/2} \qquad (1.12)$$

C(ρ) is obtained from the gradient expansion of slowly varying densities of the correlation energy of the electron gas and is usually expressed in terms of the Wigner-Seitz radius $r_s = [3/(4\pi\rho)]^{1/3}$ and a number of constants. Finally

$$\Phi(\rho,|\nabla\rho|) = 1.745 f [C(\infty)/C(\rho)][|\nabla\rho|/\rho^{7/6}] \qquad (1.13)$$

where $f = 0.11$.

Again, as described for the exchange correction, there is a functional dependence of the correlation energy on the density gradient and the use of empirical constants to fit to experimental data.

Use of these corrections has improved the value of calculated exchange and correlation energies significantly from those calculated with the LDA only. The acknowledgement that the electron density is not constant across all space for molecules is important and by treating this deficiency an improved description of these properties is achieved. Also improvements have been shown in bond energies, molecular geometries etc. over the LDA method[2]. However, the nature of these corrections, in that there is still some recourse to experimental data, suggests that improvements can still be made with a more rigorous derivation.

1.2.2.4 Practical Implementation

The implementation of the DFT method allows the computation of a large variety of molecular properties such as bond energies, geometries, vibrational frequencies, ionisation potentials, electron affinities etc. The self-consistent version of DFT requires the solution of the Kohn-Sham equation. This is accomplished in practice by deriving the potential V_{XC} from an approximate expression, E_{XC}, for the exact exchange-correlation energy, $\underline{E}_{XC}$. This leads to an approximate Kohn-Sham equation (1.14)

$$[\tfrac{1}{2}\nabla^2 + V_N(r_1) + V_C(r_1) + \underline{V}_{XC}(r_1)]\phi_i(r_1) =$$

$$h_{ks}\phi_i(r_1) = \varepsilon_i\phi_i(r_1) \qquad (1.14)$$

where h_{ks} is the Kohn-Sham Hamitonian,

$$V_N(r_1) = \Sigma Z_A[R_A - r_1]^{-1} \qquad V_C(r_1) = \int \rho(r_2)[r_1 - r_2]^{-1} dr_2$$

and $$\underline{V}_{XC}[\rho(r_1)] = [\delta E_{XC}[\rho(r_1)]]/[\delta\rho(r_1)]$$

The set of solutions $\{\phi_i(r_1), i=1, n\}$to 1.14 affords the electron density from which several expectation values can be calculated, including the total energy.

The optimisation of molecular geometries is possible via the calculation of analytical energy gradients[14]. Expressions for the derivative of the energy with respect to the Cartesian nuclear co-ordinates can be derived such that energy gradients can be calculated. These energy gradients are transformed into internal co-ordinates in order to allow partial optimisation and then the co-ordinates are updated. Any of a number of search routines can be used in order to find the minimum in the potential energy surface and hence the optimised geometry.

1.2.3 The Discrete Variational Xα (DVXα) Method

In 1973 Baerends, Ellis and Ros proposed[15] the use of a numerical integration procedure for the Hamiltonian matrix elements, coupled with a fitting of the Coulomb potential to a series of subsidiary functions. This enables fairly rapid calculations even for fairly large basis sets, since the two-electron integrals required for ab-initio methods are not required. This method is known as the discrete variational Xα (DVXα) or Hartree-Fock-Slater (HFS) method. The accurate representation of the Coulomb potential, V_C, is accomplished by fitting the molecular density to a set of one-centre auxiliary functions so that V_C can now be

evaluated by analytical or numerical integration. The advantage of using a numerical integration technique is that it allows complete freedom in the choice of basis set radial function. From this framework evolved two general methods for choosing basis sets. Firstly, numerical atomic orbital basis functions embedded in a potential well, which may be calculated by a self-consistent charge (s.c.c.) procedure (see 2.3) to reflect the calculated molecular geometries, are used. This procedure utilises the numerical freedom of the discrete variational method, but yields an accurate basis set whose size is that of a minimal basis set or larger. The second approach has been to adopt a larger Slater-type orbital basis, of double- or triple-ζ quality, including polarisation functions where necessary.

A difficulty with this method is that the number of sample points required to evaluate the total energy is much greater than that needed to determine the orbitals and one-electron energies. The incorporation of analytical integration techniques improved this situation substantially, allowing the calculation of potential curves for small molecules. The value of this method is that it allowed the calculation of energy gradients for use in geometry optimisations as well as pseudopotentials and the inclusion of relativistic effects.

1.2.4 The Hartree-Fock (HF) Method

The most popular of the *ab initio* quantum chemical molecular methods is based on the Hartree-Fock approximation[16]. The electronic structure is described in terms of a set of doubly occupied molecular orbitals(MO) and a set of higher energy vacant or virtual orbitals. All the MOs are expressed in terms of a Linear

Combination Of Atomic Orbitals (LCAO) where the number and types of atomic orbitals (AO) describe a basis set, ϕ. The molecular energy is a function of the basis set size and decreases towards a limiting value (the HF limit) as the basis is enlarged. The ground state electronic configuration usually obeys the Aufbau principle and is described by a single Slater determinant. A determinantal expression ensures that the electronic wavefunction correctly obeys antisymmetry requirements of Fermi statistics. As stated above HF scales as n^4, where n is the number of electrons in the system, essentially a measure of the size of the system.

The single determinant HF approximation only gives an averaged treatment of electron correlation. In spite of this, for a large number of systems, especially those comprising of "light" atoms, the HF approximation is remarkably good[17]. Ground state geometries can be reproduced to within a few hundredths of an Angstrom for bond distances and a few degrees for bond and torsion angles. However, a single determinant HF description is not well suited for transition metal systems .The underlying cause of the problem stems from the relatively weak nature of metal-ligand bonding and the inherent problem of HF to treat weak binding accurately.

The average treatment of correlation in single determinant HF is inadequate and several schemes exist to remedy this problem. These treatments range from Configuration Interaction (CI)[18] to the use of perturbation theory[19]. The formalism for improving HF is well defined and can, in theory, be extended to give an exact treatment. An infinite CI treatment with a complete basis set will give an exact energy of a given system. The implementation of CI is not without drawbacks. Firstly, CI scales badly (n^5 to n^8) and hence is computationally expensive, and

secondly it is not well behaved in as much as an apparently systematic improvement of the CI expansion does not necessarily lead to a systematic increase in the accuracy of the computed results. Perturbation theory expressions due to Møller and Plesset (MP)[20] are frequently used. Use of second order treatment, MP2, leads to significant improvement over HF but at the cost of an order of magnitude increase in the scaling factor. Also MP theory is only applicable to systems that are well described by a single configuration. Many problems are multi-determinantal and require more sophisticated methods such as Multi Configuration SCF (MCSCF)[21] and Complete Active Space SCF (CASSCF)[22]. However, the problem with all these methods is that of computational cost which makes them unsuitable for intensive tasks such as geometry optimisation.

1.2.5 Molecular Mechanics

1.2.5.1 Introduction

Molecular Mechanics (MM), has emerged as a popular and powerful method for modelling molecular structure and conformational energies[23] with well-parameterised force fields available for treating many "organic" problems in chemistry and biochemistry[24-28].

The MM method considers a molecule as a collection of atoms held together by elastic or harmonic forces. These forces can be described by potential energy functions of the structural features such as bond lengths, bond angles, non-bonded interactions and so on. The combination of these potential energy functions makes up the force field. The energy, E, of the molecule in the force field arises from

deviations from "ideal" structural features, and can be approximated by the sum of the energy contributions of the force field (1.15.

$$E = E_s + E_b + E_w + E_{nb} + ... \qquad (1.15)$$

where E_s is the bond stretch energy, E_b is the angle deformation energy, E_w is the torsional energy and E_{nb} is the non-bonded energy.

The total energy E is referred to as the steric or strain energy, and is the difference in energy between the real molecule and a hypothetical molecule where all the structural values such as bond lengths and bond angles are exactly at their ideal or "natural" values. The individual terms in the force field refer to the energy of a bond being stretched or compressed from its natural bond length, E_s, the energy of bending bond angles from their natural values, E_b, the torsional energy due to twisting about bonds, E_w , and the energy of non-bonded interactions, E_{nb}. If there are other intramolecular mechanisms affecting the energy, such as electrostatic (Coulombic) interactions or hydrogen bonding, then these too may be added to the force field.

It is important to recognise that the energy, E, computed by a set of force field terms is only a measure of intramolecular strain relative to a hypothetical situation, and by itself E has no physical meaning. It is, however, the differences in E for a given set of calculations that are important, and hence it is these energy differences that are appropriate for comparison with experimentally observable physical

properties such as the rotational barriers or conformer populations of a given molecule.

Once the force field has been constructed using appropriate potential functions, as will be described in the next section, and suitable parameters, such as natural bond lengths, natural bond angles etc. have been chosen, a trial geometry is specified in terms of atomic co-ordinates and an initial strain energy is calculated. Thereafter the geometry is optimised, using one of the many gradient search or analytical methods of minimisation, to render the inherent strain energy as small as possible.

1.2.5.2 Potential Functions of Force Fields

In the molecular mechanics model the atoms of a molecule may be thought of as being joined together by mutually independent springs, restoring "natural" values of bond lengths and angles. Most force fields employ a harmonic potential with Hooke's law functions for both bond stretching and angle bending, V_r and V_q respectively, as shown in Equations 1.16 and 1.17.

$$V_r = 1/2k_r(r - r_o)^2 \qquad (1.16)$$

$$V_q = 1/2k_q(q - q_o)^2 \qquad (1.17)$$

where k_r and k_q are the force constants for each term, r and q represent the actual bond length and angle, and r_o and q_o represent the ideal values of the bond length and angle.

At very large deformations from the ideal bond length one would expect deviations from the harmonic potential, however, and a Morse function would be the more general potential. The Morse potential is of the form show by Equation 1.18, where D_b is the depth of the potential well, a is the force constant, b is the actual bond length and b_o is the ideal bond length.

$$V_r = D_b[1-e^{-a(b-b_o)}]^2 - D_b \qquad (1.18)$$

The harmonic angle bending term does not seem to suffer from the same problem for large angle deformations. For organic species, angles that are opened to unusually large values show a deformation from normal of only about 15^o. There is no compelling evidence that the quadratic function is inadequate for deformations of this size.

The torsional energy term has usually been thought of as resulting from a repulsion between bonds not covered by van der Waals interactions. Modern MM force fields describe the change in energy of the molecule as the torsion angle, ω, changes in terms of the Fourier series shown in Equation 1.19.

$$V_{tor} = K(1 + S(\cos n\omega)) \qquad (1.19)$$

where K is the force constant, S is the sign applied to the cos function and n is the number of minima/maxima in the torsion barrier.

The fourth term in Equation 1.15 is the potential energy term relating to the pairwise non-bonded interaction of atoms as a function of distance between nuclei. As two atoms approach one another, there is the usual attraction due to London dispersion forces and finally a van der Waals repulsion as the atoms become too close. Two of the more common potential energy functions that describe this behaviour are the Lennard-Jones potential, Equation 1.20, and the Buckingham potential, Equation 1.21;

$$V_{LJ} = A/r^{n} - B/r^{6} \qquad (1.20)$$

$$V_{Buck} = A'\exp(B'/r) - C/r^{6} \qquad (1.21)$$

where n is usually either 6 or 10 for the Lennard-Jones potential and A, B and C are constants.

By use of the force field potentials described above, molecular mechanics models are able to provide accurate predictions of both structure and energetics of a wide range of organic species, and have become a popular and powerful tool in organic chemistry. There are at least two reasons for the popularity of the MM method. Firstly the method is considerably faster than other theoretical approaches such as quantum mechanical treatments, thus allowing a full energy minimisation of relatively large molecules (>1000 atoms) in a reasonable computational time.

Secondly, if and when a molecular orbital treatment is necessary, the MM optimised geometry can provide excellent input for a molecular orbital calculation, an approach that is becoming increasingly popular among theoretical chemists[29].

A major drawback of MM is that many molecules of interest to chemists are outside the range of molecules for which the molecular mechanics programs are currently parameterised. It is, of course, possible to estimate the appropriate parameter values with some degree of confidence from existing parameterisation schemes, but any new applications should be tested on related molecules whose structures are known, if at all possible. MM is also not suitable for studying properties where electronic effects, such as orbital interactions or bond breaking and making, are predominant.

1.2.5.3 Molecular Mechanics Calculations of Co-ordination Compounds

The application of simple valence force field computations to co-ordination compounds, although possible, is problematic. The first type of problem is revealed by the large variation of ligand-metal-ligand (L-M-L) bond angles observed at transition metal centres. This variation in bond angle is well illustrated by $CuCl_4^{2-}$ which, depending on the counterion present, can exist with Cl-Cu-Cl angles ranging from 180° (square planar) to c.120° found in distorted tetrahedral complexes. Obviously one term can not account for such variations. Bond lengths are also seen to vary considerably, but not as markedly as the bond angles. These difficulties are in part caused by the presence of ionic species and their counterions, the nature of the counterion (both size and charge) being particularly important.

Also metals are found in a variety of oxidation states and this cannot be accounted for within a MM treatment without the use of a different force field for each state. Therefore as treatment for a system which undergoes a change of oxidation state would not be at all possible.

An additional problem that is encountered in the application of MM to transition metal species is the definition of unique angles and corresponding equilibrium values, referred to as the "unique labelling problem". For example, *cis*-diaminodichloroplatinum(II) requires two N-Pt-Cl equilibrium angle values (90^{O} and 180^{O}). MM force fields have overcome the unique labelling problem by the incorporation of multiple equilibrium positions and redundant atom labelling schemes at the cost of tedious over-definition of the molecular topology. A more common strategy, however, to circumvent both the unique labelling problem and the problems encountered due to the use of harmonic angular potential functions, is to set the angle bend force constants for the L-M-L angles to zero, and to allow ligand-ligand 1-3 non-bonded interactions to determine the angular geometry of the complex.

Recent work by Burton *et al.*[30] has suggested that the modelling of transition metal complexes may be possible within a MM frame by the inclusion of a d-electron energy term derived from a cellular ligand field treatment[31]. Such work is currently limited to a small range of systems, but may in the future be capable of treating any transition metal complex. However, such a treatment will still not be able of treating reactions due to the inherent limitations of MM.

References

1. M.Born and J.R.Oppenheimer, *Ann. Phys-Leipzig*, 1927, **84**, 457.

2. T.Ziegler, *Chem. Rev.*, 1991, **91**, 651.

3. (a) L.H.Thomas, Proc. *Cambridge Philos. Soc.*, 1927, **23**, 542. (b) E.Fermi, *Z. Phys.*, 1928, **48**, 73. (c) P.A.M.Dirac, *Cambridge Philos. Soc.*, 1930, **26**, 376. (d) E.P.Wigner, *Phys. Rev.*, 1934, **46**, 1002.

4. W.Kohn and L.J Sham, *Phys. Rev. A*, 1965, **140**, 1133.

5. (a) P.Hohenberg and W.Kohn, *Phys. Rev. A*, 1964, **136**, 864. (b) M.Levy, *Proc. Natl. Acad. Sci. U.S.A.*, 1979, **76**, 6062.

6. (a) A.D.Becke, *J. Chem. Phys.*, 1988, **88**, 1053. (b) A.D.Becke, *ACS Symp. Ser.*, 1989, 394. (c) R.McWeeney and B.T.Sutcliffe, Methods Of Molecular Quantum Mechanics; Academic Press: New York, 1969. (d) W.L.Luken and D.N.Beraten, *Theoret. Chim. Acta.*, 1982, **61**, 265. (e) O.Gunnarsson and I.Lundquist, *Phys. Rev.*, 1974, **B10**, 1319. (f) O.Gunnarsson and I.Lundquist, *Phys. Rev.*, 1976, **B13**, 4274. (g) O.Gunnarsson and I.Lunquist, *Phys. Rev.*, 1979, **B20**, 3136.

7. W.Kohn and P.Vashishta, In Theory Of Inhomogeneous Electron Gas; S.Lundqvist and N.H.March, Eds; Plenum: New York, 1984, pp79-147.

8. M.Buijse, E.J.Baerends and J.G.Snijders, *Phys. Rev.*, 1989, **A40**, 4190.

9. S.J.Vosko, L.Wilk and M.Nussair, *Can. J. Phys.*, 1980, **58**, 1200.

10. D.M.Ceperley and B.J.Alder, *Phys. Rev. Lett.*, 1980, **45**, 566.

11. (a) J.C.Slater, *Phys. Rev.*, 1951, **81**, 385. (b) K.Schwarz, *Phys. Rev*, 1972, **B5**, 2466. (c) M.S.Gopinathan and M.A.Whitehead, *Phys. Rev.*, 1976, **A14**, 1.

12. A.D.Becke, *Int. J. Quantum Chem.*, 1983, **23**, 1915.

13. J.P.Perdew, *Phys. Rev. Lett.*, 1985, **55**, 1665.

14. (a) P.Pulay, *Chem. Phys. Lett.*, 1969, **17**, 197. (b) J.Pople, R.Krishnan, H.B.Schlegel and J.S.Binkley, *Int. J. Quantum. Chem.*, 1978, **S12**, 169.

15. E.J.Baerends, D.E.Ellis and P.Ros, *Chem. Phys.*, 1973, **2**, 41.

16. (a) D.R.Hartree, *Proc. Camb. Phil. Soc.*, 1928, **24**, 89. (b) V.Fock, *Z. Physik.*, 1930, **61**, 126. (c) C.C.J.Roothan, *Rev. Mod. Phys.*, 1951, **23**, 69.

17. (a) C.F.Bunge, J.A.Barrientos and A.V.Bunge, *Atomic Data and Nuclear Data Tables*, 1993, **53**, 113. (b) C.F.Bunge, J.A.Barrientos, A.V.Bunge and J.A.Cogordin, *Phys. Rev.*, 1980, **72**, 4654.

18. R.Krishnan, H.B.Schlegel and J.A.Pople, *J. Chem. Phys.*, 1980, **72**, 4654.

19. (a) B.Huron, J.P.Malrieu and O.Rancrel, *J. Chem. Phys.*, 1973, **58**, 5745.

(b) S.Evangelisti, J.P.Dacudey and J.P.Malrieu, *J. Chem. Phys.*, 1983, **75**, 91.

20. C.Møller and M.S.Plesset, *Phys. Rev.*, 1934, **46**, 618.

21. (a) K.Rudenburg, M.W.Schmidt, M.M.Gilbert and S.T.Ellbert, *Chem. Phys.*, 1982, **71**, 41. (b) K.Rudenburg, M.W.Schmidt and M.M.Gilbert, *Chem. Phys.*, 1982, **71**, 51. (c) K.Rudenburg, M.W.Schmidt, M.M.Gilbert and S.T.Elbert, *Chem. Phys.*, 1982, **71**, 65.

22. (a) B.O.Roos, *Adv. Chem. Phys.*, 1987, **69**, 399. (b) P.E.M.Siegbahn, J.Almlöf, A.Heiberg and B.O.Roos, *J. Chem. Phys.*, 1981, **74**, 2364. (c) P.E.M.Siegbahn, A.Heiberg, B.O.Roos and B.Levy, *Phys. Scr.*, 1980, **21**, 323. (d) B.O.Roos, P.R.Taylor and P.E.M.Siegbahn, *Chem. Phys.*, 1980, **48**, 157. (e) B.O.Roos, *Int. J. Quantum Chem. Suppl.*, 1980, **14**, 175.

23. V.Burkert and N.L.Allinger, "Molecular Mechanics", ACS monograph 177, Washington, 1982.

24. N.L.Allinger, Y.H.Yuh and J.H.Lii, *J. Am. Chem. Soc.,* 1989, **111**, 8551.

25. R.Brooks, R.E.Bruccoleri, D.B.Olafsen, D.J.States, S.Swaininathan and M.Karplus, *J. Comput. Chem.*, 1983, **4**, 187.

26. P.K.Weiner and P.A.Kollman, *J. Comput. Chem.*, 1981, **2**, 287.

27. S.J.Weiner, P.A.Kollman, D.A.Case, V.C.Singh, C.Ghio, G.Alagona, S.Profeta and P.K.Weiner, *J. Am. Chem. Soc.,* 1984, **106**, 765.

28. S.L.Mayo, B.D.Olafson and W.A.Goddard, *J. Phys. Chem.*, 1990, **26**, 8897.

29. N.L.Allinger and S.Profeta Jr., *J. Comput. Chem.*, 1980, **1**, 181.

30. (a) V.J.Burton, R.J.Deeth, P.J.Gilbert and C.M.Kemp, *J. Am. Chem. Soc.*, 1995, **117**, 8407. (b) V.J.Burton and R.J.Deeth, *J. Chem. Soc., Chem. Comm.*, 1995, 573.

31. (a) M.Gerloch, "*Magnetism and Ligand Field Analysis*", Cambridge University Press, 1984. (b) M.Gerloch, J.H.Harding and R.G.Woolley, *J. Chem. Soc. Dalton Trans.*, 1981, 1714. (c) M.Gerloch and R.G.Woolley, *Inorg. Chem.*, 1984, **23**, 3853, *ibid.*, 1985, **24**, 4490.

Chapter 2

Molecular Properties of Chlorocuprates

2.1 Introduction

Significant interest has been shown by both the experimental[1,7c] and theoretical[2] chemist in the series of chlorocuprates. The interest in these systems originates from the diversity of co-ordination numbers and stereochemistry and also from their relatively simple electronic and chemical properties. From a computational point of view chlorocuprates have served as simple models for various complex metalloprotein moieties such as the Blue Copper Proteins (BCP)[3]. Examples of these systems include plastocyanin, azurin and stellacyanin. Interest has focused on the BCPs because of their unusual properties and their role in biological processes such as electron transfer within plant photosynthesis (plastocyanin). BCPs are characterised by an intense (ε>5000$M^{-1}cm^{-1}$) charge transfer band at around 660nm, an unusually small hyperfine splitting in the $g_{||}$ region of the ESR spectrum and an unusually high reduction potential. Ligand field studies of small inorganic copper complexes have proved to be invaluable in elucidating spectroscopically the effective active site of BCPs prior to their crystallographic structure determination[4].

The range of chlorocuprates is given by $CuCl_n^{(n-2)-}$ (n=2,4,5,6). Regular geometries are found for n=2,5,6 (linear, square based pyramid and tetragonal) whereas $CuCl_4^{2-}$ exists in a wide variety of geometries from square planar through to tetrahedral, the exact stereochemistry depending on the counter-ion.

The tetrachlorocuprate ion is perhaps the most intensively crystallographically studied of all transition metal complexes. At least 60 different structures have been characterised[1]. These structures can be classified in terms of the trans Cl-Cu-Cl angle and the Cu-Cl bond length. By applying a rough criterion these complexes can be classified into one of three groups. Firstly a group of three structures of approximate tetrahedral symmetry with an average bond angle of 110° (range 105.2°-115.0°) with an average bond length of 2.24Å (range 2.23Å -2.25Å). Secondly a much larger group of distorted tetrahedral (D_{2d}) symmetry with an average bond angle of 136° (range 125.6°-159.3°) and an average bond length of 2.24Å (range 2.21Å-2.27Å). Finally a group of approximate square planar (D_{4h}) symmetry with an average bond angle of 179.7° (range 178.5°-180.0°) and average bond length 2.26Å (range 2.25Å-2.28Å). This variety in structure as noted above is a consequence of the nature of the counterion present in the crystal lattice and of various crystal packing forces. This diversity has implications for the computationalist, namely that it is impossible to compare calculated and experimental structures without some account being taken of the crystal environment. Structural calculations usually refer to the gas phase with no inclusion of the crystal environment. Hence it is only possible to compare calculated structures with average crystallographic structures and even so it is not realistic to expect the level of agreement found with complexes which are far less dependent on external forces. Whilst this is so for the tetrachlorocuprates it will be much less pronounced for other members of the series where structures are far more regular and less variable.

The transition energies of the chlorocuprates have also attracted significant attention[2]. Again, this is caused by a number of factors. Firstly the wide variety of species that exist within this series provides a wealth of experimental data. Secondly, the interest in them as models for biologically active species. Finally, and perhaps most importantly, their chemical and electronic simplicity. This is exemplified by the fact that only d^1 and d^9 systems are possible to treat rigorously within a one-electron framework. Despite the simplicity of the d^9 system the assignment of the electronic spectra of these systems, especially the tetrachlorocuprates, has proved less than simple. In the D_{2d} case the d-d transitions are electric dipole allowed; the polarised single-crystal spectral studies of Ferguson[5] have generated the order $^2B_2(x^2\text{-}y^2)$(ground state) < $^2E(xz,yz)$ < $^2B_1(xy)$ < $^2A_1(z^2)$. Assignment of the square-planar case has been more difficult, as this geometry possesses an inversion centre, and the d-d transitions are therefore made allowed through vibronic coupling. Hitchman[6] has studied the highly vibrationally structured d-d transitions in the bis(N-methylphenethylammonium) tetrachlorocuprate (II) complex and applied vibronic selection rules to determine the square-planar ordering: $^2B_{1g}(x^2\text{-}y^2)$(ground state) < $^2B_2(xy)$ < $^2E_g(xz, yz)$ < $^2A_{1g}(z^2)$. The observed shifts between these two geometries have been explained through ligand-field theory[7], one-electron molecular orbital bonding theory[8] and through many-electron bonding calculations[9,2a]. These ligand-field spectral studies of small molecule inorganic copper complexes have proved to be invaluable in elucidating spectroscopically the effective active site of the BCPs prior to their crystallographic structure determination.

2.2 Optimised Geometries of Chlorocuprates

2.2.1 Introduction

The series of chlorocuprates has attracted considerable interest from the theoretical chemist in line with the properties outlined above. Whilst the spectral features have been investigated by a large number of groups and a variety of methods[2], structural studies have been far less common. The reluctance to study these ionic systems computationally can in part be attributed to the fact that ionic species are expected to suffer from the need to include lattice effects. In general, geometries may or may not be affected by the influence of counterions. The structural diversity of the $CuCl_4^{2-}$ ion is an extreme case of a pronounced lattice effect. By explicitly ignoring any counterions and/or crystal packing forces within these calculations it is hoped to show that it is still a viable approximation in the calculation of molecular geometries. It has been shown[10] that for the calculation of transition energies the neglect of the crystal environment affects only the absolute transition energies but not the relative energies.

As was described above the chlorocuprates exist in a wide range of co-ordination numbers and geometries. Investigations have been made on five of these complexes, namely: linear $CuCl_2$, square-planar $CuCl_4^{2-}$, distorted tetrahedral $CuCl_4^{2-}$, square based pyramidical $CuCl_5^{3-}$ and tetragonal $CuCl_6^{4-}$.

The aim of this work is to carry out a comprehensive study of a series of chlorocuprates in terms of their structure and electronic characteristics. Also to gain insights into the effects on geometry calculations of the quality of basis sets, the use of polarisation functions in basis sets, the use of the frozen core approximation[11]

and the effect of the size of the frozen core chosen and finally the effect of spin unrestricted as opposed to spin restricted calculations.

2.2.2 Computational Details

Geometry optimisations are performed within the HFS-LCAO method[12] using the Amsterdam Density Functional (AMOL/ADF) program system due to Baerends *et al.*[12]. This method employs Slater-type orbital (STO)[13] basis sets. The uniform electron gas local density approximation (LDA)[14] was used in conjunction with analytical energy gradients[15] for all geometry optimisations. The LDA correlation energy was computed according to Vosko, Vilk and Nussair's parameterisation[16] of electron gas data and includes Stoll's correction for self-interaction[17]. Non-local gradient corrected functionals are not employed. The lower core shells on the atoms (2p on chlorine and 2p/3p on copper) were treated by the frozen-core approximation. The total molecular electron density was fitted in each SCF cycle by auxiliary s, p, d, f and g STO functions.

The basis sets are labelled according to whether they are double-ζ (DZ) or triple-ζ (TZ). In addition, the bases were, in some cases, augmented by including an extra 4p function on the copper and 3d functions on chlorine. This should allow sufficient basis set flexibility where used. It has been shown[18] that DFT is less sensitive than HF to the inclusion of multiple polarisation functions and our experience suggests that no significant improvements arise from bases with additional diffuse functions to those described above.

Relativistic corrections are not included as it has been shown[19] that the geometries

and energies of complexes containing atoms even as large as 1st-row transition metals are not affected significantly by the inclusion of these effects.

Calculations have in general used a spin-restricted formalism whereby up-spin and down-spin electrons have been treated in the same way. However, occasionally spin polarisation has been introduced where up- and down-spin electrons have been treated separately.

2.2.3 $CuCl_2$

2.2.3.1 Introduction

The simplest of the chlorocuprates is $CuCl_2$. No structural reports of isolated units have been made. Although, there are some systems with an empirical $CuCl_2$ structure, these are generally polymeric species. Calculations by Bauschlicher and Roos[20] using the Coupled Pair Functional (CPF) method, show the system to be linear and the Cu-Cl bond length to be 2.056Å. In light of the dearth of experimental data it is only possible to compare DFT calculated values with this result.

Geometry optimisations were carried out with $D_{\infty h}$ symmetry, bond lengths are kept equal and the system is restrained to be linear. Variations in basis set are made by altering the quality of the basis set, the size of the frozen core and the inclusion of spin polarisation effects. In Table 2.1 below the nomenclature of the basis sets is as follows; XX.YY.ZZ(P) where XX is the atom symbol, YY is the size of the

frozen core (every orbital up to and including this orbital is treated by the frozen core approximation), ZZ is the basis set quality (dz for double-ζ tz for triple-ζ) and

P indicates the use of a polarisation function.

2.2.3.2 Results and Discussion

Table 2.1 below shows the effect on calculated bond lengths of altering the nature of the basis set. Several comparisons can be made from these results:

i) the effect of (metal) frozen core size.

ii) the effect of basis set quality.

iii) the effect of polarisation functions.

Copper Basis Set	Chlorine Basis Set	Cu-Cl (Å)
Cu.3p.dz	Cl.2p.dz	2.051
Cu.3p.dzp	Cl.2p.dzp	2.003
Cu.3p.tz	Cl.2p.tz	2.107
Cu.3p.tzp	Cl.2p.tzp	2.039
Cu.2p.dz	Cl.2p.dz	2.034
Cu.2p.dzp	Cl.2p.dzp	1.989
Cu.2p.tz	Cl.2p.tz	2.076
Cu.2p.tzp	Cl.2p.tzp	2.007
HF-CPF		2.056

Table 2.1: Comparison of calculated Cu-Cl bond lengths with the HF-CPF value (for basis set nomenclature see text).

The size of the frozen core can be seen to have a noticeable effect on the Cu-Cl bond length. When a smaller frozen core is used the bond lengths are found to be

shorter by 0.01Å-0.03Å. A larger frozen core means that a larger part of the core space is treated by a reduced number of exponents. This is an obviously less exact treatment and leads to underbinding of the ligands so that the representation of the core must be incomplete or incorrect. The frozen core provides a charge density and Coulomb potential for the core space. If this charge density is incorrect, or at least incomparable to that generated by a smaller frozen core, and the charge density is reduced the valence orbitals become contracted and so the overlap of valence orbitals on metal and ligand are reduced and bond lengths are increased. The smaller the frozen core the smaller the effect on the valence orbitals. This is due to the outer valence orbitals being shielded from the effects of the frozen core by inner valence orbitals with the smaller frozen core. An alternative is to use an all-electron approach to provide a more complete treatment of both the core and valence orbitals. The disadvantage of this approach is the scaling problem of DFT and the large increase in computational effort that would be required for such calculations. The effects are likely to be less pronounced because, as stated above, the outer valence orbitals are already shielded from the effects of the core by the inner valence orbitals and so a more accurate treatment of the core would have its effects reduced by the damping action of the core and inner valence orbitals. The need to use only the smaller frozen cores is also justified in light of work by Baerends and Buisje[21], where it is suggested that the relative sizes of the 3s, 3p and 3d functions are similar and so it is important to include all these functions in the valence set for an accurate treatment of the bonding picture.

The quality of basis set (double-ζ vs. triple-ζ) also has a significant effect on the

molecular geometry ranging from 0.02Å to 0.05Å. In all case the triple-ζ basis sets give longer bonds.

Finally the inclusion of polarisation functions causes a universal decrease in the calculated bond lengths of 0.04Å to 0.07Å. Polarisation functions are normally orbitals with higher angular momentum than is required to describe the ground state of the neutral atom. For copper this would require a f-function and for chlorine a d-function. However in this case a copper p auxiliary function is used as it has been shown by Ellis[18] that it is not the nature of the polarisation function that is important for metals but that a function is included. The use of a p-function oriented along the metal ligand axis could allow greater metal-ligand overlap and hence forming a stronger and consequently shorter bond.

2.2.3.3 Conclusions

The results of these calculations on $CuCl_2$ have illustrated a number of points. By altering the basis set used it is possible to introduce a large variation in bond length ranging from 1.989Å to 2.107Å. Therefore care must be taken when choosing basis sets for geometry calculations and these general guidelines are proposed. The frozen core should be kept as small as possible, although the need to carry out all-electron calculations is not considered necessary or practical due to the increase in computational cost. The increase in cost in changing the metal frozen core from the 3p level to the 2p level is quite small and this is more than compensated for in the calculated results. Basis sets should be of at least the triple-ζ level, again the relatively small increase in cost is justified by the calculated results. The inclusion

of polarisation functions should be expected to improve the calculated geometry by allowing the distortion of atom centred orbitals such as is likely to be found in bond formation. Comparing the calculated results presented above with that of Bauschlicher and Roos gives a closest agreement with the value calculated with what would be considered the worst basis set (large frozen core, double-ζ basis set, no polarisation function). However, considering that this is not an experimental value the comparisons are of little real use and so it is really only possible to draw some conclusions about the effect of altering certain parameters in relative and not absolute terms.

2.2.4 $CuCl_4^{2-}$

2.2.4.1 Introduction

The relatively simple chemical, structural and electronic nature of the tetrachlorocuprates has led to them being used as models for the active sites of biological complexes[3]. Much work has been carried out on the electronic properties of these complexes whilst relatively little attention has been paid to the geometries of these complexes. This is due in part to the multitude of structural forms that exist and their ionic nature. The work presented below provides a complete study of the geometries of the tetrachlorocuprates.

2.2.4.2 Results and discussion

The results of geometry optimisations of $CuCl_4^{2-}$ complexes are presented in Tables 2.2-2.5 below. In all cases these calculations have been performed with

frozen cores for both copper (2p) and chlorine (2p). For the square-planar case the geometry has been optimised within D_{4h} symmetry and so all Cu-Cl bond lengths were equivalent and all *cis* Cl-Cu-Cl bond angles fixed at 90°. This has been shown to be a reasonable assumption as when the geometry was optimised with no symmetry restraints the average bond lengths and angles were found to be within 0.01Å and 1° respectively of the values calculated when symmetry restrictions were applied.

With the distorted tetrahedral geometry D_{2d} symmetry was applied such that all Cu-Cl bond lengths were equivalent and the two trans Cl-Cu-Cl angles were also kept identical.

Basis Set	Atomic Charges		Bond Length (Å)
	Cu	Cl	
Dz (spin restricted)	0.5008	-0.6252	2.259
Dzp (spin restricted)	0.0602	-0.5150	2.224
Dzp (spin unrestricted)	0.0643	-0.5161	2.223
Tz (spin restricted)	0.5106	-0.6276	2.382
Tzp (spin restricted)	0.2074	-0.5508	2.308
Tzp (spin unrestricted)	0.2126	-0.5532	2.307
Experimental	-	-	2.265

Table 2.2: Comparison of calculated bond lengths and atomic charges of $CuCl_4^{2-}$ (D_{4h}) with experiment (For experimental values see reference 1).

Looking at the square-planar case first, the same trends are seen as were observed

for $CuCl_2$ namely that tz basis sets give bond lengths longer than dz and the inclusion of a polarisation function reduces the bond lengths. Spin polarised calculations, up-spin and down-spin electrons treated differently, do not appear to have a significant effect, as would be expected, on the geometries for d^9 systems with a single unpaired electron. Analysis of atomic charges shows that there is contradictory evidence as to whether changing basis set quality affects the calculated charges. However, it is clear that polarisation functions bring about a significant reduction in charge separation. An additional metal p-function can polarise metal orbitals in the bond directions so metal orbitals are able to accept more charge from ligand orbitals oriented in the bond direction. This greater exchange of charge is reflected in the shorter metal-ligand bond distances. As for the bond lengths, the use of spin polarisation does not have a significant effect on charges.

Basis Set	Atomic Charges (electrons)		Bond Length (Å)	Bond Angle (°)
	Cu	Cl		
Dz	0.6312	-0.6533	2.313	129.88
Dzp	0.1164	-0.5291	2.243	127.00
Tz	0.6618	-0.6654	2.355	134.00
Tzp	0.2688	-0.5672	2.253	126.94
Experimental	-	-	2.24(av.)	136 (av.)

Table 2.3: Comparison of calculated bond lengths, bond angles (trans Cl-Cu-Cl) and atomic charges of $CuCl_4^{2-}$ (D_{2d}) with experiment (For experimental values see reference 1).

For the distorted tetrahedral case the choice of basis set is varied as above but no spin un-restricted calculations were performed in light of the previous findings that it would have little effect on calculated properties. Again the same points are noted, reduction in bond length (and in this case angle) with the addition of a polarisation function and tz basis sets giving longer bonds and larger angles than dz. The effect on bond angle of a change in basis set is comparable to the effect on bond lengths. In general a larger ligand charge leads to a larger bond angle and this can be attributed to the greater repulsion between two like charges.

2.2.4.3 Conclusions

In general the results presented for $CuCl_4^{2-}$ provide similar conclusions to those found for $CuCl_2$ regarding the effect of basis set choice on calculated geometries. That is the general shortening of bonds with the inclusion of polarisation effects and a lengthening when changing the basis set from double-ζ to the higher quality triple-ζ. The effects of spin un-restricted calculations on d^9 systems is insignificant.

A comparison of calculated geometries with experimental values reveals that best the best agreement is found for dz (D_{4h}) and for D_{2d} the case is less clear. However, bearing in mind that the experimental values are only averages and the range of values is quite large, it is not possible to state categorically that one basis set gives a more accurate result than any other.

Westbrook and Krogh-Jespersen[22] have also calculated structures for these two complexes using all-electron Hartree-Fock (HF) calculations with basis sets up to the triple-ζ level. They calculate bond lengths in the region of 2.42-2.50Å for the

square planar case and bond lengths of 2.40-2.47Å and angles of 116-117° for the distorted tetrahedral case. When a limited treatment of correlation (MP2 level) is included the improvement is in the of the region of 0.01-0.03Å in the bond lengths and 3-4° in the bond angles over the HF values. This shows the general inaccuracy of the HF method when applied to transition metal systems due to the explicit neglect of correlation, introducing even limited correlation effects can improve calculated geometries but at the incursion of additional cost.

Waizumi *et al.*[23] have also carried out DFT calculations on these complexes using double-ζ split-valence GTO basis sets. For the square planar case they calculate a bond length of 2.30Å and for the distorted tetrahedral case values of 2.28Å and 138°. These results are comparable in accuracy to the results presented here and emphasises the accuracy of DFT compared to HF regardless of the choice of basis set and the functional form of the exchange-correlation term. They also calculate relative bond energies and show that the D_{2d} structure is 7.3kJmol^{-1} more stable than the D_{4h} structure. This explains the relative excess of structures having a D_{2d} geometry as compared to those with a D_{4h} geometry that can only be stabilised by large bulky ligands. Similar calculations for the $CuBr_4^{2-}$ ion show a relative stabilisation energy of 28.6 kJmol^{-1} which is reflected in the absence of any D_{4h} structures being found.

2.2.5 $CuCl_5^{3-}$

2.2.5.1 Introduction

Pentaco-ordinated complexes can exist in a number of structural forms those

based on square-pyramids and those based on a trigonal bipyramid. The energy differences between these structures should be small but in general it is expected that the trigonal bipyramidal structure would be favoured, with respect to the square-pyramidal one, whenever the five ligands are equivalent or nearly so and there are no particular constraints. Apparently examples of both structures are known, but the trigonal bipyramidal structure seems to be an artefact of a dynamic averaging process between differently ordered polyhedra with C_{4v} geometry[24a]. Therefore only the square pyramidal case is examined. The structure of this complex is of $CuCl_5^{3-}$ and $[N(2amet)\text{-}pipzH_3]^{3+}$ ions and two water molecules of crystallisation[24b]. Bond distances and angles indicate a slightly distorted square-pyramidal co-ordination. The mean Cu-Cl bond distance of the four equatorial Cl atoms (Cl_e) is 2.318Å (maximum deviation 0.043Å) and that of the axial Cl (Cl_a) is 2.570Å. The average trans Cl_e-Cu-Cl_e bond angle is 165.0° (164.9° and 165.1°), the average cis Cl_e-Cu-Cl_e is 89.04 (maximum deviation 2.77°)and the mean value of the four Cl_a-Cu-Cl_e angles is 97.48° (maximum deviation 5.53°). For these calculations the geometry is idealised to C_{4v} symmetry so that all the equatorial bond lengths are equivalent and a four-fold rotation axis is imposed.

2.2.5.2 Results and Discussion

Presented in Table 2.4 below are calculated geometries for $CuCl_5^{3-}$. The basis sets are varied and compared with the experimental value. Calculations could not be converged with the tzp basis set but, extrapolating the difference in the dz and dzp results and applying it to the tz results gives the figures given in parentheses. The

reasons behind the failure of the SCF procedure to converge are not clear. Several methods have been applied to try and resolve this problem. These include the freezing of molecular orbital populations, varying the amount of the SCF potential that is used in generating the next value in the SCF procedure and altering the initial geometry. None of these methods have proved successful, suggesting that it maybe the very nature of these species that is the cause of this problem. As five co-ordinate copper complexes are quite unusual they need to be stabilised by external forces, consequently they cannot be thought of as real species when considered in the gas phase.

The shorter equatorial bonds show the pattern observed above for $CuCl_2$ and $CuCl_4^{2-}$ in that the addition of a polarisation function causes a decrease in bond lengths and tz basis sets give longer bonds than dz. However, the longer axial bond shows the reverse effect with the axial bond calculated with the larger tz basis calculated to be shorter than with the smaller dz basis set. This bond can be considered as an extremely long bond within transition metal chemistry. The LDA approach may be a poor approximation for complexes containing long bonds such as these. In addition highly charge species such as this one may introduce further complications that the LDA method is not capable of treating accurately. All bond angles are found to be within 2° of each other regardless of the choice of basis set. Hence the choice of basis set does not significantly affect the bond angles or the agreement with experiment. The poor agreement with the experimental value may again be in part due to the presence of the long axial bond.

Basis Set	$Cu-Cl_a$ (Å)	$Cu-Cl_e$ (Å)	$Cl_a-Cu-Cl_e$ (Å)	$Cl_e-Cu-Cl_e$ (Å)
Dz	2.600	2.359	101.67	156.65
Dzp	2.611	2.339	101.21	157.58
Tz	2.529	2.388	102.21	155.58
Tzp	(2.54)	(2.37)	(101.7)	(156.5)
Experiment	2.570	2.312	97.48	165.0

Table 2.4: Calculated geometries of $CuCl_5^{3-}$ compared to experimental.

2.2.5.3 Conclusions

In the absence of the tzp basis calculations it is not possible to comment on the agreement with experimental values but extrapolation again suggests that the higher quality basis set gives more accurate geometries. The reason as to why these calculations cannot be converged are unclear, as stated above. Also the quality of the calculated geometries, which are in error from the experimental values by as much as 0.07Å and 10°, are lower than is expected. These two observations may be as a consequence of the essentially esoteric nature of these species in the gas phase (see 2.2.7 for further discussion of this point).

2.2.6 $CuCl_6^{4-}$

2.2.6.1 Introduction

The $CuCl_6^{4-}$ complex exhibits Jahn-Teller distortion of the regular octahedral environment to a tetragonally elongated geometry. The $(cyclamH_4)CuCl_6$ system[25]

has the equatorial Cu-Cl bond lengths as almost equal at 2.229Å and 2.302Å, the axial bonds are much longer at 3.175Å and the Cl-Cu-Cl angles involving equatorial ligands vary from 90° by less than a degree. Whereas the angles involving the axial ligands are 89.0° and 85.3°. The average of the Cu-Cl bonds is 2.589Å which conforms to that expected when the metal-chloride bond length of the divalent transition ions are plotted as a function of atomic number. Conversely, using the Jahn-Teller displacement factor, Q, of Reinen and Freibel[26];

$$Q = [2(\delta x)^2 + 2(\delta y)^2 + 2(\delta z)^2]^{1/2} \qquad (2.1)$$

where δx, δy and δz are the displacements from the average bond length along each axis gives a value of Q of 1.00Å. This considerably larger than that found for ligands such as NO_2^- and H_20 (0.3-0.4Å) and although the cause of this discrepancy is not clear it is possibly just a reflection of the fact that Cu-Cl bonds are inherently longer than those to oxygen and nitrogen. However. it may also be of a consequence of the lattice environment as , for example, $Cu(H_20)_6^{2+}$ exhibits a variety of values of Q depending on the crystal environment.

2.2.6.2 Results and Discussion

Calculations on the $CuCl_6^{4-}$ species were carried out with the geometry constrained to D_{4h} symmetry, all equatorial and axial bond lengths were kept identical but the axial bonds were allowed to differ from the equatorial ones. All bond angles were fixed at 90° or 180°. Calculations were performed with only the

tzp basis set with 2p frozen cores and spin restricted. Both LDA and GC calculations, using Becke's correction to exchange[27] and Perdew's correlation correction[28], were made.

Shown graphically in Figure 2.1 below is the variation of axial and equatorial bond length during the optimisation process. Initial values are 2.0Å and 3.0Å respectively for equatorial and axial. As can be seen the initial tendency is for both the equatorial and axial bonds to lengthen. However, the equatorial bond length reaches a maximum and then begins to shorten once more whilst the axial bond stretches more rapidly. At the limiting point of this calculation the axial bond has been stretched beyond the point that would be considered to be a bonding interaction and the equatorial and bonds approach the observed length in $CuCl_4^{2-}$ complexes. This suggests that within the constraints of the symmetry and the gas phase approximation, $CuCl_6^{4-}$ is unstable with respect to $CuCl_4^{2-} + 2Cl^-$. Evidence of this dissociation is shown by the charge distribution of the axial and equatorial chlorines at the end of the final cycle. The equatorial chlorines show a negative charge of -0.6137, whereas the axial values are -0.9998. This shows a distinct separation into the tetrachloro species and two chloride ions, and hence dissociation is seen to have occurred.

The changing nature of the metal-ligand interaction can be rationalised in terms of ligand to metal charge donation. Initially both the axial and equatorial bond lengths increase as towards the equilibrium bond lengths of the square planar complex (approximating this system to square planar $CuCl_4^{2-}$ and two distant chloride ligands). The equatorial bond length exceeds this value as charge donation to the

metal from the axial ligands is still weakly present. However, as the axial bond is stretched beyond the bonding limit the equatorial bond must shorten to provide the extra charge. The axial ligands are now non-bonded and the metal-ligand distance increases rapidly whilst the equatorial ligands converge towards the square planar limit.

Further calculations incorporating the gradient corrections of Becke and Perdew do not significantly improve this picture of bonding illustrating that the difficulty with this system is not in the poor treatment of long bonds but by the inherent instability of the $CuCl_6^{4-}$ complex in the gas phase.

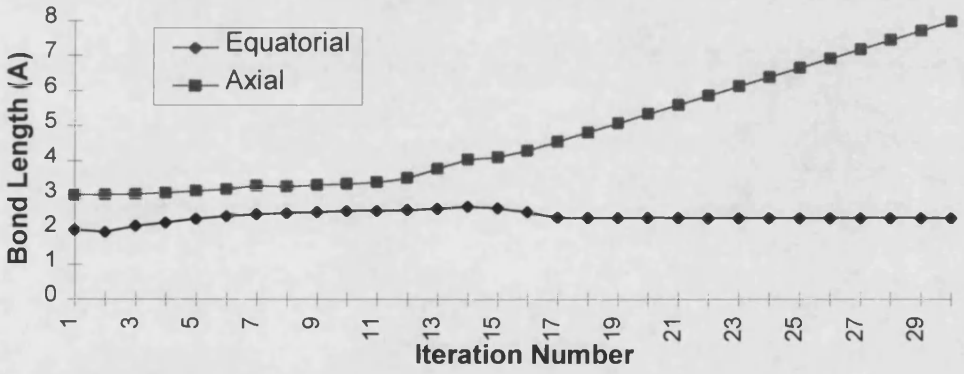

Figure 2.1: Variation of the axial and equatorial bond lengths of $CuCl_6^{4-}$ during geometry optimisation.

2.2.6.3 Conclusions

$CuCl_6^{4-}$ has been shown to be unstable in the gas phase with respect to dissociation to $CuCl_4^{2-}$. Geometry optimisations of complexes which are stabilised by the crystal environment may need to take into account the influence of the environment if accurate results are to be achieved. Of course this situation may be

prevented if by maintaining the symmetry of the system the pathway to the lower energy state is blocked.

The inclusion of gradient corrected functionals in these calculations does not significantly improve the treatment of this molecule as the problem is the instability of the system and not the nature of the long axial bonds.

2.2.7 Conclusions

The results presented above for the geometry optimisation of a series of chlorocuprates have produced a number of key points to use to obtain maximum accuracy:

a) Triple-ζ basis sets are generally more accurate than double-ζ (and generally lead to longer bond lengths) and do not lead to a significant increase in cost.

b) Polarisation functions should be used on all atoms, but it is not necessary for them to be true polarisation functions (i.e. of higher orbital angular momentum).

c) The frozen core approximation can produce accurate results and reduces cost but for 1st-row transition metals a frozen core of no larger than 2p should be used.

d) Spin restricted calculations are sufficient for d^9 systems, although systems with more unpaired electrons may be expected to require a spin unrestricted approach (see Chapter 3 for further investigation of this point).

These points should enable the accurate calculation of transition metal complex geometries to be made within the DFT formalism.

Difficulties have been found with both $CuCl_5^{3-}$ and $CuCl_6^{4-}$. In the former case the calculated geometries are found to significantly in error from the experimental

value. With the latter, a stable six co-ordinate structure is not found and dissociation occurs to a four co-ordinate species. This suggests that there is some source of error that increases with co-ordination number/charge. This may be a consequence of the neglect of the effects of the crystal environment and further investigation may be required to see whether the inclusion of some treatment of lattice effects improves these calculations.

2.3 Transition Energies of Chlorocuprates Using the DVXα Method

2.3.1 Introduction

The chlorocuprate systems, as stated above are found in a variety of co-ordination numbers and stereochemistries. They are also chemically and electronically simple with a d^9 electronic configuration with a single unpaired electron. Further they have also been the subjects of numerous theoretical and experimental investigations[1,2]. The absorption spectrum of these complexes can be divided into two regions. Firstly, a set of relatively weak, low-energy bands associated with Laporte-forbidden d-d transitions. Secondly, at higher energies a set of much more intense Laporte-allowed charge transfer (c.t.) transitions.

The Xα (or Hartree-Fock-Slater (HFS))[29] method is the simplest of the DFT methods. It has been shown relative to the HF method to give accurate results for a much reduced computational cost. Results are often in better agreement with experiment than corresponding HF calculations. Whether a theoretical method is capable of predicting transition energies is a good test of that particular method. The Xα transition state method (see below) provides a computationally inexpensive method for the calculation of transition energies. This all-electron method can, in principle, be used to study d-d and c.t. transitions simultaneously. However, since a one-electron, single-determinant gives an incomplete treatment of many-electron multiplet states, a direct comparison between calculated and experimental transition energies is only possible for d^1 and d^9 systems. Also, use of a spin-restricted formalism is justifiable for a system with only a single unpaired electron.

2.3.2 Computational Details

The details of the DVXα method[30] have been explained previously (see 1.2.3) so only a brief outline is presented here. The DVXα method uses Slater's exchange-correlation operator, $V_{X\alpha}$;

$$V_{X\alpha} = -3\alpha[(3/4\pi)\rho]^{1/3} \qquad (2.2)$$

Where α is an adjustable parameter and ρ is the charge density. This simple relationship facilitates the solution of the one-electron Schrödinger equation. A value of 0.7 for α has been found to give good results in a variety of calculations and is used throughout this work. The LDA value of α is 2/3, by using 0.7 instead includes some empirical treatment of correlation.

The Coulomb and exchange integrals are approximated numerically by the weighted summation over a three-dimensional grid of distinct points[30]. The number of sample points, N, can be varied to provide the required accuracy depending on the property being studied. In these calculations N is between 3000 and 4000. The distribution of points is such that approximately 1000 points are used for the central copper atom and the remainder shared equally among the chlorine ligands. Coulomb potentials are calculated via the self-consistent charge (s.c.c.) procedure[31] which provides a good approximation to the molecular potential particularly for heteropolar interactions like the Cu-Cl bond. The potential is constructed from the gross atomic orbital populations obtained from a Mulliken population analysis.

As a numerical method, the DVXα s.c.c. method is not restricted to analytical Gaussian or Slater basis sets. Any convenient radial functions may be used. A particularly compact set of double-ζ quality may be generated from accurate solutions of the atomic Schrödinger equation within the Xα approximation. However, only bound atomic functions have suitably contracted radial properties and there are relatively few of these for each atom. To increase the variational freedom of the molecular calculation the diffuse unbound functions can be localised by placing the atom in a local potential well. This approach has been taken previously by Deeth[32] where both ligand-field (d-d) and charge-transfer (c.t.) spectra have been calculated for a series of chlorocuprates.

The DVXα s.c.c. basis sets are optimised by performing a series of calculations starting with ionic basis sets. After each calculation the new Mulliken populations are used to construct new bases and the procedure is repeated until self consistency is reached. The advantage of this method is that it generates unique basis sets for each complex which are effectively optimised for each molecule.

Transition energies for d-d transitions are calculated via a simple difference in orbital energies, c.t. transition energies are calculated via the transition state approximation[33]. The calculation of transition energies can be made in a number of ways within a given computational method. Assuming the generation of molecular orbital energies is possible, then a simple difference between occupied and empty orbitals can be calculated. A second method, ΔSCF (Self Consistent Field), involves independent SCF calculations for the ground and excited states. The energy difference of these two states is the transition energy. Thirdly, Slater's

transition state approximation involves the excitation of half an electron to a higher energy orbital. The transition energy is a simple difference in the energies of these two orbitals. The first of these three methods ignores the effects of relaxation which occur when an electron is removed from an orbital and replaced in another, higher energy, orbital. This causes the remaining orbitals to decrease in energy due to the reduction in screening effects. The other two methods include some treatment of correlation. However, the advantage of the transition state approach is that only a single SCF calculation is required as opposed to the two required for the ΔSCF method. It has been shown[32] that for d-d transitions transition state calculations are unnecessary. Conversely, for c.t. spectra it is necessary, to give good splittings of the c.t. states.

For these calculations, unless stated, the basis sets used are of approximate double-ζ quality and near minimal basis sets: 1s-4p on copper and 1s-3p on chlorine. Of these, the copper 1s-3p and chlorine 1s-2p core orbitals are frozen and orthogonalised against the valence functions. Where these basis sets are altered in any way the alterations are reported in the text.

2.3.3 Results

Deeth[32] has previously used the DVXα method to calculate transition energies for chlorocuprates. A funnel potential of depth -2 a.u. at a radius of 4 a.u., decreasing linearly to zero at a radius of 6 a.u., was employed around each atom in order to localise the diffuse unbound functions as outlined above. This has led to good results for d-d transition energies, but c.t. energies differ from experimental results

by at least several thousand wavenumbers. In this work in order to improve on this method, the well potentials, and hence the basis sets, are optimised for a single chlorocuprate. Once both d-d transition energies and c.t. energies are well reproduced these values can be refined for a second member of the series and in an iterative way, a set of well parameters are sought that will allow a reasonable fit of experimental values for these species. This should allow further predictions about the transition energies of other members of the series to be made.

This investigation looks only at the two four-co-ordinate chlorocuprates, that is the square-planar (D_{4h}) and the distorted-tetrahedral (D_{2d}) cases. These two fairly similar systems enable the hypothesis that one set of well parameters should be sufficient for the chlorocuprates. The square-planar case was studied first and then the distorted-tetrahedral case followed. In both cases calculations were performed at the experimental geometry of the complex in question. The complexes chosen were for the D_{4h} system $[NMe(CH_2CH_2Ph)H_2][CuCl_4]$[34], and for the D_{2d} system $Cs_2[CuCl_4]$[35]. Geometric parameters for each of these complexes are:

Compound	Cu-Cl Bond Length (Å)	Cl-Cu-Cl Bond Angle (°)
$[NMe(CH_2CH_2Ph)H_2][CuCl_4]$ (D_{4h})	2.26	180.0
$Cs_2[CuCl_4]$ (D_{2d})	2.23	129.2

Table 2.5: Bond lengths and angles for $CuCl_4^{2-}$ (D_{4h} and D_{2d}).

Note that not all the results will be presented, as a large number of calculations were performed and only those meriting special explanation will be presented.

Initially square-sided potential wells were used so that the inner and outer radii were the same. It was found that the use of such wells tended to overestimate the $3a_{1g} \rightarrow 3b_{1g}$ transition by 3-8000cm^{-1} (c.20-50%) and at the same time the order of the two lowest energy d-d transitions ($2b_{2g} \rightarrow 3b_{1g}$ and $2e_{2g} \rightarrow 3b_{1g}$) was found to be reversed. Table 2.6 shows an example where such a result is found. Straight sided wells have been used with radii of 6a.u.

Transition	Calculated Energy		Experiment
	eV	cm^{-1}	cm^{-1}
$2b_{2g} \rightarrow 3b_{1g}$ (d-d)	1.7624	13924	12500
$2e_g \rightarrow 3b_{1g}$ (d-d)	1.6854	13594	14300
$3a_{1g} \rightarrow 3b_{1g}$ (d-d)	2.7019	21792	17000
$1a_{2g} \rightarrow 3b_{1g}$ (c.t.)	2.9841	24068	23700
$3e_u \rightarrow 3b_{1g}$ (c.t.)	3.5828	28897	26050
$2e_u \rightarrow 3b_{1g}$ (c.t.)	4.9986	40316	39040

Table 2.6: d-d and c.t. transition energies for $CuCl_4^{2-}$ (D_{4h}) (for experimental values see references 6 and 2d).

These results show that, in general, good agreement is found with experimental data. However, certain discrepancies are, as stated above, evident and it is necessary to improve the accuracy of all calculated values to bring them into line with experiment.

Transition	Calculated Energy		Experiment
	eV	cm^{-1}	cm^{-1}
$2b_{2g} \rightarrow 3b_{1g}$ (d-d)	1.5587	12572	12500
$2e_g \rightarrow 3b_{1g}$ (d-d)	1.7924	14457	14300
$3a_{1g} \rightarrow 3b_{1g}$ (d-d)	2.0247	16330	17000
$1a_{2g} \rightarrow 3b_{1g}$ (c.t.)	7.0421	59702	23700
$3e_u \rightarrow 3b_{1g}$ (c.t.)	7.7713	62680	26050
$2e_u \rightarrow 3b_{1g}$ (c.t.)	9.2157	74330	39040

Table 2.7: d-d and c.t. transition energies for $CuCl_4^{2-}$ (D_{4h}) (for experimental values see references 5 and 2d).

Transition	Calculated Energy		Experiment
	eV	cm^{-1}	cm^{-1}
$1a_{2g} \rightarrow 3b_{1g}$ (c.t.)	2.8120	22680	23700
$3e_u \rightarrow 3b_{1g}$ (c.t.)	3.2489	26204	26050
$2e_u \rightarrow 3b_{1g}$ (c.t.)	4.8033	38741	39040

Table 2.8: c.t. transition energies for $CuCl_4^{2-}$ (D_{4h}).

A number of approaches have been tested, from different well radii for copper and chlorine to introducing funnel-shaped wells and altering the well depth. The single factor that has characterised the failure in these calculations is that the $3a_{1g}$ level is calculated to be too low in energy. To correct this problem required some drastic alterations to the dimensions of the potential wells. By using funnel-shaped wells

of outer radius 3.5 a.u. and inner radius 1 a.u. for copper and 6 a.u. and 1 a.u. for chlorine (depth at outer radius 0 a.u., depth at inner radius -2 a.u.) it is possible to get good agreement with experiment for the d-d transitions (see Table 2.7).

Unfortunately the errors in the calculated c.t. transitions using these parameters were extremely large and in the order of 35000cm^{-1} (90-150%). This suggests that it is not possible to calculate d-d and c.t. transitions using the same parameters, which reinforces the result shown previously by Deeth[32]. However, it may be possible to calculate d-d and c.t. transitions separately. Table 2.8 shows results of c.t. bands calculated with straight-sided wells of radius 6 a.u. for copper and 4 a.u. for chlorine respectively. The values of the d-d transitions are omitted, but it is noted that again large errors were found for these.

Transition	Calculated Energy		Experiment
	eV	cm^{-1}	cm^{-1}
$5_e \rightarrow 4b_2$ (d-d)	0.6105	4924	4880
$2b_1 \rightarrow 4b_2$ (d-d)	0.8640	6969	7900
$4a_1 \rightarrow 4b_2$ (d-d)	1.0549	8508	9050
$1a_2 \rightarrow 4b_2$ (c.t.)	2.7541	22213	22700
$4e_u \rightarrow 4b_2$ (c.t.)	2.8627	23089	24730
$3e_u \rightarrow 4b_2$ (c.t.)	3.2908	26542	28880
$2e_u \rightarrow 4b_2$ (c.t.)	4.0341	32537	33480
$2a_1 \rightarrow 4b_2$ (c.t.)	5.2449	42303	43000

Table 2.9: d-d and c.t. transition energies for $CuCl_4^{2-}$ (D_{2d}).

Having established that it was possible to reproduce both the d-d and c.t. bands, albeit with separate well parameters, investigations were carried out to see if these results were transferable to the distorted-tetrahedral case. Table 2.9 shows the results of these calculations. Different well parameters for the d-d and c.t. bands have been used in these calculations and are as described above. It is seen quite clearly that the parameters obtained for the square-planar case give good agreement with the experimental values of the distorted-tetrahedral complex.

Finally, the occupations of the copper and chlorine valence orbitals are calculated for each of the two complexes and with each of the well parameter sets required for the d-d and c.t. transitions respectively.

	Copper			Chlorine	
	3d	4s	4p	3s	3p
D_{4h} d-d	9.219	0.464	0.480	1.974	5.736
D_{2d} d-d	9.167	0.452	0.567	1.970	5.733
D_{4h} c.t.	9.475	0.645	0.794	1.948	5.574
D_{4h} c.t.	9.456	0.567	0.816	1.953	5.588

Table 2.10: Valence orbital occupations for $CuCl_4^{2-}$ (D_{4h} and D_{2d}) for d-d and c.t. transitions.

2.3.4 Discussion

From the results that have been presented above it is quite clear that it is possible to reproduce separately the d-d and c.t. transitions for two different chlorocuprates by using separate well parameters for each type of transition. Results of this study

and other calculated results from various methods along with the experimental results are presented below for the d-d transitions of both systems.

$CuCl_4^{2-}$ (D_{4h})

Method	$2b_{2g} \rightarrow 3b_{1g}$	$2e_g \rightarrow 3b_{1g}$	$3a_{1g} \rightarrow 3b_{1g}$
Wolfsberg-Helmholz[8c]	5856	6887	9278
RHF[2a]	7500	9400	10100
UHF[9b]	7300	8500	9500
INDO[9b]	12950	14050	13080
MSXα (overlapping spheres)[2c]	14407	14788	17035
DVXα1[32]	13340	14032	17774
DVXα2[a]	12572	14457	16330
Experiment[2d]	12500	14300	17000

$CuCl_4^{2-}$ (D_{2d})

Method	$5e \rightarrow 4b_2$	$2b_1 \rightarrow 4b_2$	$4a_1 \rightarrow 4b_2$
Extended Hückel[8a]	8641	11521	12962
INDO[9b]	4622	6535	6852
MSXα (tangent spheres)[9b]	5500	11380	10850
MSXα (overlapping spheres)[2c]	5575	8946	9709
DVXα1[32]	5375	8125	9126
DVXα2[a]	4924	6969	8508
Experiment[5]	4800, 5550	7900	9050

Table 2.11: Comparison of calculated transition energies (cm^{-1}) from various methods with the present DVXα and experimental results. [a] - this work.

Comparing the results achieved using the DVXα and other methods (see Table 2.11), shows that the former method gives better agreement with experimental d-d transition energies than either the HF or MSXα approaches. It can be clearly seen that the extended Hückel, HF (both spin-restricted (RHF) and spin-unrestricted (UHF)) and the Wolfsberg-Helmholz give poor agreement with experiment. The MSXα and INDO methods give results numerically comparable with experiment but with the incorrect assignment. The HF results are assigned correctly but the observed values are about 40% lower than observed. With the DVXα method it appears that it is possible to reproduce accurately the transition energies, to within $1000cm^{-1}$ or 12%, and the their assignments. It is possible to vary the well parameters used in the calculations and obtain a fit of equal quality. This suggests some flexibility that may become important when transferring these parameters to other systems.

The calculation of c.t. transitions by this method is shown to be accurate in terms of both the energy of the transition and its assignment when compared to experimental values. Absolute errors are in all cases less than $2500cm^{-1}$ (less than 9%). This compares favourably with other methods which tend to over or underestimate considerably. In some cases the assignment of these transitions is also incorrect. Significantly the results presented here are nearer the experimental values than those reported by Deeth[32] ,who used the same well parameters for both d-d and c.t. transitions within the DVXα method.

Of further interest is to examine the orbital occupations of the valence copper and chlorine orbitals, especially how they vary as the well parameters (and hence basis

sets) are altered to reproduce d-d transitions as opposed to those required for the c.t. transitions, see Table 2.10. Quite clearly, there is a significant change in orbital occupation with the two well types. The more constrained wells required for the d-d transitions cause a greater amount of charge to reside on the chlorines than is found in the more open wells used for the c.t. transitions. This is what would be expected intuitively as no electron transfer from ligand orbitals to metal orbitals occurs during d-d transitions. Whereas during c.t. transitions electron density is removed from essentially ligand-based orbitals to metal-based orbitals so there is a build up of charge in the metal valence orbitals. The tighter well conditions required for d-d transitions are unsuitable for c.t. transitions as the orbitals are tightly constrained around each atom and hence transfer to a second atom is less facile. This raises the question as to whether it is possible to treat both phenomena simultaneously. A lack of freedom in the d-orbital basis sets (as d-orbitals are involved as acceptors and donors) prevents a good description of both d-d and c.t. transitions. Introducing a greater degree of flexibility, i.e. more d-orbital exponents, in the same basis sets will allow a more complete treatment of ground and excited states at the same time. This will hopefully allow a simultaneous treatment of both d-d and c.t. spectra.

Deeth[32] has shown for a series of chlorocuprates that the difference between calculated and observed c.t. energies increases as a function of molecular charge. The use of embedded clusters to model the crystal environment may be able to overcome this systematic error. The inclusion of a set of point charges around the complex to reflect the environment will have the effect of altering the orbital energies within the complex. The ligand orbitals will be more susceptible to this

field because of their closeness as compared with the central copper atom that is more distant and also shielded by the ligand atoms. Therefore, the effect will be minimal in the d-d transitions since the d-orbitals are metal based and largely unaffected, but much more significant for the c.t. transitions that involve the ligand orbitals as well.

2.3.5 Conclusions

The DVXα method has been shown to be quite capable of reproducing electronic transitions of chlorocuprates in terms not only of the transition energies but also of their assignments. Separate treatments are necessary for d-d transitions and c.t. transitions, although this may be due to inflexibility in the d-orbital bases. Better agreement with experiment is found using this method than with other one-electron m.o. approaches. Absolute errors are less than $1000cm^{-1}$ for d-d transitions and less than $2500cm^{-1}$ for c.t. transitions (relative errors are respectively less than 12% and less than 9%). The use of independently optimised wells may be compensating for lattice effects that are not explicitly treated by any of these methods. Further optimisation of basis sets, by the use of different well potentials could be expected to reduce these errors still further. Transition state calculations are found to be unnecessary for d-d transitions but are essential for an accurate treatment of c.t. transitions.

It was hoped that a simultaneous treatment of all transitions would be possible. This has proved unsuccessful here as found previously. Greater flexibility in the d-orbital basis or the use of embedded clusters may yet solve this problem.

By introducing different ligand types parameter sets could be obtained for a variety of ligands. If it can be shown reliably that a single set of well parameters can be used for a single ligand type then the only variable that would affect the electronic spectra of the system will be its geometry. This point has been shown here as it has proved possible to reproduce the transition energies of two complexes with the same ligands but in different geometries with the same well parameters although it is quite possible that the same atom type may need different parameters depending on its functionality. For example a nitrogen atom of an imidazole may need different parameters from an amine nitrogen. Once other ligands have been parameterised it would be possible to apply this method to the elucidation of the structures of biological systems. These systems usually have well defined electronic spectra and EXAFS can often determine metal-ligand distances. So by using predetermined parameters for the well potentials the geometry could be varied until the experimental spectrum is reproduced. This method would not be capable of delivering the same accuracy as crystallographic studies but since obtaining structures of the metal centre in these systems is at best difficult it should prove to be a helpful tool in calculating approximate geometries. A similar method could be envisaged using the Cellular Ligand Field model of Gerloch and Woolley[36], however this method can only calculate d-d transitions and so may be limited by a lack of experimental data that would be less likely to effect this method based on both the d-d and c.t transitions.

The development of such a method will require further work but it may prove to be a useful tool in the elucidation of molecular structure. Compared to other

computational methods, such as the LDA, this method would be computationally less expensive and would also have the advantage that any *ab initio* method would have to introduce approximations into calculations in order to represent the influence of the surrounding ligands on the molecular structure as full geometry optimisations would be prohibitively expensive.

References

1. K.E.Halvorson, C.Patterson and R.D.Willett, *Acta. Cryst.*, 1990, **B46**, 508.

2. (a) J.Demuynck, A.Veillard and U.Wahlgren, *J. Am. Chem. Soc.*, 1973, **95**, 5563. (b) R.G.McDonald, M.J.Riley and M.A.Hitchman, *Inorg. Chem.*, 1988, **27**, 894. (c) A.Bencini and D.Gatteschi, *J. Am. Chem. Soc.*, 1983, **105**, 5535. (d) S.R.Desjardins, K.W.Penfield, S.L.Cohen ,R.Musselman and E.I.Solomon, *J. Am. Chem. Soc.*, 1983, **105**, 4590.

3. (a) R.B.Bereman, M.R.Churchill and G.Shields, *Inorg. Chem.*, 1979, **18**, 3117. (b) J.Van Rijn, W.L.Driessen, J.Reedijk amd J.-M.Lehn, *Inorg. Chem.*, 1984, **23**, 3584. (c) T.Sakurai, S.Suzuki and A.Nakahara, *Bull. Chem. Soc. Jpn.*, 1981, **54**, 2313. (d) R.H.Petty and L.J.Low, *J. Chem. Soc. Chem. Comm.*, 1978, 483.

4. (a) E.I.Solomon, J.W.Hare, D.M.Dooley, J.H.Dawson, P.J.Stephens and H.B.Gray, *J. Am. Chem. Soc.*, 1980, **102**, 168. (b) E.I.Solomon, J.W.Hare and H.B.Gray, *Proc. Natl. Acad. Sci. U.S.A.*, 1976, **73**, 1389.

5. J.Ferguson, *J.Chem.Phys.*, 1964, **40**, 3406.

6. M.A.Hitchman and P.J.Cassidy, *Inorg.Chem.*, 1979, **18**, 1745.

7. (a) P.Day, *Proc.Chem.Soc*, 1964, 18. (b) W.E.Hatfield and T.S.Piper, *Inorg.Chem.*, 1964, **3**, 841. (c) D.W.Smith, *J.Chem.Soc.A*, 1969, 1529. (d) D.W.Smith, *Ibid.*, 1970, 2900. (e) D.W.Smith, *Inorg.Chim.Acta.*, 1977, **22**, 107.

8. (a) L.L.Lohr and W.N.Lipscomb, *Inorg.Chem.*, 1963, **2**, 911. (b) P.Day and K.C.Jorgensen, *J.Chem.Soc.*, 1964, 6226. (c) P.Ros and G.C.A.Schuit, *Theor.Chim.Acta.*, 1966, **4**, 1.

9. (a) K.H.Johnson and U.Wahlgren, *Int. J. Quantum Chem., Quantum Chem. Symp.* 1972, **6**, 243. (b) P.Correa de Mello, M.Hehenberger, S.Larsson and M.Zerner, *Ibid.*, 1980, **102**, 1278. (c)M.Barker, J.D.Clark and A.Hinchcliffe, *J. Chem. Soc., Faraday Trans. II*, 1978, **74**, 681

10. H.Johansen and N.K.Anderson, *Mol. Phys.*, 1986, **58**, 965.

11. E. J. Baerends D. E. Ellis and P. Ros, *Theoret. Chim. Acta*, 1972, **27**, 339.

12. E. J. Baerends D. E. Ellis and P. Ros, *Chem. Phys.*, 1973, **2**, 41.

13. J.G.Snijders, P.Vernooijs and E.J.Baerends, *At. Data. Nucl. Data. Tables*, 1981, **26**, 483.

14. O.Gunnarsson and I.Lundquist, *Phys. Rev.*, 1976, **B13**, 4274.

15. (a) P.Pulay, *Chem. Phys. Lett.*, 1969, **17**, 197. (b) J.Pople, R.Krishnan, H.B.Schlegel and J.S.Binkley, *Int. J. Quantum. Chem.*, 1978, **S12**, 169.

16. S.J.Vosko, L.Wilk and M.Nussair, *Can. J. Phys.*, 1980, **58**, 1200.

17. H.Stoll, E.Golka, H.Preuss, *Theor. Chim. Acta*, 1978, **49**, 143.

18. B.Delley and D.E.Ellis, *J. Chem. Phys.*, 1982, **76**, 1949.

19. J.Li, G.Schreckenbach and T.Ziegler, *J. Phys. Chem.*, 1994, **98**, 4838.

20. C.W.Bauschlicher and O.B.Roos, *J. Chem. Phys.*, 1989, **91**, 4785.

21. E.J.Baerends and M.A.Buisje, *Theor. Chim. Acta.*, 1991, **79**, 389.

22. J.Westbrook and K.Krogh-Jespersen, *Int. J. Quantum. Chem.*, 1988, **22**, 245.

23. K.Waizumi, H.Masuda, H.Einaga and N.Fukushima, *Chem. Lett.*, 1993, 1145.

24. (a) M.Atanasov, W.Konig, R.Craubner and D.Reinen, New J. Chem., 1993, 17, 115. (b) L.Antolini, G.Marcotrigiano, L.Menabue and G.C.Pellacani, *J. Am. Chem. Soc.*, 1980, **102**, 1303.

25. M.Studer, A.Riesen and T.A.Kaden, *Helv. Chim. Acta.*, 1989, **72**, 1253.

26. D.Reinen and C.Freibel, *Struct. Bonding (Berlin)*, 1979, **37**, 1.

27. A. J. Becke, *Chem. Phys.*, 1986, **84**, 4524.

28. J. P. Perdew, *Phys. Rev.*, 1986, **B33**, 8822.

29. (a) J.C.Slater, *Adv. Quantum Chem.*, 1972, **6**, 1. (b) J.C.Slater and K.H.Johnson, *Phys. Rev. B*, 1972, **5**, 844.

30. D.E.Ellis and G.S.Painter, *Phys. Rev. B*, 1970, **2**, 2887.

31. A.Roser, D.E.Ellis, H.Adachi and F.W.Averill, *J. Chem. Phys.*, 1976, **65**, 3629.

32. R.J.Deeth, *J.Chem. Soc. Dalton*, 1990, 355.

33. J.C.Slater, *Quantum Theory of Molecules and Solids*, McGraw-Hill, U.S.A., 1974, vol. 4.

34. R.L.Harlow, W.J.Wells (III), G.W.Watt and S.H.Simonsen, *Inorg. Chem.*, 1974, **13**, 2106.

35. J.A.McGinnety, *J. Am. Chem. Soc.*, 1972, **94**, 8406.

35. (a) M.Gerloch, "*Magnetism and Ligand Field Analysis*", Cambridge University Press, 1984. (b) M.Gerloch, J.H.Harding and R.G.Woolley, *J. Chem. Soc. Dalton Trans.*, 1981, 1714. (c) M.Gerloch and R.G.Woolley, *Inorg. Chem.*, 1984, **23**, 3853, *ibid.*, 1985, **24**, 4490.

Chapter 3

Molecular Properties of Transition Metal Tetrachlorides

3.1 Introduction

In the previous chapter it was shown that DFT was capable of modelling both the structural and electronic properties of transition metal complexes accurately and efficiently. Comparisons between other methods, in particular HF were shown to be favourable. Conclusions drawn from the studies of chlorocuprates are employed in this chapter and applied to a wider range of complexes, that is 1st-row transition metal tetrachlorides. These complexes are relatively simple and have attracted a great deal of attention from the theoretical chemist[1]. However, the majority of studies have centred on electronic structure and bonding and neglect any optimisation of geometry. This may be due to the suspicion that the crystal environment will have a significant effect on molecular geometries. The calculations presented below are all made in the gas phase with no attempt to model the crystal environment.

In comparison with the tetrachlorocuprates that were investigated in Chapter 2, the tetrachlorides of the other elements of the first transition series are found in much more regular stereochemistries. According to ligand field theory[2], the set of d-orbitals in a regular tetrahedral field splits into a doublet e orbital (d_{z^2} and $d_{x^2-y^2}$) and

a triplet t_2 orbital (d_{xy}, d_{xz} and d_{yz}). However, the Jahn-Teller effect[3] predicts that the most stable configurations of the tetrahedral complexes of Cr^{2+} (d^4), Fe^{2+} (d^6), Ni^{2+} (d^8) and Cu^{2+} (d^9) in the high spin state will be distorted tetrahedral. Weak-field ligands such as chloride, in a tetrahedral environment, will always give a high-spin state because of the relatively low promotion energy compared to the cost of pairing electrons in the same orbital (electronic repulsion). In the case of Cr^{2+} and Cu^{2+}, the tetrahedral complexes should be flattened, where the d_{xy} orbital is destabilised and the d_{xy} and d_{yz} orbitals are stabilised. Whereas for Ni^{2+} the tetrahedron will be elongated along an S_4 axis where the d_{xy} orbital is destabilised and the d_{xz} and d_{yz} orbitals are stabilised. The Jahn-Teller effect cannot predict whether the flattened or elongated tetrahedron is the more stable configuration for Fe^{2+}.

Experimental structures are known for the entire series[4], with the exceptions of chromium and scandium. These are of the $[M^{II}Cl_4]^{2-}$ formula apart from vanadium and titanium (M^{IV}). In addition, the $Fe^{III}Cl_4^-$ complex is also known[4b]. As predicted by the Jahn-Teller effect, the structures of the Ni^{2+}, Cu^{2+} and Fe^{2+} species are distorted tetrehedra whilst the remainder of the series are regular tetrahedra (*vide infra*).

D-electron configurations of these complexes range from d^0 (Ti^{IV}) to d^{10} (Zn^{II}) and consequently the number of unpaired d-electrons varies from 0 (Ti^{IV} and Zn^{II}) to 5 (Mn^{II} and Fe^{III}). Therefore the inclusion of spin-unrestricted calculations is expected to be necessary, the more unpaired electrons the greater the effect.

It is also been suggested that for an accurate treatment of transition metal complexes it may be necessary to include gradient corrections to the functionals employed in the LDA[5]. The nature of these gradient corrected functionals and the fact that they were derived from atomic properties, might lead to difficulties when applied to these transition metal complexes.

3.2 Computational Details

The computational details were as described in detail in section 2.2.2. Alterations to the computational procedure were as follows. Firstly, from the results of the previous chapter the frozen core approximation was used, however cores were frozen only to the 2p level for both the metal and chlorine. Polarisation functions were employed as additional functions in all basis sets; these functions were an extra p function for the metals and a d function for chlorine.

As was outlined above calculations were carried out with both spin-restricted and spin-unrestricted formalisms i.e. up-spin and down-spin electrons are treated differently in the spin-unrestricted formalism.

Finally, the gradient corrected functionals of Becke[6] and Perdew[7] were used to modify the potential generated within the LDA.

3.3 Results and Discussion

Results are presented for geometry optimisation calculations for the series of complexes of the formula $M^nCl_4^{(4-n)-}$, where M is a transition metal of the 1st series and n is the oxidation state of that metal. The range of complexes covered here are

those where M is Ti^{IV}, V^{IV}, Mn^{II}, Fe^{III}, Fe^{II}, Co^{II}, Ni^{II} and Zn^{II}. No tetrachloro species is known for either chromium or scandium. As the aim of this work is to investigate the accuracy of DFT calculations on transition metal systems and to investigate the properties of the complexes studied no calculations were made on these two species.

Calculations were generally constrained to tetrahedral. Those complexes that are Jahn-Teller active, Fe^{II} and Ni^{II}, are additionally modelled with reduced symmetry (C_2) allowing the structure to deviate from tetrahedral symmetry. This will confirm whether the DFT model is capable of accounting for Jahn-Teller distortions or not. Certainly these deviations are not comparable to those exhibited by the d^9 Cu^{II} complexes. Those complexes that are not expected to show a Jahn-Teller distortion have been modelled with rigorous tetrahedral symmetry only.

Although the structures of these complexes all approximate to tetrahedral geometry and are less varied than those of $CuCl_4^{2-}$ there is still some variation depending on crystal forces. In most cases the average of a number of structures is taken as the experimental value. Experimental bond lengths and the number of structures from which they were derived (in parentheses) are as follows; Ti 2.17Å[4c] (1), V 2.14Å[4c] (1), Mn 2.35Å[4a] (3), Fe^{III} 2.19Å[4b] (4), Fe^{II} 2.31Å[4a] (8), Co 2.27Å[4a] (36), Ni 2.26Å[4a] (5) and Zn 2.27Å[4a] (55).

The results presented below show the effect of basis set, spin polarisation and gradient corrected functionals on geometry (Tables 3.1 and 3.2), atomic charge (Table 3.4), d-orbital population (Table 3.5) and Δ_{tet} values (Tables 3.6 and 3.7).

Looking at the geometries first, and in this case because the angles are fixed at the tetrahedral values, the only variables are the metal-chlorine bond lengths.

	Dzpr	Dzpu	Tzpr	Tzpu	Expt.
$TiCl_4$	2.16	2.16	2.16	2.16	2.17
VCl_4	2.12	2.12	2.11	2.12	2.14
$MnCl_4^{2-}$	2.31	2.37	2.30	2.36	2.35
$FeCl_4^{-}$	2.17	2.20	2.17	2.19	2.19
$FeCl_4^{2-}$	2.28	2.32	2.27	2.31	2.31
$CoCl_4^{2-}$	2.26	2.28	2.25	2.27	2.27
$NiCl_4^{2-}$	2.27	2.28	2.26	2.27	2.26
$ZnCl_4^{2-}$	2.32	2.32	2.32	2.32	2.27
Av. Error	0.024	0.019	0.028	0.013	-
RMS Error	0.024	0.008	0.011	0.007	-

Table 3.1: Comparison of calculated bond lengths using different basis sets and the effect of spin-polarisation (Å). All calculations using Local Density Approximation (LDA). Basis sets: Dzpr - double-ζ with polarisation function spin restricted, Dzpu - double-ζ with polarisation function spin unrestricted, Tzpr - triple-ζ with polarisation function spin unrestricted, Tzpr - triple-ζ with polarisation function spin unrestricted.

The results obtained from the LDA are, in general, in very good agreement with experimental values despite the approximations that are inherent not only within the LDA method itself but also in the way in which it has been applied here, particularly the imposed symmetry constraints and the neglect of the crystal environment. Average errors are not larger than 0.03Å regardless of basis set and the maximum single error is found for $ZnCl_4$ at 0.05Å (for all basis sets). In comparison, the inclusion of gradient corrected functionals (Table 3.2) causes a

dramatic lengthening of bonds by as much as 0.08Å leading to an overestimation of bond lengths.

	Dzpr	Dzpu	Tzpr	Tzpu	Expt.
$TiCl_4$	2.19	2.19	2.18	2.18	2.17
VCl_4	2.15	2.15	2.14	2.15	2.14
$MnCl_4^{2-}$	2.38	2.45	2.37	2.43	2.35
$FeCl_4^{-}$	2.22	2.18	2.21	2.23	2.19
$FeCl_4^{2-}$	2.35	2.39	2.34	2.38	2.31
$CoCl_4^{2-}$	2.33	2.36	2.32	2.35	2.27
$NiCl_4^{2-}$	2.34	2.35	2.33	2.34	2.26
$ZnCl_4^{2-}$	2.38	2.38	2.37	2.37	2.27
Av. Error	0.048	0.064	0.038	0.059	-
RMS Error	0.028	0.024	0.017	0.022	-

Table 3.2 Comparison of calculated bond lengths using different basis sets and the effect of spin-polarisation (Å). All calculations with gradient corrected functionals. Basis sets: Dzpr - double-ζ with polarisation function spin restricted, Dzpu - double-ζ with polarisation function spin unrestricted, Tzpr - triple-ζ with polarisation function spin unrestricted, Tzpr - triple-ζ with polarisation function spin unrestricted.

Average errors are now in the region of 0.04-0.07Å which is, significantly, worse than the worst results achieved with the LDA. It has been proposed that it may be necessary to include gradient corrected functionals for the accurate calculation of molecular geometries of transition metal systems[5]. However the results presented here indicate that this is not so, the LDA geometries being far more in agreement than when the gradient corrected functionals are included. A number of considerations can be taken into account when viewing this situation. Firstly, the inclusion of crystal forces might be expected to alter the geometry of these

complexes. Unfortunately, it is not possible to attribute a value on the size of this effect without having experimental values for the same molecule in the solid and gas phases. Gas phase structures are not available for the complexes studied and so the effects of the lattice are, at present, indeterminable.

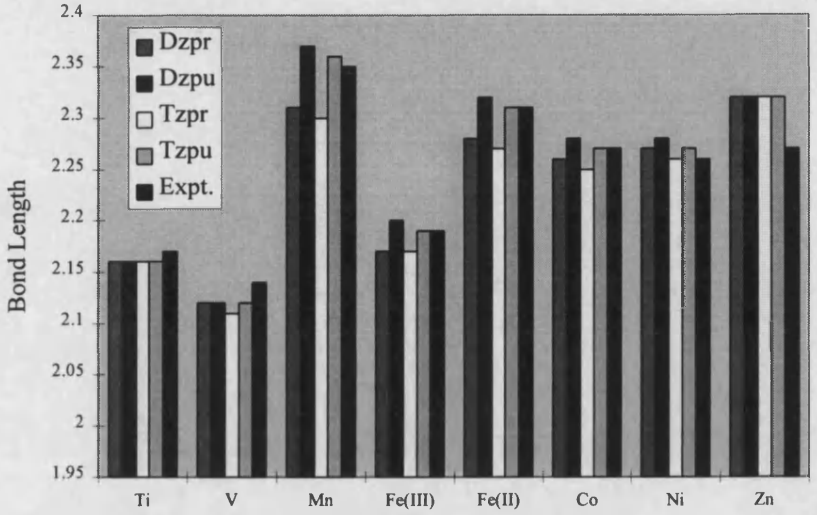

Figure 3.1: Calculated bond lengths (Å) using the LDA showing the effect of spin-polarisation and basis set size.

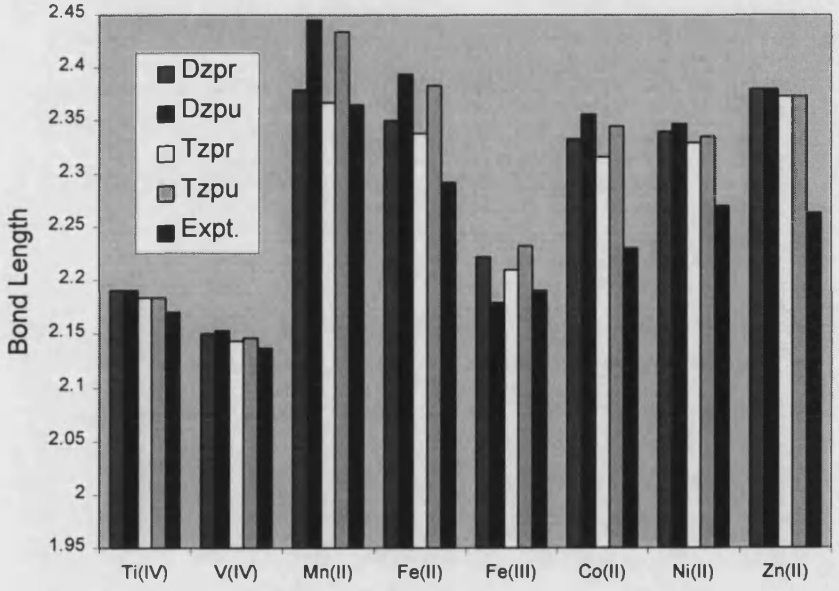

Figure 3.2: Calculated bond lengths (Å) using gradient corrected functionals showing the effect of spin-polarisation and basis set size.

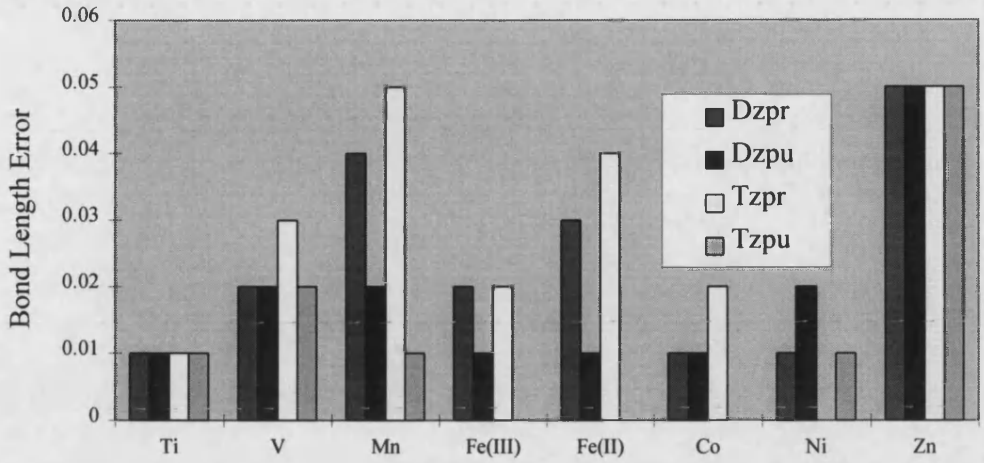

Figure 3.3: Errors in calculated bond lengths (Å) using the LDA showing the effect of spin-polarisation and basis set size.

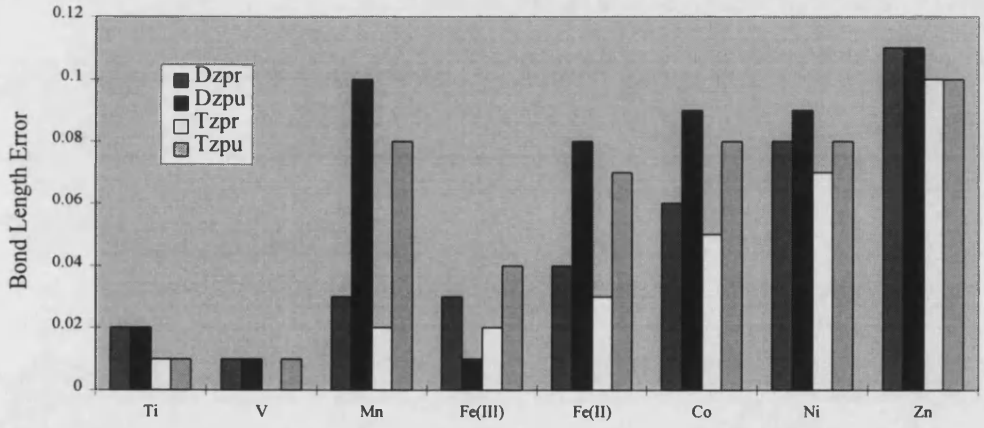

Figure 3.4: Errors in calculated bond lengths (Å) using gradient corrected functionals showing the effect of spin-polarisation and basis set size.

The problem may lie in the fact that the LDA is derived from the homogeneous electron gas where the electron density is constant across the whole system. Therefore, it will be best suited to treating systems in which similar behaviour is exhibited. Few real systems have a constant electron density (bulk metals are an example) but the nearer a system is to this ideal the more accurate LDA calculations should be. Complexes with a slowly varying electron density gradient may be good approximations to the homogeneous electron gas. This situation is typical of complexes with covalent bonding such as organometallic species. Hence, it would be expected that for such systems the LDA would give a reasonable treatment of geometries but that the inclusion of gradient corrected functionals would lead to an improvement in line with experimental values (see below). The gradient corrected functionals were originally designed to improve binding energies calculated by the LDA method. The LDA tends to calculate binding energy values that are too high[8], i.e. the bonds are too strong and strong bonds are shorter than weak bonds (relative to the same bond type). Hence, it has been shown that the LDA tends to underestimate bond lengths. The inclusion of the gradient corrections to both the exchange and correlation energies leads to a better treatment of binding energies[8,9] (lower values) and hence the calculated bond lengths are also improved. The nature of the way in which the gradient corrections improve the picture of bonding has been analysed by Baerends and Van Leeuwen[10]. The correction to the exchange energy is larger (and opposite in sign) to the correlation correction term, and so dominates the effects of the latter. The influence of the exchange correction is important in the tail of the valence density where the local exchange hole

incorrectly has its maximum around the reference electron rather than at larger values of the inter-electron distance. On bond formation, parts of the valence tail disappear as the two atoms are brought together. As a consequence this correction is more important (stabilising) in the constituting atoms than when the bond has been formed. Thus, the overall influence of the exchange correction is to reduce the binding energy and as a consequence lead to an increase in bond lengths.

This situation is illustrated by comparing calculated molecular geometries of some organometallic species using various methods[5,17,18] (Table 3.3). Comparing the results achieved with these methods with the experimental values shows that the Hartree-Fock (HF) method gives poor agreement with experiment, bond lengths being always too long and in error by as much as 0.25Å. As expected the Hartree-Fock-Slater and Local Density Approximation (LDA) methods give very similar results that are a significant improvement on the HF values but still too short by as much as 0.05Å. Finally the LDA with gradient corrections to exchange and correlation (LDA/GC) are in excellent agreement with the experimental values and the errors are only of the order of 0.01Å or less. Therefore to model accurately the geometries of transition metal organometallic complexes it appears that gradient-corrected functionals are essential to correct the shortcomings of the LDA.

However, for Werner-type complexes, such as are presented here, it appears that the situation is not the same as that found for organometallic complexes. The difference can be attributed to the differences in bonding in these two types of systems. The more ionic nature of the bonding in Werner-type complexes should be poorly treated by methods that are developed from the uniform electron gas such as

the LDA. However, the results presented here do not reflect this, in fact the opposite situation is found, where LDA results are good and those with gradient corrected functionals are less so. On first examination this appears to show that the uniform electron gas is not a poor approximation to ionic systems. This is counter-intuitive and suggests that there is an additional factor to consider. The apparent accuracy of the geometries calculated in this work for Werner-type complexes may be as the result of a fortuitous cancellation of errors.

Complex	Bond	Method[a]				Experiment[a]
		HF	HFS	LDA	LDA/GC	
$Fe(CO)_5$	$Fe\text{-}C_{ax}$	2.047	1.774	1.769	1.819	1.807
	$Fe\text{-}C_{eq}$	1.874	1.798	1.766	1.817	1.827
$Fe(C_5H_5)_2$	Fe-C[b]	1.88	1.60	-	-	1.65
$HCo(CO)_4$	$Co\text{-}C_{eq}$	2.02	1.753	-	-	1.764
	$Co\text{-}C_{ax}$	1.96	1.779	-	-	1.818
$Cr(CO)_6$	Cr-C	-	1.868	1.862	1.917	1.918
$Ni(CO)_4$	Ni-C	1.921	1.805	1.781	1.844	1.838

Table 3.3: Comparison of bond lengths (Å) calculated by various methods (see text for details) with experimental values for some organometallic complexes .
[a] references 5, 17, 18 and references cited therein.b distance from Fe to middle of plane of Cp ring.

As stated above, the LDA is expected to be most accurate for a system in which the electron density is slowly varying, and even though in such cases the treatment gives reasonable bond lengths they are found to be too short by 0.04-0.06Å. Inclusion of gradient corrected functionals reduces this error to 0.01Å or less. If the LDA is capable of calculating bond lengths only to this level of accuracy for

complexes to which it is best suited then it would be expected that, for complexes where the approximation is even less valid, the agreement would be worse. Therefore, there must be a further error in the LDA. The nature of this error is not currently apparent and further investigation is required to determine its source and magnitude. However, it is also apparent that the gradient corrected functionals still lead to a general increase in bond lengths over those calculated using the LDA. The fact that the inclusion of the corrections leads to bond lengths that are longer than experiment is not an indication that they are not required or incorrect (although some alteration may be required for ionic species) but that they are correcting what is already a relatively poorer approximation (the LDA). This may seem contradictory in that the LDA, from calculated values, does not appear to be a poor approximation at all to ionic systems. However, the results generated with the LDA for these ionic species must be treated with some caution as it cannot accurately represent the electron density in ionic systems. There must be some form of systematic error that cancels out the errors that are introduced by the use of the homogeneous electron gas.

Many *ab initio* calculations on metal species concentrate on closed shell diamagnetic species or treat paramagnetic molecules using a spin-restricted method. The latter approximation minimises the effects of spin contamination. The effects of spin contamination are caused by the mixing of states of higher spin multiplicity into the ground state. This leads to a decrease in energy of the system and unrealistic spin densities. The value of the spin operator $\langle S^2 \rangle$ is found to be greater than the expectation value for a given spin multiplicity. Although spin

contamination has been shown to be a problem for unrestricted Hartree-Fock (UHF) calculations[11], recent work by Andzelm *et al.*[12] shows that, for density functional theory, the effect is significantly reduced primarily by an improved treatment of the exchange term.

Studies of the chlorocuprates in Chapter 2 have shown that spin-unrestricted calculations do not have significant effects on molecular geometries. Other studies on $[MO_4]^{2-}$ (M=Cr, Mn and Fe) complexes[13] confirm these results. However, these systems have, at most, only two unpaired electrons and, in the case of the oxo-species, the high covalency further diminishes any spin polarisation effects. The complexes presented in this work have a variety of numbers of unpaired electrons and so it is possible that they may be affected more by the inclusion (or neglect) of spin polarisation.

The effect of spin-polarisation on geometries is considerable, causing a systematic lengthening of metal-ligand bonds by as much as 0.07Å compared to the equivalent spin-restricted calculations. However, the effect is not uniform and is most pronounced for manganese and has no effect for titanium and zinc. This correlates well with the number of unpaired electrons in each system; Manganese having five and titanium and zinc each having none. A spin-restricted calculation implies that the (spatial) orbitals and the occupation numbers are identical for spin-α and spin-β respectively. In an unrestricted calculation the orbitals may be different (i.e. different linear combinations of the same set of basis functions).

The exchange energy term is expressed as a function of the number of unpaired electrons. Therefore the more unpaired electrons the more stabilising is the

exchange energy. The size of the metal based orbitals can be significantly affected by the inclusion of spin polarisation effects. With a spin restricted approach there is an averaging of α and β electrons so that the orbitals are identical in size. When spin polarisation is introduced, α and β are treated separately. This leads to a relative reduction in size of the majority spin orbitals and an expansion of the ones describing the minority spins. The difference depends on the number of electrons involved, and, for these chloro complexes , is largest in the d-orbitals because this is where most of the spin density is found. The M-Cl overlap in the spin polarised case is reduced because more electrons are in the contracting orbitals than in the expanding ones. If the overlap is reduced then the binding energy will also be reduced and this leads to increased bond lengths. This effect will be most pronounced with a large number of unpaired electrons (Mn^{II}) .Conversely there will be no effect where α- and β- spin populations are equal (Zn^{II}). This correlation between number of unpaired electrons and the relative increase in bond length from spin polarisation is exactly what is observed.

The effect of basis set size has also been investigated and the results presented above show the differences in geometries calculated with double-ζ and triple-ζ basis sets (polarisation functions are included in all cases). As expected the triple-ζ basis set gives a more accurate geometry, although the difference between the average errors are only in the region of 0.005-0.010Å for equivalent calculations with the different basis sets. Using the LDA with the triple-ζ basis set and with spin polarisation gives average errors in bond lengths of only 0.013Å (RMS error 0.006Å), this is approximately half the size of the error found when spin

polarisation is not included. The results calculated with the inclusion of gradient corrections show average errors of 0.03-0.07Å, significantly worse than LDA calculations and in all cases the bond lengths are increased so that they are always too long. Therefore, the LDA is seen to give accurate geometries when combined with a triple-ζ basis set and the inclusion of spin polarisation (although the latter is only necessary for species containing more than two unpaired electrons).

Finally, the complexes $[FeCl_4]^{2-}$ and $[NiCl_4]^{2-}$ are known to be susceptible to a Jahn-Teller distortion although the calculations presented above have not allowed for this possibility. In order to investigate whether the DFT method is capable of reproducing these effects optimisations of these complexes were carried out in much lower symmetry (C_2). This symmetry allows a greater variation of geometries but still maintains enough symmetry to specify the occupation of the correct d-orbitals easily. Introducing these symmetry constraints represents an approximation in that all degrees of freedom should be allowed so that the potential energy surface can be explored completely, However, Waizumi *et al.*[15] have shown for similar calculations that the removal of all symmetry restraints leads to bond lengths and angles that are equivalent in these calculations to within 0.01Å and 0.1° respectively. All bond lengths are kept equivalent but the angles are allowed to vary to allow the flattening or elongation of each complex. Calculations were performed using the LDA with triple-ζ basis sets and spin-polarisation.

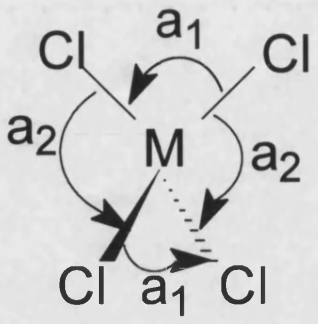

Figure 3.5: Definition of bond angles for MCl_4 complexes.

The results show that the iron complex is a flattened tetrahedron with bond lengths of 2.32Å and the angles a_1 118.7° and a_2 105.1° respectively This compares to experimental values of 2.31 and 103-121°Å[4a], and 2.31Å and 112°(a_1) and 108°(a_2) calculated by Waizumi *et al.*[4a] using the local spin density method with Gaussian-type basis sets. The reverse distortion is seen for the nickel complex with the bond lengths of 2.26Å and the angles a_1 98.6° and a_2 115.2° respectively (see Figure 3.5 for definitions of angles a_1 and a_2). Again comparisons with experimental data[4a] (bond length 2.26Å, bond angles 103-114°) and calculated values[4a] (bond length 2.26Å, a_1 97°, a_2 116°) are favourable.

This shows that DFT is capable of reproducing the Jahn-Teller effect in these complexes and also that bond lengths do not change significantly when Jahn-Teller effects are incorporated.

Gross atomic charges computed from Mulliken analyses for both the metal and chlorine of all the species studied are presented in Table 3.4. Calculations are performed with both the LDA and LDA plus gradient corrected functionals. Basis sets have been varied and the effect of spin polarisation is also investigated.

Absolute Mulliken charges are of little significance, what is more important is the relative variation from complex to complex and the qualitative trends are the same irrespective of the choice of basis set. For comparable complexes (those with the same formal charge), the magnitudes of the atomic charges decrease from left to right across the series indicating a greater covalency and hence a greater departure from the formal oxidation states of the constituent ions. Such an increase is expected on the basis of the increasing effective nuclear charge, Z_{eff}, on the metal. This trend is reversed at zinc, where the charges now increase indicating a more ionic character in the bonding relative to $[NiCl_4]^{2-}$. The increase in formal oxidation state from $[FeCl_4]^{2-}$ to $[FeCl_4]^{-}$ is also accompanied by greater covalency in the latter and hence a larger departure from the formal charge of Fe^{3+} and Cl^{-}.

	R(DZP)	U(DZP)	R(TZP)	U(TZP)
$TiCl_4$	1.0774	1.0774	0.9826	0.9826
VCl_4	0.8743	0.8820	0.7673	0.7746
$MnCl_4^{2-}$	0.5434	0.6959	0.5670	0.6997
$FeCl_4^{-}$	0.5120	0.6390	0.4296	0.5395
$FeCl_4^{2-}$	0.5104	0.6198	0.5198	0.6080
$CoCl_4^{2-}$	0.4560	0.5372	0.4681	0.5373
$NiCl_4^{2-}$	0.4695	0.5071	0.4460	0.4785
$ZnCl_4^{2-}$	0.7018	0.7018	0.5924	0.5924

Table 3.4: Atomic charges calculated using the LDA showing the effect of basis set.

Significantly, the charges calculated with the gradient corrected functionals included show more ionic charge distributions than with the LDA method (see

Figure 3.6). This suggests that the former leads to a more ionic description of bonding that is typical of these complexes. The same trend is seen even if the charges are calculated at the experimental geometry and so the nature of the charge distribution is inherent in the method and not a function of geometry. This adds further evidence to the theory that due to the inherent limitations of the LDA the gradient corrected functionals must be included to treat systems where the electron density is not constant.

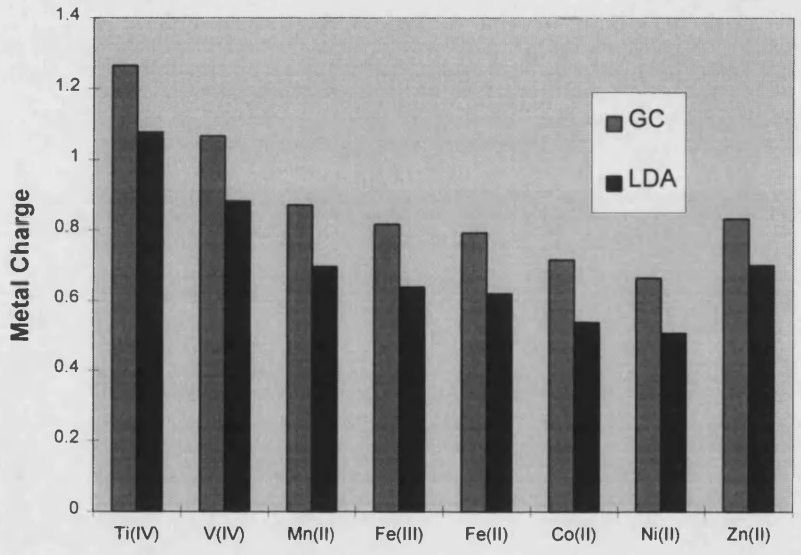

Figure 3.6: Calculated metal atomic charges showing the effect of gradient corrected functionals.

The increasing covalence is also monitored by the deviation of the total d-orbital populations from their formal values. Again, the absolute values are basis set dependent while the qualitative trends are not. For the formally d^0 $TiCl_4$, the computed d-orbital population is approximately 2.5. For VCl_4, there is an increase

of about 0.04 electrons above the additional electron expected for the formal d^1 configuration.

Similar extra increments of around 0.05 to 0.16 electrons are found for the $[MCl_4]^{2-}$ series from Mn to Zn, with populations of 5.42, 6.45, 7.53, 8.79 and 9.94 compared to the formal configurations of d^5, d^6, d^7, d^8 and d^{10}.

Comparing the e and t_2 components of the d-orbital population shows that the increasing covalence is spread across all the d-orbitals. Thus, while the extra electron in VCl_4 relative to $TiCl_4$ formally would occupy an e function, the e population increases by only 0.8 electrons with the remainder appearing in the t_2 orbitals. A similar picture emerges for the other complexes apart from $[ZnCl_4]^{2-}$ which, being closed shell, has a completely filled d level.

	Ti	V	Mn	Fe^{III}	Fe^{II}	Co	Ni	Zn
e	0.88	1.68	2.12	2.42	3.06	3.96	3.96	4.00
t_2	1.56	1.80	3.30	3.84	3.39	3.57	4.83	5.94
Total	2.44	3.48	5.42	6.26	6.45	7.53	8.79	9.94

Table 3.5: d-orbital populations calculated using the LDA with a double-ζ basis set and spin polarisation included.

Values of the ligand field splitting parameter, Δ_{tet}, have also been calculated by a simple difference of the e and t_2 MO energies. The unpaired electrons in these systems are invariably found in the anti-bonding d-orbitals of e and t_2 symmetry. For the spin polarised calculations this corresponds to the difference between up-spin MOs for configurations d^1-d^5 and down-spin MOs for configurations d^6-d^8 (configurations d^0 and d^{10} are unaffected by spin-polarisation). Electronic

relaxation effects have therefore been omitted although previous Xα calculations suggest[14] the effects for nominally d-d transitions are small in such species.

The relevant data are collected in Tables 3.6 and 3.7 and in Figure 3.7. As with the M-Cl bond lengths, the value of Δ_{tet} does not change significantly as a function of basis set. There is no particular correlation between the number of unpaired electrons for the spin unrestricted calculations which are somewhat worse than the spin-restricted results. The spin restricted data indicate that the tetravalent metal complexes are in poorer agreement with experiment than the di- and trivalent species. Previous Discrete Variational Xα calculations on VCl_4[14], which include relaxation effects via Slater's transition state formalism[15], gave very similar results suggesting that this shortcoming is inherent to the model.

Comparing the calculated values with experimental values shows that there are some large discrepancies although average errors are in the region of $1000cm^{-1}$ except for spin-unrestricted gradient-corrected where errors are much larger. This latter point may be due to the fact that these values are calculated at the calculated geometries which for the gradient corrected calculations are significantly different from the experimental values. However, calculations at the experimental geometries do not appear to alter the values significantly indicating that the Δ_{tet} values are fairly geometry independent, at least at or around the experimental geometry.

Best agreement with experiment is found with the gradient corrected calculations without spin-polarisation. If spin contamination is affecting the calculated spin unrestricted values then it appears to be much worse with gradient corrected

calculations. However, if as is indicated, the Δ_{tet} value is relatively unchanged by a change in geometry at or around the experimental geometry, then relatively accurate values can be calculated from geometries obtained from LDA calculations and then calculating orbital energies with the gradient corrections included.

	R(DZP)	U(DZP)	R(TZP)	U(DZP)	Expt.
$TiCl_4$	6629	6629	6654	6654	7501[a]
VCl_4	6589	8073	6637	8105	9034
$MnCl_4^{2-}$	3791	4565	3847	4621	3629
$FeCl_4^{2-}$	5670	4791	5734	5516	4033
$FeCl_4^{-}$	3234	4758	3291	4783	5001
$CoCl_4^{2-}$	2524	6113	2581	6137	3307
$NiCl_4^{2-}$	3234	5105	3282	5145	3549
$ZnCl_4^{2-}$	1782	1782	1790	1790	-
Av. Error	1140	1147	1138	1271	-

Table 3.6: Δ_{tet} values calculated using the LDA showing the effect of basis set (experimental values from reference 16).

Comparing Δ_{tet} values calculated for the doubly charged species using the spin restricted treatment with gradient corrected functionals, a trend can be seen to emerge. Whilst the absolute energies are in reasonable agreement, the relative differences between complexes are well reproduced. The overall energies are likely to be affected by the molecular environment. Therefore, the inclusion of some potential field to represent the crystal environment may increase the accuracy of calculated Δ_{tet} values.

	R(DZP)	U(DZP)	R(TZP)	U(DZP)	Expt.
$TiCl_4$	6291	6291	6323	6323	7501
VCl_4	6823	9479	6871	9525	9034
$MnCl_4^{2-}$	3307	4033	3317	4129	3629
$FeCl_4^{2-}$	5129	4460	5226	4662	4033
$FeCl_4^{-}$	3379	7767	3444	7783	5001
$CoCl_4^{2-}$	3242	11315	3299	11356	3307
$NiCl_4^{2-}$	3379	7178	3436	7242	3549
$ZnCl_4^{2-}$	1355	1355	1387	1387	-
Av. Error	957	2384	932	2474	-

Table 3.7: Δ_{tet} values calculated using gradient corrected functionals showing the effect of basis set (experimental values from reference 16).

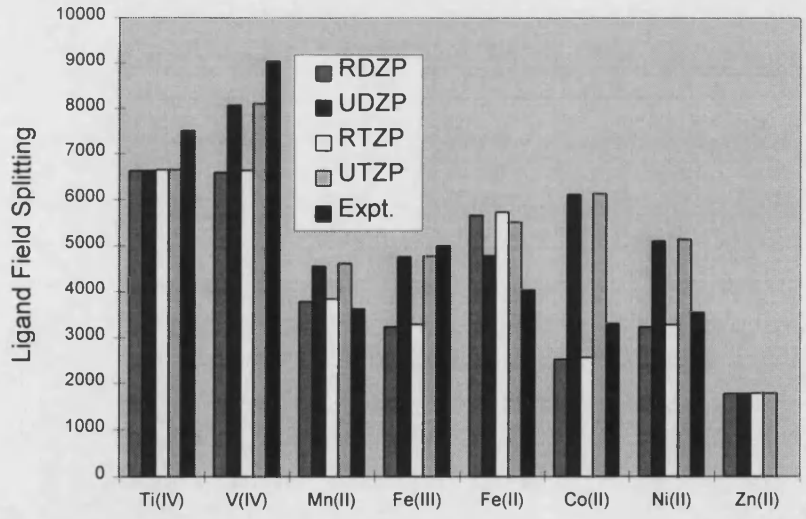

Figure 3.7: Comparison of calculated Δ_{tet} values (cm^{-1}) with experimental values (all calculations using LDA).

3.4 Conclusions

In this chapter studies of transition metal tetrachloro species have been presented. Geometry optimisations have been shown to be capable of reproducing experimental values very accurately within a LDA approach. The inclusion of gradient corrected functionals gives significantly less accurate geometries. The use of spin-polarisation is shown to be essential, especially for complexes with two or more unpaired electrons. There is also a significant correlation between the change in bond length and the number of unpaired electrons when these effects are included.

Gross atomic charges and d-orbital populations, although not comparable with experiment, do indicate an increasing covalency across this series.

Calculated Δ_{tet} values are compared with experimental values and average errors are found in the region of $1000cm^{-1}$ (with the exception of gradient corrected calculations with spin polarisation). Best agreement is found for gradient corrected calculations without spin-polarisation and the calculated values seem to be relatively insensitive to the M-Cl bond lengths. Thus, these values can be calculated at the experimental geometry or that calculated using the LDA without a significant reduction in accuracy.

References

1. D.W.Smith, *Coord. Chem. Rev.*, 1976, **21**, 93.

2. J.H.Van Vleck, *Phys. Rev.*,1932, **41**,208.

3. H.A.Jahn and E.Teller, *Proc. Roy. Soc.*, 1937, **A161**, 220.

4. (a) K.Waizumi, H.Masuda, H.Einaga and N.Fokushima, Chem. Lett., 1993, 1145. (b) F.A.Cotton and C.A.Murillo, *Inorg. Chem.*, 1975, **14**, 2467. (c) Y.Morino and H.Vehara, *J. Chem. Phys.*, 1966, **45**, 4543.

5.T.Ziegler, *Chem. Rev.*, 1991, **91**, 651.

6. A. J. Becke, *Chem. Phys.*, 1986, **84**, 4524.

7. (a) J. P. Perdew, *Phys. Rev.*, 1986, **B33**, 8822. (b) J. P. Perdew, *Phys. Rev.*, 1987, **B34**, 7406 (erratum).

8. A.D.Becke, ACS Symp. Ser., 1989, 394.

9. T.Ziegler, V.Tschinke and C.Ursenbach, *J. Am. Chem. Soc., 1987*, **109**, 4825.

10. R.Van Leeuwen and E.J.Baerends, *Int. J. Quantum Chem.,* 1994, **52**, 711.

11. (a) N.C.Handy, P.J.Knowles and K.Somasundram, *Theoret. Chim. Acta.*, 1985, **68**, (b) R.H.Nobes, J.A.Pople, L.Radom, N.C.Handy and P.J.Knowles, *Chem. Phys. Lett.,*. 1987, **138**, 481. (c) J.Baker, *J. Chem. Phys.*, 1989, **91**, 1789. (d) C.Sosa and H.B.Schlegel, *Int. J.Quantum Chem.*, 1986, **29**, 1001. (e) F.Jensen, *Chem. Phys. Lett.*, 1990, **169**, 519.

12. J.Baker, A.Scheiner and J.Andzelm, *Chem. Phys. Lett.*, 1993, **216**, 380.

13. R.J.Deeth, *J. Chem. Soc., Faraday Trans.*, 1993, **89**, 3745.

14. R.J.Deeth, *J. Chem. Soc. Dalton*, 1991, 1467.

15. J.C.Slater, *Quantum Theory Of Molecules and Solids*, McGraw-Hill, New

York, 1974, vol.4.

16. R.Fenske and D.Radtke, *Inorg. Chem.*, 1968, **7**, 479.

17. L.Versluis and T.Ziegler, *J. Chem. Phys.*, 1988, **88**, 322.

18. A.Béces and T.Ziegler, *J. Phys. Chem.*, 1995, **99**, 11417.

Chapter 4

Theoretical Vibrational Energies of $[CrO_4]^{2-}$, $[MnO_4]^{2-}$ and $[FeO_4]^{2-}$

4.1 Introduction

This chapter investigates the calculation of vibrational frequencies for some transition metal oxo complexes. Accurate second derivatives are required for characterising potential energy surface features. For example, a minimum gives all real eigenvalues while a saddle point corresponding to a transition state will have exactly one imaginary eigenvalue. At present, computation is the only way to obtain detailed transition state geometries. In addition, vibrational energies derived from the second derivatives can be used to compute zero point energies and, using the techniques of statistical mechanics, thermodynamic quantities like enthalpy and the entropy.[1] A completely theoretical estimation of reaction energetics requires the accurate estimation of the second derivatives and molecular vibrational energies.

Terminal metal-oxygen bonds are a common feature of the high oxidation state chemistry of the transition elements.[2] They often participate in the important process of oxo transfer.[3]

$$X + AO \rightleftharpoons XO + A \qquad (4.1)$$

Among the metals of the left half of the transition series a variety of metal-oxo subunits exists, ranging from simple mono-oxo to tetra-oxo species. When two or more terminal oxygen ligands are present, several geometric arrangements become possible and examples of virtually every isomeric configuration can be found. For example, *cis* and *trans* O=M=O units, trigonal planar and trigonal pyramidal MO_3 units, tetrahedral and 'see-saw' MO_4 units etc. Among the latter, a range of discrete, tetrahedral tetra-oxo complexes are found for each element of the vanadium through to iron triads. These species represent some of the simplest metal-oxo molecules.[3]

The richness of metal-oxo chemistry has stimulated a good deal of theoretical interest. Other studies have investigated; (i) the electronic transition energies of a range of d^1 complexes of CrO^{3+},[4] VO^{2+} [5] and MoO^{3+},[6] (ii) the optimised structures and vibrational energies of Mo_2X_2 species (M = Cr, Mo; X = F, Cl)[7] and (iii) the optimised bond lengths and electronic structures of $[MO_4]^{2-}$ compounds (M= Cr, Mn, Fe)[8]. In each case, a theoretical model based on Density Functional Theory (DFT) was employed and found to give good agreement with experimental data. This contrasts with the results of Hartree-Fock treatments of the M=O bonding in, for example, tetrahedral oxyanions which are qualitatively and quantitatively poor.[9,10]

4.2 Computational Details

All DFT calculations were based on the Amsterdam Density Functional (ADF) program system due to Baerends *et al.*[11]. STO basis sets of double-ζ plus

polarisation (DZP) and triple-ζ plus polarisation (TZP) are used[25,26]. All geometry optimisations were constrained to T_d symmetry. The local density approximation[27] (LDA) employed Vosko *et al.*'s functional[28] and included Stoll *et al.*'s[29,30] correction for self-interaction. Gradient Corrections (GC) to the LDA exchange and correlation terms employed the formulations of Becke[12] and Perdew[13,14] respectively. The lower core shells on the atoms (1s on O and up to 2p on the metal atoms) were treated by the frozen core approximation.[15]

Harmonic vibrational energies were estimated via finite difference of the analytical first derivatives. The calculations were run without T_d symmetry constraints (i.e. with all nine degrees of freedom) with two additional points used to estimate each second derivative. The resulting nine computed vibrational energies were then averaged over symmetry equivalent components assigned by reference to the computed eigenvectors. Notionally equivalent vibrational components never differed from each other by more than about 15 cm^{-1} which indicates the approximate level of numerical 'noise' inherent in this procedure.

A previous DFT study[8] on these complexes gave optimised M=O distances within 0.02Å of experiment. Test calculations using the experimentally observed bond lengths and the DFT-optimised bond lengths gave computed vibrational energy differences of around $10cm^{-1}$. This error is of the same order as the numerical 'noise' described above and hence the averaged experimental bond lengths were employed throughout, viz. 1.658Å,[16] 1.659Å [17] and 1.656Å [18] for Cr=O, Mn=O and Fe=O respectively.

The formally d^1 $[MnO_4]^{2-}$ ion possesses a ^2E Jahn-Teller active ground state. In principle, a regular T_d geometry would not correspond to a minimum on the potential energy surface and would yield an imaginary vibrational frequency. However, there is no experimental evidence for a marked Jahn-Teller distortion.[17] To circumvent this problem and maintain the high symmetry for comparison with the other two molecules, the unpaired electron was divided equally between the two components of the 2e partially occupied MO. The DFT formalism remains consistent even with non-integral MO occupations.[19] This procedure then generates a $^2A_1$ state which now corresponds to a (constrained) energy minimum. The fact that this state is not the global minimum does not appear to affect adversely the computed vibrational energies (*vide infra*).

4.3 Results and Discussion

The calculated and observed data for three complexes are collected in Table 4.1 along with various error estimates in terms of percentage differences. Generally speaking, there is a marginal improvement with the larger basis sets but the difference between local and non-local functionals is slight (*vide infra*).

Turning first to the question of the order of the vibrational bands, in each case, the theoretical assignment, labelled **I** below, yields energies which increase in the order:

$$E < F_2 < A_1 < F_2 \qquad \mathbf{I}$$

The experimental assignment for $[CrO_4]^{2-}$ has been reported by Weinstock *et al*[20] while Griffith has given assignments for the other two complexes on two separate occasions.[21,22] Assignment **I** is suggested for both $[MnO_4]^{2-}$ and $[FeO_4]^{2-}$ in the earlier study[21]. However, in the later work,[22] an alternative assignment (**II**) (see below) was proposed for $[FeO_4]^{2-}$ based on the polarisation of lines in the Raman spectrum.

$$F_2 < E < F_2 < A_1 \qquad \textbf{II}$$

Complex	Method	E	F_2	A_1	F_2
$[CrO_4]^{2-}$	Expt.[20]	349	378	846	890
	LDA,DZP	322	356	836	894
	LDA,TZP	323	356	866	912
	GC,TZP	330	380	870	926
$[MnO_4]^{2-}$	Expt. 1[22]	325	332	812	820
	Expt. 2[21]	325	328	816	862
	LDA,DZP	307	330	856	909
	LDA,TZP	311	336	844	876
	GC,TZP	321	353	853	889
$[FeO_4]^{2-}$	Expt. 1[21]	320	340	778	800
	Expt. 2[22,a]	340	322	832	790
	Expt. 3[22,b]	322	340	790	832
	LDA,DZP	292	314	810	864
	LDA,TZP	304	328	833	867
	GC,TZP	311	341	845	885

Table 4.1: Observed and calculated vibrational energies (cm^{-1})for tetrahedral $[MO_4]^{2-}$ complexes. (See text for explanation of methods and assignments.)
[a] based on assignment **II**, [b] based on assignment **I.**

This conflicts with the present DFT results. However, given the similarity of the species and the otherwise good numerical agreement, a revision back to the original assignment **I** is suggested.

Turning now to a comparison of computed and observed energies, the most favourable agreement uses the earlier data on $[MnO_4]^{2-}$ with the more recent band maxima for $[FeO_4]^{2-}$ but now reassigned. Under these conditions, the average deviation among the TZP results is between 3 to 5% with the largest percentage error on any one band being 7.6% for the lower F_2 vibration of $[MnO_4]^{2-}$ while the biggest energy difference is 55 cm^{-1} for the A_1 band of $[FeO_4]^{2-}$ at the GC TZP level. The largest percentage deviation for **any** TZP result is 12% corresponding to the highest F_2 band for $[FeO_4]^{2-}$ which at the GC TZP level is 95cm^{-1} higher than experiment provided one is prepared to accept assignment **II**. If only assignment **I** is considered, but with any of the reported experimental data, the largest error is 7% corresponding to a deviation of 55 cm^{-1} between observed and calculated (GC TZP) A_1 vibrations for $[FeO_4]^{2-}$. The difference between best and worst cases is therefore not too large with the best case comparison as far as the experimental data are concerned being illustrated in Figure 4.1.

At a detailed level, theory tends to slightly overestimate the energies of the highest two bands. These correspond to M=O stretching vibrations.[23] The LDA is well-known to lead to overbinding[24] which could lead to steeper potential wells and hence to computed energies which are too high. However, the non-local GC results, which should correct the overbinding, always give a slightly increased energy relative to the comparable LDA TZP data. Evidently, the depth of the potential well

is improved using GC functionals but its shape is virtually unchanged. The GC results for the two high energy bands therefore tend to be in slightly worse agreement with experiment.

In contrast, the LDA calculations for the lower two bands tend to slightly underestimate experiment such that the increase found for the GC results brings the latter into slightly better agreement with experiment.

Complex	Expt.	Method	E Δ%	$1F_2$ Δ%	A_1 Δ%	$2F_2$ Δ%	|av. Δ%|
$[CrO_4]^{2-}$	1	LDA,DZP	-7.7	-5.8	-1.2	+0.5	3.8
	1	LDA,TZP	-7.5	-5.8	+2.4	+2.5	4.6
	1	GC,TZP	-5.4	+0.5	+2.8	+4.0	3.2
$[MnO_4]^{2-}$	1	LDA,DZP	-5.5	-0.6	+5.4	+10.9	5.6
	2	LDA,DZP	-5.5	+0.6	+4.9	+5.5	4.1
	1	LDA,TZP	-4.3	+1.2	+3.9	+6.8	4.1
	2	LDA,TZP	-4.3	+2.4	+3.4	+1.6	2.9
	1	GC,TZP	-1.2	+6.3	+5.1	+8.4	5.3
	2	GC,TZP	-1.2	+7.6	+4.5	+3.1	4.1
$[FeO_4]^{2-}$	1	LDA,DZP	-8.8	-7.7	+4.1	+8.0	7.2
	2	LDA,DZP	-14.1	-2.5	-2.6	+9.4	7.2
	3	LDA,DZP	-9.3	-7.7	+2.5	+3.9	5.9
	1	LDA,TZP	-5.0	-3.5	+7.1	+8.4	6.0
	2	LDA,TZP	-10.6	+1.9	+0.1	+9.8	5.6
	3	LDA,TZP	-5.6	-3.5	+5.4	+4.2	4.7
	1	GC,TZP	-2.8	+0.3	+8.6	+10.6	5.6
	2	GC,TZP	-8.5	+5.9	+1.6	+12.0	7.0
	3	GC,TZP	-3.4	+0.3	+7.0	+6.4	4.3

Table 4.2: Percentage deviations (Δ%) and the average magnitude of Δ% (|av. Δ%|) for tetrahedral $[MO_4]^{2-}$ complexes. Where multiple sets of experimental data are available, corresponding sets of Δ% and |av. Δ%| are also given. (See text for explanation of methods and assignments.)

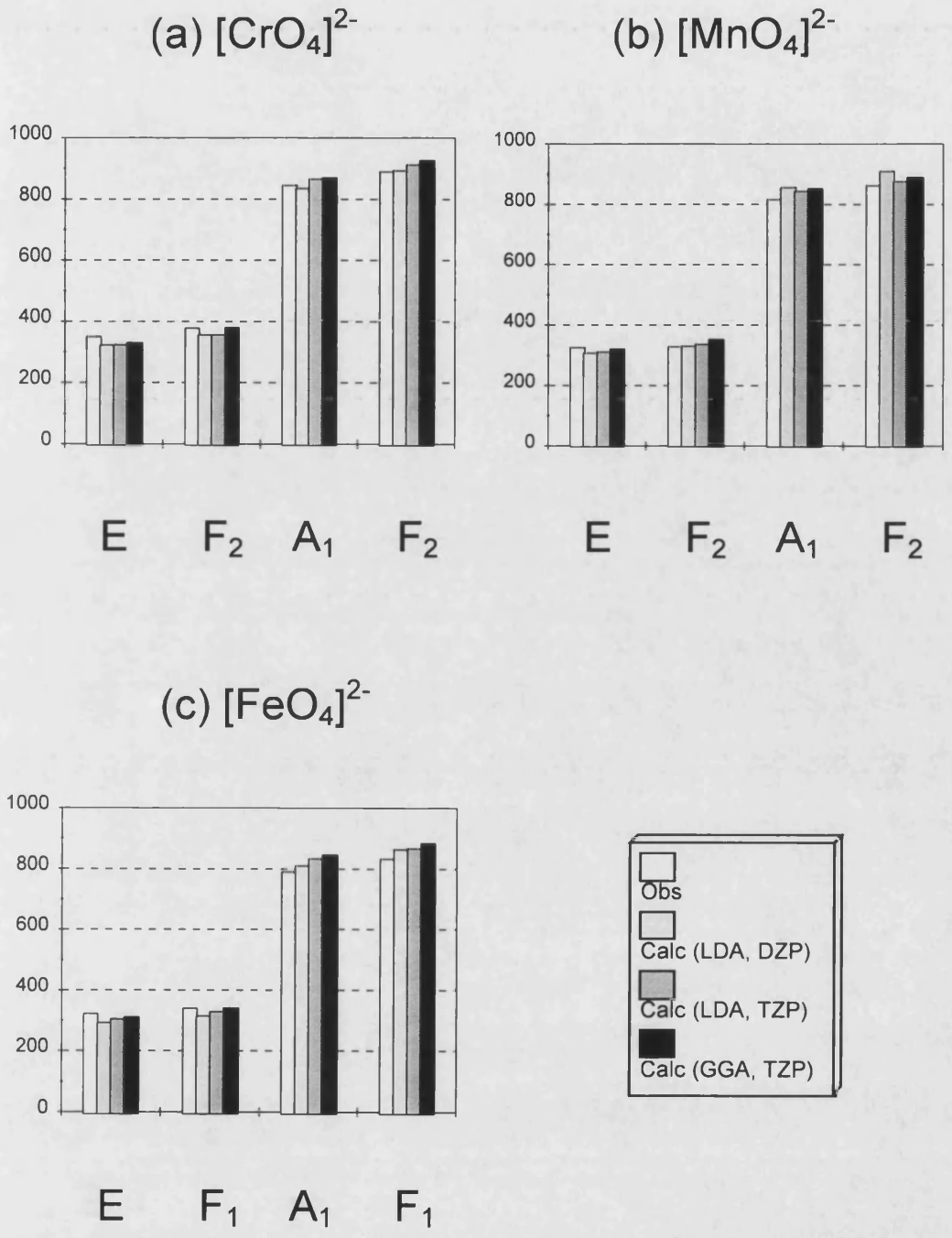

Figure 4.1: Observed and calculated vibrational energies (cm^{-1}) for $[MO_4]^{2-}$ complexes.

In summary, the LDA data are slightly better than the GC results for the two higher energy bands and slightly worse for the two lower energy bands. However, it is clear that the effects of changing basis set and functional are all relatively small

and of a similar order to the numerical 'noise' of around 10-15 cm^{-1}. This range can be considered a rough guide to the theoretical error bars and essentially implies that the LDA DZP, LDA TZP and gradient corrected TZP results are fairly comparable.

As found for the dioxodihalides of Cr and Mo,[7] harmonic vibrational energies from DFT reproduce the experimental data which are intrinsically anharmonic. Evidently, these systems either obey the harmonic oscillator approximation quite well or there is a fortuitous cancellation of errors in the DFT calculations. Either way, the DFT method appears to give consistently reliable results.

Assuming assignment **I** throughout, then, one sees that each band tends to decrease in energy in the order $[CrO_4]^{2-} > [MnO_4]^{2-} > [FeO_4]^{2-}$. The comparison between theory (LDA TZP) and experiment is displayed in Figures 2 and 3. The only discrepancy seems to be that the lower energy F_2 band observed in $[MnO_4]^{2-}$ is anomalously low. Otherwise, there appears to be a relatively systematic discrepancy between experiment and the DFT results. As noted above, however, a special procedure was adopted for the Mn anion in order to avoid a ground state orbital degeneracy. It is possible that this procedure is responsible for the apparent anomaly but, given the agreement found for the other three bands, it seems possible that the experimental data may be suspect. The two low energy bands of $[MnO_4]^{2-}$ are reported to be only three to seven wavenumbers apart and presumably overlap. It may be that the exact positions of the band maxima are subject to a larger uncertainty. An increase of only 20 cm^{-1} for the lower F_2 band would establish a consistent trend. However, in the absence of the actual spectra, one cannot judge the reliability of this assertion.

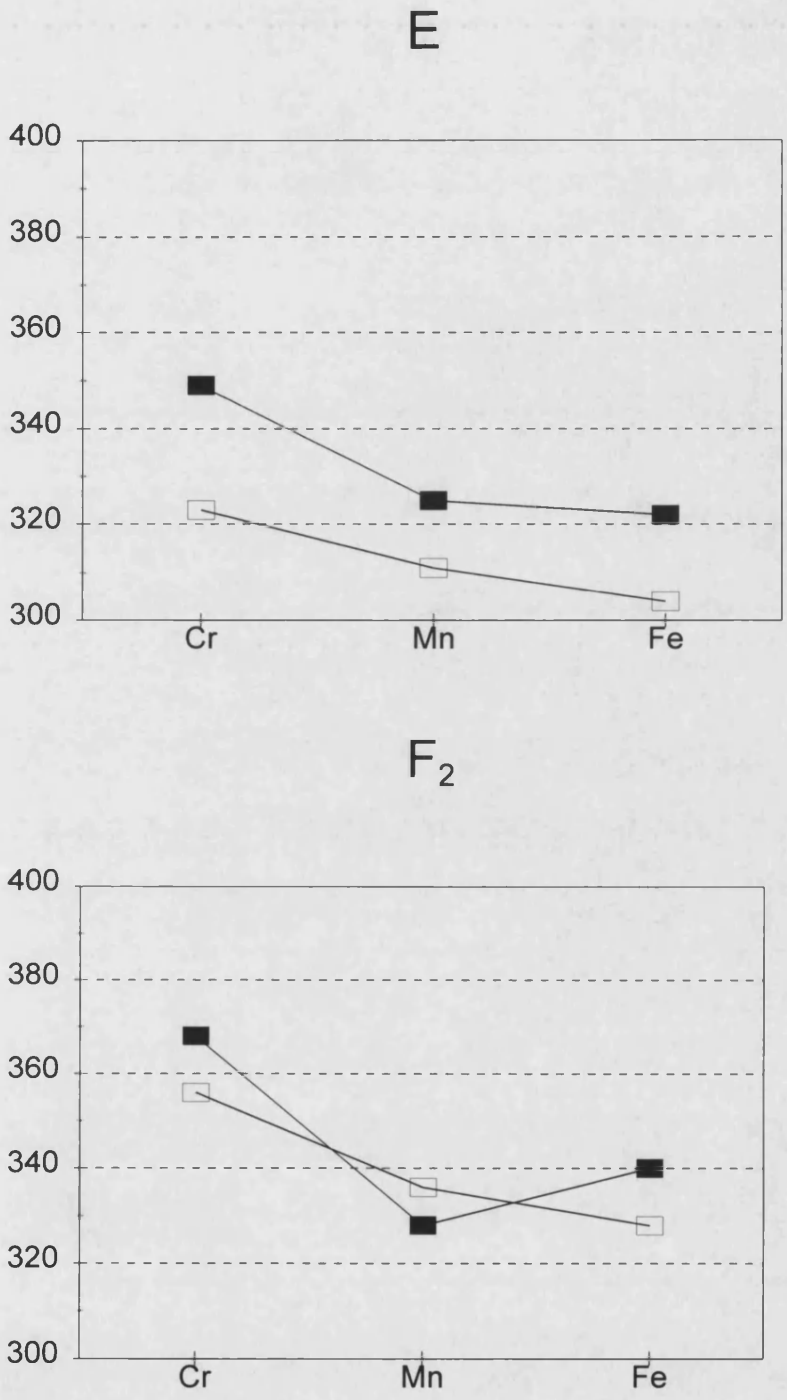

Figure 4.2: Systematic deviations between observed (solid) vibrational energies (cm^{-1}) and those calculated at the LDA TZP level (open).

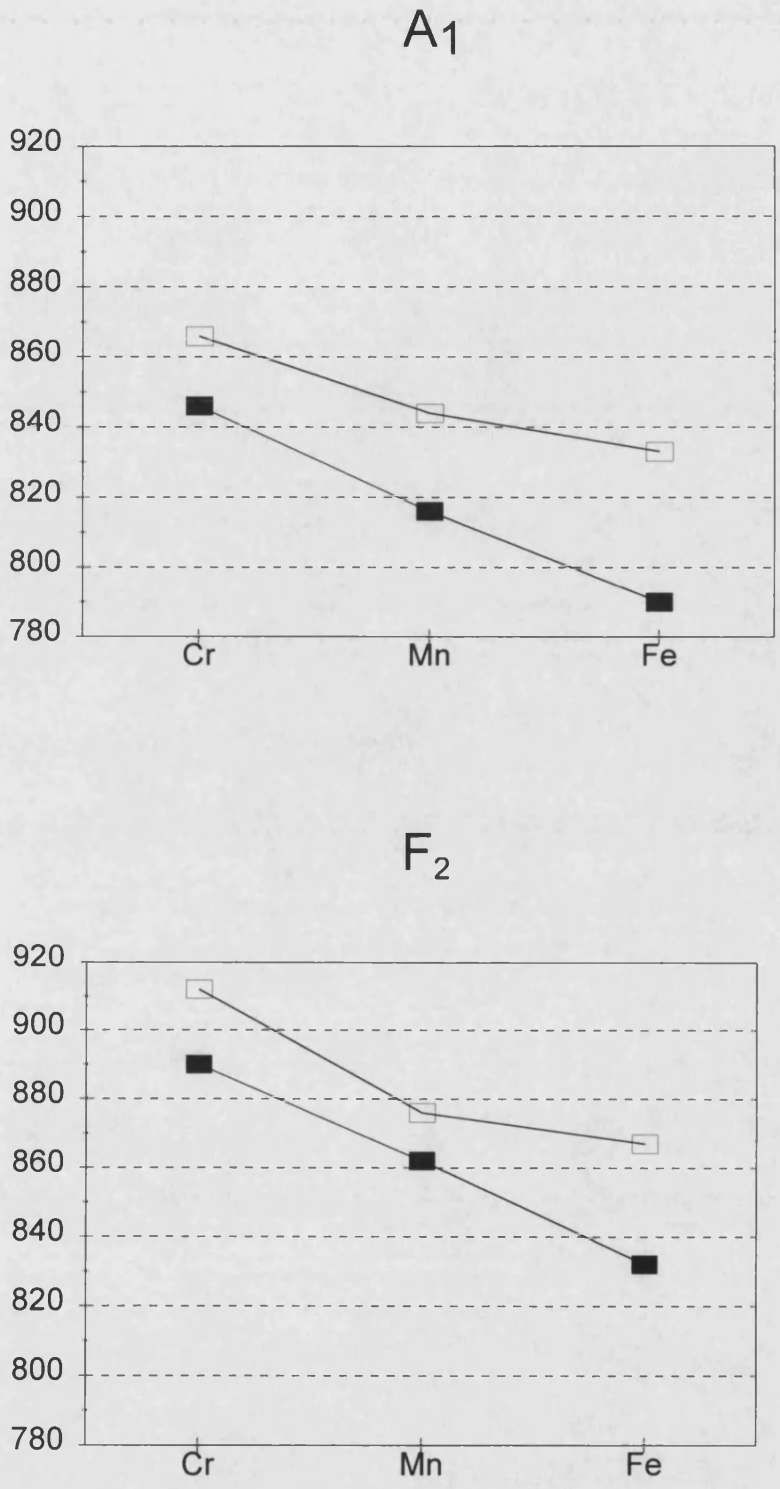

Figure 4.3: Systematic deviations between observed (solid) vibrational energies (cm^{-1}) and those calculated at the LDA TZP level (open).

4.4 Conclusions

Density Functional Theory calculations of the vibrational energies of $[CrO_4]^{2-}$, $[MnO_4]^{2-}$ and $[FeO4]^{2-}$ using double and triple-ζ basis sets give accurate agreement with experiment subject to a revision of the assignment of $[FeO_4]^{2-}$ back to the original proposal. The average error for the larger basis sets using both local and non-local functionals is only about 4% with a maximum average deviation of about 7% depending on with which experimental data one compares it. Theoretical estimates for the two high energy stretching modes tend to be slightly too large while those for the lower energy bending and torsional modes tend to be slightly too small. These errors are of the same order as the numerical noise, which is around 10-15 cm^{-1}. This study, together with the previous work on these complexes,[8] demonstrates that DFT provides a very satisfactory description of the potential energy surface of these molecules in the vicinity of the ground state.

References

1. N.Weinstock, H.Schulze and A.Müller, *J. Chem. Phys.*, 1973, **59**, 5063.

2. F.A.Cotton and G.Wilkinson, *Advanced Inorganic Chemistry (5^{th} ed.)*, Wiley-Interscience, New York, 1988.

3. R.H.Holm, *Chem. Rev.*, 1987, **87**, 1401.

4. R.J.Deeth, *J. Chem. Soc., Dalton Trans.*, 1990, 365.

5. R.J.Deeth, *J. Chem. Soc., Dalton Trans.*, 1991, 1467.

6. R.J.Deeth, *J. Chem. Soc., Dalton Trans.*, 1991, 1895.

7. R.J.Deeth, *J. Phys. Chem.*, 1993, **97**, 11625.

8. R.J.Deeth, *J. Chem. Soc., Faraday Trans.*, 1993, **89**, 3745.

9. P.W.Fowler and ESteiner, *J. Chem. Soc., Faraday Trans.*, 1993, **89**, 1915.

10. M.A.Buijse and E.J.Baerends, *Theoret. Chim. Acta*, 1991, **79**, 389.

11. E.J.Baerends, D.E.Ellis and P. Ros, *Chem. Phys.*, 1973, **2**, 41.

12. A.J.Becke, *Chem. Phys.*, 1986, **84**, 4524.

13. J.P.Perdew, *Phys. Rev.*, 1986, **B33**, 8822.

14. J.P. Perdew, *Phys. Rev.*, 1987, **B34**, 7406 (erratum).

15. E.J.Baerends D. E. Ellis and P. Ros, *Theoret. Chim. Acta*, 1972, **27**, 339.

16. J.S.Stephens and D.W.J.Cruckshank, *Acta Cryst*, 1970, **B26**, 437.

17. G.Wilkinson, R.G.Gillard and J.A.McClavarty (eds.), *Comprehensive Coordination Chemistry, Vol 4*, Pergamon, Oxford, 1987, pp109.

18. R.J.Audette, J.W.Quail, W.H.Black and B.E.Robertson, *J. Solid State Chem.*, 1973, **8**, 43.

19. J.C.Slater, *Quantum Theory of Molecules and Solids Vol. 4*, McGraw-Hill, New York, 1974.

20. N.Weinstock, H.Schulze and A.Müller, *J. Chem. Phys*, 1973, **59**, 1467.

21. W.P.Griffith, *J. Chem. Soc. A*, 1966, 1467.

22. F.Gonzalez-Vichez and W.P.Griffith, *J. Chem. Soc., Dalton Trans.*, 1972, 1416.

23. K.Nakamoto, *Infrared and Raman Spectra of Inorganic and Coordination Compounds (3rd ed.)*, Wiley-Interscience, New York, 1978.

24. T.Ziegler, *Chem. Rev.*, 1991, **91**, 1416.

25. J.G.Snijders, P.Vernooijs and E.J.Baerends, *At. Data Nucl. Data Tables*, 1981, **26**, 483.

26. J.G.Snijders, P.Vernooijs and E.J.Baerends, *Slater Type Basis Functions for the Whole Periodic System.*, Internal Report, Free University, Amsterdam, 1981.

27. J.C.Slater, *Adv. Quantum. Chem.*, 1972, **6**, 1.

28. S.H.Vosko, L.Wilk and M.Nussair, *Can. J. Phys.*, 1980, **58**, 1200.

29. H.Stoll, E.Golka and H.Preus, *Theor. Chim. Acta.*, 1980, **55**, 29.

30. H.Stoll, C.M.E.Pavlidou and H.Preus, *Theor. Chim. Acta.*, 1978, **49**, 143.

Chapter 5

Combined Quantum Mechanical and Molecular Mechanical Methods

5.1 Introduction

As has been shown in Chapters 2-4, Density Functional Theory (DFT)[1] provides an accurate method for the study of transition metal complexes. However, despite its improved scaling properties compared to Hartree-Fock (HF) Theory[2] and the various Post Hartree-Fock (PHF) methods[3], it will become unfeasibly expensive for large transition metal systems. Examples of what one might include as large molecules range from, at the lower end, transition metal catalysts used in organic synthesis such as Wilkinson's catalyst ($RhCl(PPh_3)_3$) to biologically important species such as Carbonic Anhydrase (Molecular weight c.30,000) and Galactose Oxidase (Molecular weight 68,000). Obviously, there is a great range in the size of transition metal systems, and whilst it would not be impossible to model molecules such as $RhCl(PPh_3)_3$ using a DFT method, the heavier proteins would be totally impossible given today's levels of computer power. Biological enzymes are known to carry out reactions much faster and with greater specificity than is currently possible using laboratory methods[4]. For example the production of ammonia using the Haber process[5] involves the use of extreme conditions of temperature and pressure and the use of catalysts and hence is extremely expensive. In spite of this the demand for ammonia production world-wide is enormous, and even a small reduction in the cost of ammonia production would lead to significant financial

benefits. In nature this very process is carried out by nitrogenase enzymes under ambient conditions. By using computational methods to investigate the reaction profiles of such a process it may become possible to produce a catalyst for this reaction that will operate under less harsh conditions and hence lessen the expense of this procedure. This is just one example of where biological systems carry out reactions that are important to man but under much less severe conditions than are currently possible using laboratory techniques, and hence the possibility for computational methods to make a real impact on this area are significant.

The difficulty with calculations on molecules of this size is the enormous computational effort required. Molecular Mechanics (MM) treatments would be one answer but they suffer, as already outlined, from their poor treatment of transition metal systems and their inability to model bond making/breaking processes. Recently several groups[6,7,13] have sought to address this problem by producing a combined Quantum Mechanical/Molecular Mechanical method which combines the accuracy of the Quantum Mechanical (QM) method for the important active site and the more efficient MM method for the generally organic based ligand backbone. Essentially, the approach has been to divide the system in question into a number of regions. The first region is the QM region, which involves all the atoms that are involved in reactive processes or that need to be modelled accurately. Secondly there is a MM region which contains the remainder of the molecule, generally the bulk of the ligand backbone. Some way is needed so join these regions together so there is a third region where the QM and MM regions meet. Two main approaches have been taken to implement a combined method,

firstly where a combined Hamiltonian is formulated for all the atoms in the system (the "Combined Potential Method") and, secondly, where separate QM and MM optimisations are carried out sequentially (the "Sequential" method). These two approaches are examined in more detail below.

5.2 The Combined Potential Method

In this method, atoms in the QM region are represented as nuclei and electrons. The potential surface for these atoms is usually determined within the Born-Oppenheimer approximation[8] and energy derivatives as a function of the nuclear co-ordinates are obtained. The MM region contains the remaining atoms of the system. They are represented as atoms rather than electrons and nuclei and their interactions are determined from an empirical potential energy function. They constitute the immediate environment for the QM atoms and are included because their interactions and dynamics will have a significant influence on the QM atoms and so require a detailed treatment. These atoms, as stated above, cannot be involved in bond making/breaking processes.

In order to calculate the energies of this system an effective Hamiltonian, H_{eff}, is constructed and the time-independent Schrödinger equation is solved for the energy of the system, E, and the wavefunction of the electrons of the QM atoms, Ψ,

$$H_{Eff}\Psi(r,R_\alpha,R_M) = E(R_\alpha,R_M)\Psi(r,R_\alpha,R_M) \qquad (5.1)$$

The wavefunction is a function of the co-ordinates of the electrons, r, and parametrically depends on the positions of both the QM atoms, R_α, and the MM atoms, R_M. The energy is calculated for each geometry of the QM nuclei and the MM atoms and generates the Born-Oppenheimer potential surface for the system. It is given by the expectation value of the wavefunction over the Hamiltonian.

$$E = \langle\Psi|H_{Eff}|\Psi\rangle/\langle\Psi|\Psi\rangle \qquad (5.2)$$

The forces on the QM nuclei, F_α, and the MM atoms, F_M, are obtained by differentiating (5.2) with respect to the nuclear or atomic Cartesian co-ordinates; that is,

$$F_\alpha = \frac{\delta E}{\delta R_\alpha} \quad \text{and} \quad F_M = \frac{\delta E}{\delta R_M} \qquad (5.3)$$

The effective Hamiltonian for the partitioned system is written as the sum of four terms,

$$H_{Eff} = H_{QM} + H_{MM} + H_{QM/MM} + H_{Boundary} \qquad (5.4)$$

where H_{QM}, H_{MM}, $H_{QM/MM}$ and $H_{Boundary}$ are respectively the Hamiltonians for the QM region, the MM region, the QM/MM interaction region and the boundary region. The total energy is the sum of the expectation values of each term in the Hamiltonian; i.e.,

$$E = E_{QM} + E_{MM} + E_{QM/MM} + E_{Boundary} \qquad (5.5)$$

Since the wavefunction depends only parametrically on R_M, the term, E_{MM} can be taken outside the integral in (5.2) and we have

$$E = \langle\Phi|H_{QM} + H_{QM/MM} + H_{Boundary(QM)}|\Psi\rangle/\langle\Psi|\Psi\rangle + E_{MM} + E_{Boundary(MM)} \qquad (5.6)$$

where the boundary term has been separated into QM and MM parts.

The first term of (5.4) is the Hamiltonian describing the QM particles of the system and their interaction with each other. The interaction between the QM and MM atoms is described by the interaction Hamiltonian, $H_{QM/MM}$, and the interaction between the QM and MM regions respectively with the boundary region are determined by the boundary Hamiltonian, $H_{Boundary(QM)}$.

The QM Hamiltonian can be obtained from a number of methods such as Hartree-Fock (HF), Density Functional Theory (DFT)[1] and quantum Monte Carlo[9]. The choice of the QM method is arbitrary with different methods being employed by different groups. The MM Hamiltonian is a function of the positions of the MM atoms. It does not depend on the co-ordinates of the electrons and nuclei of the QM atoms and so it is a number, i.e.,

$$H_{MM} = E_{MM} \qquad (5.7)$$

The nature of the MM force field has been described earlier. The interaction Hamiltonian, $H_{QM/MM}$, describes how the QM and MM atoms interact. The MM atoms in a normal force field are represented by point charges and van der Waals parameters and so the simplest interaction Hamiltonian would be written as:

$$H_{QM/MM} = -\sum_{iM} \frac{q_M}{R_{iM}} + \sum_{\alpha M} \frac{Z_\alpha q_M}{R_{\alpha M}} + \sum_{\alpha M} \frac{A_{\alpha M}}{R^{12}_{\alpha M}} - \frac{B_{\alpha M}}{R^{6}_{\alpha M}} \qquad (5.8)$$

where the subscripts i and α correspond to the QM electrons and nuclei respectively and M to the MM atoms, q_M is the charge on a MM atom, ZA is the nuclear charge on a QM atom and A and B are constants.

There are two electrostatic terms, in which the MM atoms interact with the QM electrons and nuclei respectively, and a van der Waals term. The van der Waals term is required because some MM atoms may possess no charge and so would be invisible to the QM atoms. Also, the van der Waals terms for MM atoms often provide the only difference between the interactions of, for example, a fluoride and a chloride that both have a uninegative charge and hence only differ in their van der Waals parameters. The Hamiltonian represented by (5.8) is an exact Hamiltonian for the interaction of QM electrons and nuclei and MM atoms represented by partial charges and van der Waals spheres. The last two terms are constant with respect to electronic co-ordinates and therefore can be calculated and added directly

to the total energy. The first term however, involves electronic positions and must be included in the QM procedure.

The non-bonded MM interactions are truncated to save time by including contributions from atoms or groups that are contained within a certain cut-off region. The QM interactions are expected to extend over a small enough number of atoms so that all interactions are included.

The boundary terms can be calculated using one of two common methods, periodic[10] and stochastic[11] boundary conditions.

A combined QM/MM such as the one described can be used in the same way as a normal empirical energy function.

The energy and forces may be employed to perform geometry optimisations, Molecular Dynamics (MD)[12] and Monte Carlo simulations. The advantage is that reactions (or exited states) can be described for the QM region and that information can be obtained about the electron distribution surrounding the QM nuclei. Therefore, charge analyses can be performed during an MD simulation to gain an idea of how the charge cloud distorts with time or along a reaction path under the influence of the environment.

As was stated previously, the system under investigation must be partitioned into a QM and a MM region. There are no rules for the way in which a system should be partitioned except that any part of the system involved in reactive processes will have to be treated within the QM region. Beyond this, the problem is arbitrary and will depend on the exact nature of the system, the computational resources available and a degree of chemical intuition.

A difficulty arises when parts of the same molecule contain both QM and MM regions. In such cases there are bonds between the QM and MM atom. However, the electrons and nuclei of the MM atoms are not treated explicitly and so the electron density along the QM-MM bond will not be representative of the real system. Therefore, it is necessary to introduce a method such that the interactions of the bonded MM atoms with the QM atoms should resemble, as much as possible, the interactions found in a complete QM system. There is no exact way to do this, but one method involves the use of "link" or "dummy" atoms. These atoms are used to terminate the QM system, and are normally QM hydrogen atoms which are made invisible to the MM atoms because no interactions between the link atoms and the MM atoms are calculated. The type of methods that have been discussed above are capable of modelling large systems within an acceptable time frame. It will not be possible to model all interactions with great accuracy but the important reactive and the effects that the surroundings have upon it centre can be described accurately.

Use of such methods[6] had primarily been concerned with the solvation of small molecules and both ion-ion interactions and ion-molecule interactions. Many of these applications are used in conjunction with MD treatments although a discussion of such work is beyond the scope of this work.

5.3 The Sequential Method

An alternative method to the one outlined above is what can be notionally describes as the sequential method. The procedure is greatly different to the one

outlined previously in that whilst the system is divided up into a QM and a MM region, these regions are optimised independently. Firstly, the system is divided up into its two regions, the QM region containing the central atoms of, for example, the reactive site or metal centre. Bulky ligands, with large, generally organic, substituents, are commonplace. These ligands are then replaced by smaller and less computationally demanding derivatives. For example, bulky alkyl groups are often replaced by hydrogen derivatives, i.e. PR_3 becomes PH_3. The positioning of the hydrogen atoms relative to the heteroatom is normally that found in the free ligand. This model system is then used to describe the whole system within the QM method. Geometry optimisation of this model is performed within the relevant QM schemes, although the substituted atoms are held fixed relative to the heteroatom to which they are bonded. When an optimised structure has been calculated this then serves as a QM skeleton to which is added the remainder of the system. The hydrogen atoms (or whichever atoms were used) that replaced the bulky ligands are removed and so the original molecule is regained but with the positions of the QM atoms altered by the optimisation procedure.

Once the new co-ordinates have been calculated a MM calculation is performed on this structure. The QM region is frozen so that all the MM terms that involve a alteration of the geometry of that area are explicitly removed from the MM parameterisation scheme such that only the atoms of the MM region are affected. The converged MM geometry is then the converged geometry for the whole system.

In a slight variation to this method, Hillier *et al.*[13] have included MM gradients from the surrounding MM atoms in the *ab initio* optimisation of the QM region. This is achieved by the addition of the MM gradients (exerted by the MM atoms on the QM atoms) to the QM gradients of the QM atoms.

While the method outlined above allows the quantifying of the effect of the ligand-ligand interactions on a reaction profile, it is unable to consider changes in the same profile induced by these interactions because the QM geometry is always frozen. In other words, this approach is limited to those cases where the ligand-ligand interactions are a minor perturbation to the metal-ligand interactions.

Applications of this method are widespread. This is probably due to the fact that it is a relatively simple method to implement. It is generally applied to the geometry calculation of systems containing a metal centre for which the parameterisation within a MM scheme would be at best extremely difficult. Examples of its application include the modelling of the potential energy surface of ester hydrolysis by the enzyme phospholipase A_2[13], modelling various Ru[(P-P)2"H_3^{+}"]$^{+}$ complexes[7a] and the conformational investigation of the cofactor (6R, 1'R, 2'S-)-5, 6, 7, 8-tetrahydrobiopterin[7b].

5.4 A New Approach to QM/MM Methods

DFT has been shown here and by other workers to be an accurate method when used to study transition metal complexes. Therefore, this method can be used in conjunction with MM to produce an effective combined method capable of treating large systems both quickly and accurately. In contrast to the methodology outlined

in 5.2 above, our proposed method is to treat the reactive centre (the metal site) with DFT using truncated ligands to mimic the real ligands in a way similar to the sequential method. The QM calculation will involve all atoms directly bonded to the metal plus terminal hydrogens to replace the remainder of any organic based ligands plus the complete ligand for inorganic-type ligands such as carbonyls, nitrosyls etc. Analytical first derivatives for each atom (minus the terminal hydrogens) are calculated and these derivatives are passed to the MM package. There are no MM bond stretch and angle bend terms for the atoms of the QM part of the molecule so these are replaced by these energy gradients. Cartesian energy gradients are calculated for each atom within MM and the gradients from the QM calculation are simply added to these gradients to give a net gradient for the QM atoms. Optimisation of the whole molecule is then carried out using the total energy gradients. A set of new optimised co-ordinates is computed and then passed back to DFT and a new set of derivatives calculated, for the QM atoms, and the process continued until the derivatives calculated for the QM atoms within DFT are balanced by those calculated by MM. At this point convergence will have been reached.

During the QM calculation, it is important that, at least electronically, the truncated ligand mimics behave as would the complete ligand. For example, if our molecule contains a trimethylphosphine ($P(CH_3)_3$) ligand then it can be replaced with the all hydrogen derivative phosphine (PH_3). By varying the P-H bond lengths and the H-P-H angles it may be possible to make a phosphine act (electronically) as the much larger trimethylphosphine.

In order to show the validity of such an approximation, the first part of this work involves calculations on a metal bonded to a single ligand. The donor atoms chosen are phosphorus, nitrogen, oxygen and sulphur. Methylated ligands are chosen as reference points, with the metal ligand bond lengths optimised while the ligand geometries are kept fixed. These results are then taken as reference points and then, by varying the geometries of hydrogen derivatives, an attempt is made to mimic these reference points. As a further extension, two ligands are used in a linear system using the same method as above. Once a set of parameters has been refined for each ligand and metal type, these parameters will be used in calculations on real complexes to test the validity of this assumption. Finally, the QM and MM parts will be incorporated together to give a complete treatment of both steric and electronic effects.

References

1. T.Ziegler, *Chem. Rev.*, 1991, **91**, 651.

2. (a) D.R.Hartree, *Proc. Camb. Phil. Soc.*, 1928, **24**, 89. (b) V.Fock, *Z. Physik.*, 1930, **61**, 126. (c) C.C.J.Roothan, *Rev. Mod. Phys.*, 1951, **23**, 69.

3. (a) R.Krishnan, H.B.Schlegel and J.A.Pople, *J. Chem. Phys.*, 1980, **72**, 4654. (b) B.Huron, J.P.Malrieu and O.Rancrel, *J. Chem. Phys.*, 1973, **58**, 5745. (c) S.Evangelisti, J.P.Dacudey and J.P.Malrieu, *J. Chem. Phys.*, 1983, **75**, 91. (d) C.Møller and M.S.Plesset, *Phys. Rev.*, 1934, **46**, 618.

4. (a) R..F.Hardy, R.C.Burns and C.W.Parshall, "*Inorganic Biochemistry*", G.L.Eichorn Ed., Elsevier, Amsterdam, 1973, **2**, 745. (b) J.A.Fee, Struct. Bonding, 1975, 23, 1. (c) O.Hayaishi, "*Molecular Mechanisms of Oxygen Activation*", New York Academic Press, 1974.

5. S.D.Lyon, *Chem. Ind.*, 1975, 731.

6. (a) M.J.Field, P.A.Bash and M.Karplus, *J. Comp. Chem.*, 1990, **11**, 700. (b) J.Gao and L.Shao, *J. Phys. Chem.*, 1994, **98**, 13772. (c) R.V.Stanton, D.S.Hartsough and K.M.Merz Jr., *J. Comp. Chem.*, 1995, **16**, 113. (d) H.Liu and Y.Shi, *J. Comp. Chem.*, 1994, **15**, 1311. (E) J.Gao, *J. Phys. Chem.*, 1992, **96**, 537.

7. (a) F.Maseras, N.Koga and K.Morokuma, *Organometallics*, 1994, **13**, 4008. (b) W.Estelberger, D.Fuchs, C.Murr, H.Wachter and G.Reibnegger, *Biochim. Biophys. Acta*, 1995, 23.

8. M.Born and J.R.Oppenheimer, *Ann. Phys-Leipzig*, 1927, **84**, 457.

9. D.Ceperley and B.Alder, *Science*, 1986, **231**, 555.

10. M.Born and T.V.Karman, *Physik. Z.*, 1912, **13**, 297.

11. C.L.BrooksIII and M.Karplus, *J. Chem. Phys.*, 1983, **79**, 6312.

12. N.Metropolis, A.W.Rusenbluth, M.N.Rusenbluth, A.H.Teller and E.Teller, *J. Chem. Phys.*, 1953, **21**, 1087.

13. I.H.Hillier, B.Waszkowycz, N.Gensmantel and D.W.Payling, *J. Chem. Soc. Perkin Trans. 2*, 1991, 225.

Chapter 6

Transition Metal Mono-Ligand and Di-Ligand Systems

6.1 Introduction

This chapter provides preliminary investigations into whether it is possible to model large ligands such as substituted phosphines and amines by smaller truncated hydrogen mimics. First metal plus one ligand and then metal plus two ligand systems are investigated. The aim is to show whether by altering the bond distances and angles in the mimic it is possible to reproduce the electronic nature of more complex ligands. The systems investigated are the methyl derivatives of phosphines, amines, esters and sulphides. Metal-ligand bond lengths are optimised for these systems and these are compared to results obtained with the hydrogen derivatives of these ligands with various ligand geometries.

6.2 Metal Plus One Ligand

6.2.1 Introduction

As was described in the previous chapter, in order to treat the real ligands by truncated mimics it is necessary to be able to reproduce electronic effects of the larger ligands. Initially calculations are carried out with the fully methylated ligands of phosphorus, sulphur, oxygen and nitrogen. Also several different metals are used; cobalt, nickel, copper and zinc in both the 0 and +2 oxidation states.

Calculations are simple optimisations of the metal ligand bond distance with the ligand geometry fixed. The ligand geometries are those found in the free ligand. These calculations establish an "experimental value" for the metal-ligand bond length. There are no real experimental structures for complexes of this type, but calculations on these systems provide a means of comparing the values calculated with the truncated ligands. In order for a truncated ligand to make a good mimic, it must be capable of reproducing the calculated bond length for the methylated derivative.

The methyl groups are then replaced with hydrogens, and the geometries of these ligands are varied. Taking the X-H (where X=O,N,S or P) bond lengths and the H-X-H bond angles as variables.

The values of these parameters are:

	Bond Length (Å)	Bond Angle (°)
H_2O	0.957	104.5
H_2S	1.336	92.1
NH_3	1.012	106.7
PH_3	1.420	93.3
$O(Me)_2$	1.416	112.0
$S(Me)_2$	1.807	99.1
$P(Me)_3$	1.458	110.9
$N(Me)_3$	1.847	98.6

Table 6.1: Bond lengths (Å) and angles (°) for various ligands (see reference 1).

Using for each variable the experimental value found for the methylated derivative (using X-C bond lengths and C-X-C bond angles respectively) and the hydrogen derivative produces a total of four combinations, namely:

C derivative bond angles, H derivative bond lengths.

2) H derivative bond angles, H derivative bond lengths.

3) C derivative bond angles, C derivative bond lengths.

4) H derivative bond angles, C derivative bond lengths.

Of course the range of parameter values is infinitely variable and the set chosen here is done so for simplicity. It is quite possible that other parameters may be necessary for some or all of the complexes that are studied here.

6.2.2 Computational Details

All calculations in this section are carried out with the ADF program by Baerends et. *al.*[2]. The following conditions were applied:

a) Basis sets are of the STO type[3], at the triple-ζ plus polarisation function level.

b) LDA employed using the Vosko, Wilk and Nussair functional[4].

c) The frozen core approximation[5] is used for all atoms except Hydrogen. Oxygen and nitrogen are frozen to the 1s level and sulphur, phosphorus and all metals to the 2p level.

d) All calculations are spin unrestricted (spin polarised)

e) C_{2V} (for H_2O and H_2S) or C_{3V} (for PH_3 and NH_3) symmetry is used in all cases.

6.2.3 Results

Results presented below refer to geometry optimisations of the metal-ligand bond length of a single ligand bound to each metal. 1-4 refer to the parameter sets described on page 122, the methyl value is calculated with the methylated derivative. The error value is the smallest error.

	1	2	3	4	Methyl.	Error
H_2O	1.876	1.870	1.839	1.830	1.853	0.009
H_2S	2.195	2.207	2.177	2.176	2.156	0.020
NH_3	1.979	1.956	1.911	1.920	2.002	0.023
PH_3	2.302	2.304	2.313	2.295	2.325	0.012

Table 6.2: Calculated bond lengths and smallest errors (Å) for Zn^{II} complexes.

	1	2	3	4	Methyl.	Error
H_2O	3.008	2.858	2.018	2.001	2.386	0.368
H_2S	3.095	3.085	2.632	2.648	2.980	0.105
NH_3	2.482	2.383	2.069	2.949	2.387	0.004
PH_3	3.319	3.176	2.911	2.295	3.077	0.099

Table 6.3: Calculated bond lengths and smallest errors (Å) for Zn^{0} complexes.

	1	2	3	4	Methyl	Error
H_2O	1.877	1.882	1.822	1.820	1.910	0.028
H_2S	2.203	2.257	2.202	2.101	2.177	0.025
NH_3	1.982	1.936	1.902	1.903	1.914	0.011
PH_3	2.321	2.345	2.299	2.301	2.229	0.070

Table 6.4: Calculated bond lengths and smallest errors (Å) for Cu^{II} complexes.

	1	2	3	4	Methyl.	Error
H_2O	2.116	2.076	1.827	1.822	2.005	0.071
H_2S	2.285	2.254	1.844	2.142	2.214	0.040
NH_3	2.001	2.000	1.902	1.854	2.025	0.024
PH_3	2.225	2.225	2.191	2.196	2.213	0.012

Table 6.5: Calculated bond lengths and smallest errors (Å) for Cu^0 complexes.

	1	2	3	4	Methyl	Expt.
H_2O	2.588	2.623	1.833	1.835	1.830	0.003
H_2S	1.936	2.029	1.942	1.939	1.935	0.001
NH_3	1.804	1.792	1.675	1.676	1.835	0.031
PH_3	1.957	2.022	1.954	1.950	1.960	0.003

Table 6.6: Calculated bond lengths and smallest errors (Å) for Ni^0 complexes.

	1	2	3	4	Methyl	Expt.
H_2O	1.957	1.917	1.821	1.809	1.877	0.040
H_2S	2.204	2.201	2.148	2.153	2.113	0.035
NH_3	1.999	1.936	1.894	1.891	1.898	0.004
PH_3	2.294	2.263	2.262	2.257	2.180	0.077

Table 6.7: Calculated bond lengths and smallest errors (Å) for Co^{II} complexes.

	1	2	3	4	Methyl	Expt.
H_2O	2.035	1.962	1.762	1.775	1.999	0.036
H_2S	2.114	2.115	2.146	2.145	2.254	0.086
NH_3	2.063	1.828	1.859	1.728	2.084	0.021
PH_3	1.983	2.056	2.151	2.151	1.979	0.004

Table 6.8: Calculated bond lengths and smallest errors (Å) for Co^0 complexes.

6.2.4 Discussion

Looking at the results presented above it can be seen that, in general, the agreement between the methylated derivatives and the best of the mimics is quite good. Approximately half of the systems are matched to within 0.02Å, and only a quarter are found to not be within 0.04Å. The latter are Zn^0 and H_2S, PH_3 and H_2O, Cu^{II} and PH_3, Cu^0 and H2O, Co^{II} and PH_3 and Co^0 and H_2S. Essentially, in line with the empirical nature of this investigation it should be possible to search a wider range of parameters until good agreement is found. However, having proved that this method is capable of, in most cases, replacing a methylated ligand with a simple hydrogen derivative this work is not as yet necessary. Further investigations will be required for other combinations of metal and ligand

In general, the oxidation state of the metal affects which set of parameters give the best fit. This is not true in all cases but sufficient evidence suggests that parameters need to be "tuned" to the oxidation state of the metal. This is not entirely unexpected due to the fact that electronic effects are dominant.

There does seem to be little correlation between which parameter sets give the most accurate results for any particular metal or ligand type. In general the best parameters are evenly spread between the four chosen parameter sets. These observations suggest that it will not be possible to predict which parameters will be most suitable for a particular metal and ligand on an *a priori* basis.

Comparison of these results with other work is limited as most other workers have concentrated on M^{1+} species. Magnusson and Moriarty[6] have reported HF

calculations (including correlated calculations) of the whole first row transition series of $M(H_2O)^+$ compounds, as have Rosi and Bauschlicher[7] using a Modified Coupled Pair Potential (MCPF) approach. However, work on single ligands and neutral or doubly positive charges appears to be limited to work by Siegbahn et *al.*[8] on nickel(0) water and phosphine complexes. Their bond length of 2.207Å for phosphine compares with the value calculated here of 2.022Å. This is a significant difference but the calculations carried out here were designed only to reproduce values of methylated derivatives, and it is not appropriate to make comparisons with other works.

6.2.5 Conclusion

These initial calculations suggest strongly that it is possible to model a large ligand with a much smaller truncated hydrogen derivative. By adjusting only the H-X bond length and the H-X-H bond angle it is quite possible to alter the M-X bond length by between 0.05Å and 1.0Å. This was achieved with a relatively small alteration in the ligand geometry, further alteration of these parameters could achieve a wide range of control over the metal ligand geometry.

In general the complexes that have been investigated here are not entirely representative of real complexes, therefore the conclusions that have been drawn here may be skewed by the essentially esoteric nature of the metal and one ligand system. Further investigations below centre on a more chemically feasible system containing two ligands. This will enable further investigation of the results obtained above

6.3 Metal Plus Two Ligands

6.3.1 Introduction

This section considers adding a second ligand *trans* to the first. This step produces a greater degree of confidence in the results obtained in the previous section. With a two ligand system there is no possibility of a steric interaction between atoms in separate ligand groups as each ligand is significantly distant from the other to prevent this occurring. Of course, there was no possibility at all of any such interaction in the one ligand systems. Therefore, the only factors influencing the metal ligand bond lengths will be electronic ones.

The ligands are orientated in an eclipsed formation in all cases although this will probably not be the lowest energy conformation. However, since the aim here is to determine whether a model hydrogenated system can be made to behave as if it were a methylated system this will not be a problem. As long as the calculations are made on comparable structures then the fact that each structure will not be at a global minimum will not affect the conclusions that are drawn from this work. Of course, each system will converge to a local energy minimum with respect to the metal ligand bond lengths, and this is the important point in this investigation.

In addition to the systems that were included originally, Cu^{I} and Co^{I} are added as complexes containing these oxidation states are commonly encountered. As was shown above the ligand geometries that reproduce the bond lengths in the methylated system are not consistent for one metal in different oxidation states.

Hence, calculations on real molecules will need to be parameterised according to the nature of the metal and its oxidation state.

6.3.2 Computational Details

For computational details see 6.2.2.

6.3.3 Results

Results presented below refer to geometry optimisations of the metal-ligand bond length of two ligands bound to each metal. 1-4 refer to the parameter sets described on page 122, the methyl value is calculated with the methylated derivative. The error value is the smallest error.

	1	2	3	4	Methyl	Error
H_2O	1.833	1.825	1.796	1.796	1.811	0.014
H_2S	2.183	2.180	2.186	2.182	2.160	0.020
NH_3	1.922	1.920	1.882	1.874	1.908	0.012
PH_3	2.300	2.291	2.291	2.289	2.293	0.002

Table 6.9: Calculated bond lengths and smallest errors (Å) for Zn^{II} complexes.

	1	2	3	4	Methyl	Error
H_2O	2.866	2.833	1.872	1.992	2.867	0.001
H_2S	2.041	2.038	2.534	2.502	2.055	0.014
NH_3	3.224	2.935	1.922	1.993	2.603	0.332
PH_3	2.166	2.153	3.056	3.001	2.193	0.027

Table 6.10: Calculated bond lengths and smallest errors (Å) for Zn^{0} complexes.

	1	2	3	4	Methyl	Expt.
H_2O	1.910	1.809	1.767	1.792	1.813	0.004
H_2S	2.149	2.148	2.140	2.141	2.119	0.021
NH_3	1.910	1.909	1.857	1.844	1.881	0.024
PH_3	2.275	2.295	2.231	2.226	2.138	0.088

Table 6.11: Calculated bond lengths and smallest errors (Å) for Cu^{II} complexes.

	1	2	3	4	Methyl	Expt.
H_2O	1.996	1.996	1.785	1.787	2.003	0.007
H_2S	2.063	2.061	2.154	2.161	2.061	0.000
NH_3	1.992	1.993	1.822	1.815	2.191	0.199
PH_3	2.134	2.128	2.225	2.125	2.138	0.004

Table 6.12: Calculated bond lengths and smallest errors (Å) for Cu^{0} complexes.

	1	2	3	4	Methyl	Expt.
H_2O	1.824	1.822	1.695	1.707	1.820	0.002
H_2S	2.030	2.027	2.047	2.044	2.035	0.005
NH_3	1.838	1.838	1.752	1.746	1.882	0.044
PH_3	2.077	2.072	2.069	2.064	2.089	0.012

Table 6.13: Calculated bond lengths and smallest errors (Å) for Ni^{0} complexes.

	1	2	3	4	Methyl	Expt.
H_2O	1.826	1.826	1.770	1.777	1.803	0.023
H_2S	2.162	2.159	2.145	2.060	2.041	0.018
NH_3	1.950	1.952	1.869	1.874	1.911	0.037
PH_3	2.333	2.312	2.283	2.273	2.288	0.005

Table 6.14: Calculated bond lengths and smallest errors (Å) for Co^{II} complexes.

	1	2	3	4	Methyl	Expt.
H_2O	1.861	1.858	1.754	1.760	1.820	0.038
H_2S	2.075	2.023	2.049	2.045	2.021	0.002
NH_3	1.880	1.875	1.781	1.774	1.926	0.046
PH_3	2.101	2.095	2.087	2.082	2.115	0.014

Table 6.15: Calculated bond lengths and smallest errors (Å) for Co^0 complexes.

	1	2	3	4	Methyl	Expt.
H_2O	1.872	1.866	1.725	1.803	1.840	0.026
H_2S	2.162	2.156	2.125	2.116	2.118	0.002
NH_3	1.943	1.939	1.864	1.853	1.921	0.018
PH_3	2.246	2.241	2.223	2.223	2.239	0.002

Table 6.16: Calculated bond lengths and smallest errors (Å) for Co^I complexes.

	1	2	3	4	Methyl	Expt.
H_2O	1.854	1.834	1.836	1.834	1.838	0.002
H_2S	2.190	2.190	2.196	2.197	2.168	0.022
NH_3	1.895	1.888	1.850	1.843	1.903	0.008
PH_3	2.220	2.214	2.215	2.215	2.198	0.016

Table 6.17: Calculated bond lengths and smallest errors (Å) for Cu^I complexes.

6.3.4 Discussion

Again, the results of these calculations (Tables 6.9-6.17) show that reproduction of the results obtained with the methylated derivative by the hydrogen derivative is as good as 0.02Å for the best systems. In fact, about two thirds of the systems

investigated here are reproduced to that level or better. A further quarter are found to be within 0.04Å of the methylated derivative. That leaves only five systems, Zn^0, Cu^0, Ni^0 and Co^0 with NH_3 and Cu^{II} with PH_3, where the error is greater than 0.04Å. With further investigation of the parameter set it may still be possible to improve the calculated results for these systems.

The agreement with the values calculated for the methylated derivatives has improved compared to the single ligand systems. This may be due to these systems being more chemically realistic molecules. Significantly, in the majority of cases the parameters that give the best fit for the one ligand systems also give the best fit for the two ligand systems. This is particularly emphasised when all calculated values within 0.01Å of the best value are included in the comparison. This suggests that these parameters are applicable to a particular ligand and metal with any co-ordination number. This is particularly important when real systems are considered.

Again there does not appear to be a particular correlation with the best parameter set and any metal or ligand type. However, the majority of the best results are achieved with either parameter set 1 or 2. In fact, these two sets account for approximately 90% of all the best results. These sets both use the hydrogen derivative bond lengths and this suggests that it is the bond length parameter that is more important than the angle parameter.

6.3.5 Conclusions

The use of two ligands bound to the same metal shows that it is still possible to reproduce the electronic effects of methylated ligands using the simple hydrogen

mimics. Results are often found to be as accurate as 0.02Å for the best results for each system and the largest errors are less than 0.04Å in all but a few cases. Again as seen above, small alterations in ligand geometries can have noticeable effects on metal-ligand bond distances and so even for those systems where large errors are observed it is possible that further investigation of the parameter set will enable satisfactory results to be obtained.

6.4 Conclusions

Both the single and double ligand systems show good accuracy when replacing the methyl derivatives with the simpler hydrogen systems. In most cases errors are less than 0.02Å and are generally less than 0.04Å. These levels of errors are acceptable considering that calculated values for complete systems are generally are of this level of accuracy.

Comparing the results from the double ligand systems and that of the single ligand systems a number of points can be made. Firstly the sets of ligand parameters that produces a "best fit" to the methylated derivative results is very similar in the two ligand system as was found for the one ligand system. When results that are within 0.01Å are included then the fit is almost exact. This situation is reassuring because when the number of ligands bound to the metal changes the same parameters can be used to describe the ligand system. This is an important result for future work as it appears that the same ligand parameters will be suitable for a variety of complexes.

There does not appear to be any significant correlation between the best parameter set and any metal or ligand. This has the implication that the parameters for all combinations of metal and ligand may have to be determined individually.

Overall, it is shown here that purely electronic effects in large ligands can be reproduced by much simpler and computationally more expedient hydrogen mimics. The nature of these calculations is such that steric factors are minimised and so the conclusions that are drawn here are a consequence only of the electronic effects. This bodes well for a hybrid Quantum Mechanical and Molecular Mechanical (QM/MM) treatment where electronic factors are incorporated in the QM treatment, and the steric factors to be treated with molecular mechanics. However, as the system becomes more crowded, the QM calculation will begin to include some steric interactions. The balance between the QM and MM parts should ensure that this double counting of steric interactions will not affect the calculated geometries significantly. The steric interactions of the full ligands within the MM calculation will be greater than those of the truncated mimics in the QM calculation. If necessary, some fine tuning of the MM force field may be used to overcome this situation.

References

1. D.R.Linde, *Handbook of Chemistry and Physics*, 75th edn., CRC Press, Ann Arbor, 1994, pp **9**-15 - **9**-41.

2. E.J.Baerends, D.E.Ellis and P.Ros, *Chem. Phys.*, 1973, **2**, 41.

3. (a) J.G.Snijders, P.Vernooijs and E.J.Baerends, *At. Data Nucl. Data Tables,* 1981, **26**, 483. (b) J.G.Snijders, P.Vernooijs and E.J.Baerends, *Slater Type Basis Functions for the Whole Periodic System.,* Internal Report, Free University, Amsterdam, 1981.

4. S.H.Vosko, L.Wilk and M.Nussair, *Can. J. Phys.*, 1980, **58**, 1200.

5. E.J.Baerends, D.E.Ellis and P.Ros, *Theoret. Chim. Acta.*, 1972, **27**, 339.

6. E.Magnusson and N.W.Moriarty, *J. Comp. Chem.*, 1993, **14**, 961.

7. M.Rosi and C.W.Bauschlicher, *J. Chem. Phys.*, 1989, **90**, 7264.

8. P.E.M.Siegbahn and M.R.A.Blomberg, *Chem. Phys.*, 1984, **87**, 189.

Chapter 7

Use of Truncated Ligand Mimics to Model Real Systems

7.1 Introduction

The previous chapter showed that it is possible, by altering the ligand geometry, to make a simple all hydrogen substituted ligand act electronically like an all methyl substituted derivative. As stated earlier, this is an important step towards the modelling of large systems within a combined Quantum Mechanical/Molecular Mechanical (QM/MM) method. The next step in this work is to apply this concept to a set of real complexes to determine whether this notion holds when the co-ordination sphere is more crowded by the presence of more (and different) ligands. Of course, the use of all-hydrogen ligand mimics, whilst accounting for the electronic effects, will reduce the steric bulk of the ligands considerably. Whether this will have a significant effect on the geometry of these species is uncertain at this moment although it is suggested that the steric factors are as important, if not more so, than electronic factors.

The calculations presented deal exclusively with phosphine ligands due to the abundance of species containing these ligands and also the importance in a number of catalytic species. Firstly, a number of trimethylphosphine complexes of nickel and cobalt are investigated by using the parameters obtained in the previous investigation of the metal plus one and two ligands. A slightly different approach is

applied to some nickel triphenylphosphine complexes. The parameterisation process involves the variation of the phosphine ligand geometry within a range of bond angles and bond lengths and subsequent geometry optimisation of a triphenylphosphine complex mimic. Calculated metal-ligand bond lengths are compared with the experimental values and the best parameter sets are applied to some real complexes.

7.2 Metal Trimethylphosphine Complexes

7.2.1 Introduction

A large number of complexes containing trimethylphosphine ligands are found for transition metals[1]. Especially prevalent are cobalt(I) complexes and also nickel(0) complexes. Using parameters derived from the one and two ligand systems, geometry optimisations are carried out with all trimethylphosphine ligands replaced by phosphines (PH_3). The remaining ligands are modelled completely. No symmetry constraints are applied to allow full exploration of the potential energy surface.

In total seven cobalt and two nickel complexes have been studied. These contain between four and two trimethylphosphine ligands, the remaining co-ordination sphere consisting mainly of other simple ligands such as carbonyls, nitrosyls and halides. All the complexes have either four or five ligands in the co-ordination sphere.

7.2.2 Computational Details

The details of the ADF[2] scheme have been given previously. Important points of the calculations performed here are:

a) Triple-ζ STO[3] basis sets are used in all cases with additional polarisation functions.

b) All calculations include spin-polarisation where appropriate.

c) No symmetry constraints are applied.

d) Minimal frozen cores[4] are applied, that is 2p for Co, Ni, P, and Cl, 3p for Br, 4p for I and 1s for C, O, N. Hydrogen has no frozen core.

e) H-P-H angles and H-P bond lengths are kept constant. The values are 118.83° and 1.420Å for Co and 122.69° and 1.420Å for Ni. These are the values that were found in Chapter 6 to give the best treatment of the methylated ligands.

7.2.3 Results and Discussion

Presented in Tables 7.1-7.9 are the results of geometry optimisations of nine cobalt and nickel trimethylphosphine complexes. In Figures 7.1-7.9 are illustrations of each molecule and the atom labelling system that is used in the corresponding table of results.

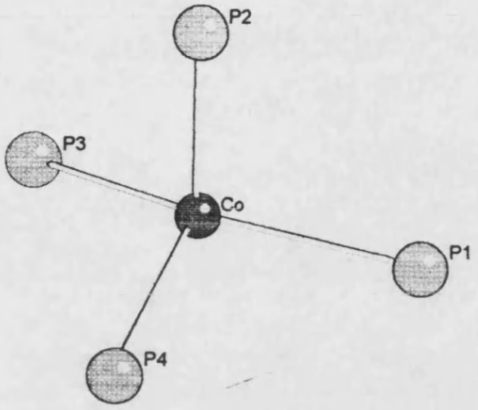

Figure 7.1: Definition of atom labels in $[Co^{I}(PMe_3)_4]^+$.

Bond	Calculated	Expt.	Error	Bond	Calculated	Expt.	Error
$Co\text{-}P_1$	2.24	2.22	0.02	$P_1\text{-}Co\text{-}P_2$	100.7	101.7	1.0
$Co\text{-}P_2$	2.29	2.25	0.04	$P_1\text{-}Co\text{-}P_3$	102.9	104.7	1.8
$Co\text{-}P_3$	2.23	2.19	0.04	$P_1\text{-}Co\text{-}P_4$	102.1	106.4	4.3
$Co\text{-}P_4$	2.29	2.25	0.04	$P_2\text{-}Co\text{-}P_3$	101.8	103.4	1.6
				$P_2\text{-}Co\text{-}P_4$	108.6	113.1	4.5
				$P_3\text{-}Co\text{-}P_4$	136.4	125.4	11.0
Av. Error			0.04	Av. Error			3.7

Table 7.1: Comparison of experimental and calculated bond lengths (Å) and angles (°)for $[Co^{I}(PMe_3)_4]^+$ (For experimental values see reference 5).

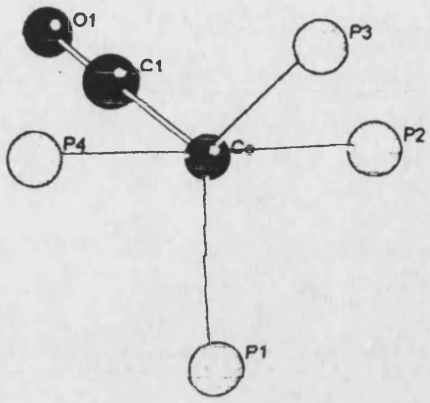

Figure 7.2: Definition of atom labels in $[Co^{I}(PMe_3)_4CO]^{+}$.

Bond	Calculated	Expt.	Error	Bond	Calculated	Expt.	Error
$Co\text{-}P_1$	2.16	2.25	0.09	$P_1\text{-}Co\text{-}P_2$	92.0	92.6	0.6
$Co\text{-}P_2$	2.13	2.21	0.08	$P_1\text{-}Co\text{-}P_3$	114.7	109.6	5.1
$Co\text{-}P_3$	2.16	2.25	0.09	$P_1\text{-}Co\text{-}P_4$	89.6	95.9	6.3
$Co\text{-}P_4$	2.13	2.22	0.09	$P_1\text{-}Co\text{-}C_1$	122.3	134.0	11.7
$Co\text{-}C_1$	1.75	1.73	0.02	$P_2\text{-}Co\text{-}P_3$	89.2	95.6	6.4
$C_1\text{-}O_1$	1.15	1.17	0.02	$P_2\text{-}Co\text{-}P_4$	176.6	163.6	13.0
				$P_2\text{-}Co\text{-}C_1$	88.3	81.6	6.7
				$P_3\text{-}Co\text{-}P_4$	92.2	95.3	3.1
				$P_3\text{-}Co\text{-}C_1$	122.9	116.4	6.5
				$P_4\text{-}Co\text{-}C_1$	88.3	82.6	5.7
				$Co\text{-}C_1\text{-}O_1$	179.9	177.3	2.6
Av. Error			0.07	Av. Error			6.2

Table 7.2: Comparison of experimental and calculated bond lengths (Å) and angles (°)for $[Co^{I}(PMe_3)_4CO]^{+}$ (For experimental values see reference 6).

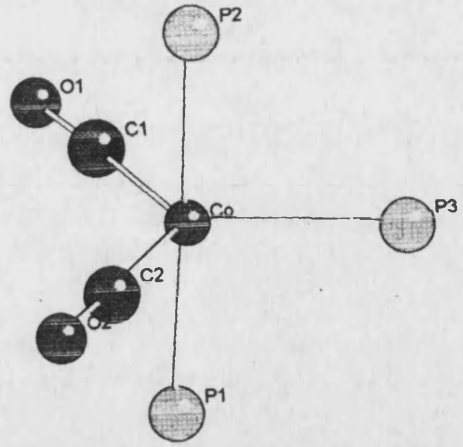

Figure 7.3: Definition of atom labels in $[Co^{I}(PMe_3)_3(CO)_2]^+$.

Bond	Calculated	Expt.	Error	Bond	Calculated	Expt.	Error
$Co\text{-}P_1$	2.14	2.21	0.07	$P_1\text{-}Co\text{-}P_2$	178.4	162.3	16.1
$Co\text{-}P_2$	2.15	2.21	0.06	$P_1\text{-}Co\text{-}P_3$	91.0	98.6	7.6
$Co\text{-}P_3$	2.17	2.25	0.08	$P_1\text{-}Co\text{-}C_1$	90.7	86.4	4.3
$Co\text{-}C_1$	1.76	1.74	0.02	$P_1\text{-}Co\text{-}C_2$	88.8	87.4	1.4
$Co\text{-}C_2$	1.76	1.77	0.01	$P_2\text{-}Co\text{-}P_3$	90.7	99.1	8.4
$C_1\text{-}O_1$	1.15	1.14	0.01	$P_2\text{-}Co\text{-}C_1$	89.4	87.4	2.0
$C_2\text{-}O_2$	1.15	1.14	0.01	$P_2\text{-}Co\text{-}C_2$	90.2	86.1	4.1
				$P_3\text{-}Co\text{-}C_1$	118.2	109.9	8.3
				$P_3\text{-}Co\text{-}C_2$	117.8	112.2	5.6
				$C_1\text{-}Co\text{-}C_2$	123.9	137.9	14.0
				$O_1\text{-}C_1\text{-}Co$	178.2	178.7	0.5
				$O_2\text{-}C_2\text{-}Co$	178.1	179.5	1.4
Av. Error			0.04	Av. Error			11.0

Table 7.3: Comparison of experimental and calculated bond lengths (Å) and angles (°)for $[Co^{I}(PMe_3)_3(CO)_2]^+$ (For experimental values see reference 7).

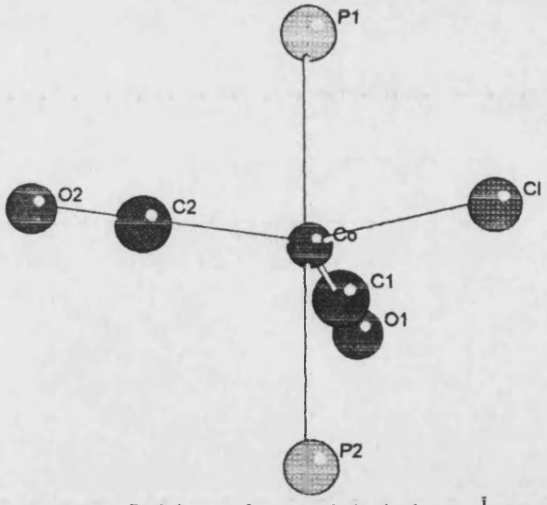

Figure 7.4: Definition of atom labels in $Co^{I}(PMe_3)_2(CO)_2Cl$.

Bond	Calculated	Expt.	Error	Bond	Calculated	Expt.	Error
$Co-P_1$	2.36	2.20	0.16	$Cl-Co-P_1$	84.9	87.6	2.7
$Co-P_2$	2.38	2.19	0.19	$Cl-Co-P_2$	84.1	87.4	3.1
Co-Cl	2.29	2.33	0.04	$Cl-Co-C_1$	129.7	122.3	6.4
$Co-C_1$	1.76	1.82	0.06	$Cl-Co-C_2$	129.0	122.3	6.7
$Co-C_2$	1.76	1.82	0.06	P_1-Co-P_2	169.0	177.0	8.0
C_1-O_1	1.17	1.09	0.08	P_1-Co-C_1	93.4	92.7	1.7
C_2-O_2	1.17	1.18	0.01	P_1-Co-C_2	93.4	92.7	4.5
				P_2-Co-C_1	93.1	88.9	4.2
				P_2-Co-C_2	94.0	88.9	5.1
				C_1-Co-C_2	101.4	115.4	14.0
				O_1-C_1-Co	178.7	175.3	3.4
				O_2-C_2-Co	178.2	179.5	1.3
Av. Error			0.08	Av. Error			5.1

Table 7.4: Comparison of experimental and calculated bond lengths (Å) and angles (°)for $Co^{I}(PMe_3)_2(CO)_2Cl$ (For experimental values see reference 8).

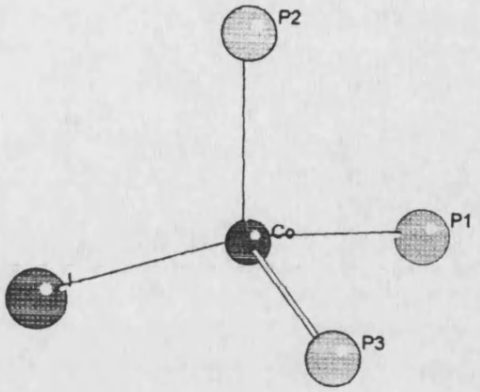

Figure 7.5: Definition of atom labels in $Co^{I}(PMe_3)_3I$.

Bond	Calculated	Expt.	Error	Bond	Calculated	Expt.	Error
Co-I	2.43	2.55	0.12	P_1-Co-P_2	101.4	105.3	3.9
Co-P_1	2.22	2.23	0.01	P_1-Co-P_3	100.9	105.3	4.4
Co-P_2	2.22	2.24	0.02	P_1-Co-I	114.2	119.3	5.1
Co-P_3	2.24	2.21	0.03	P_2-Co-P_3	102.3	106.8	4.5
				P_2-Co-I	112.6	109.8	2.8
				P_3-Co-I	122.8	109.8	13.0
Av. Error			0.05	Av. Error			5.6

Table 7.5: Comparison of experimental and calculated bond lengths (Å) and angles (°)for $Co^{I}(PMe_3)_3I$ (For experimental values see reference 9).

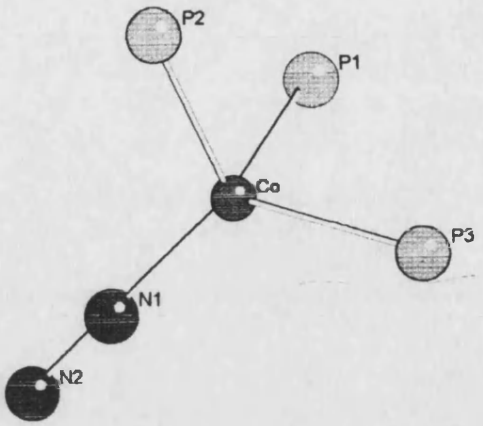

Figure 7.6: Definition of atom labels in $[Co^{I}(PMe_3)_3N_2]^{-}$.

Bond	Calculated	Expt.	Error	Bond	Calculated	Expt.	Error
$Co\text{-}P_1$	2.09	2.17	0.08	$P_1\text{-}Co\text{-}P_2$	105.7	103.5	2.2
$Co\text{-}P_2$	2.10	2.15	0.05	$P_1\text{-}Co\text{-}P_3$	106.1	103.4	2.7
$Co\text{-}P_3$	2.10	2.15	0.05	$P_1\text{-}Co\text{-}N_1$	112.0	107.4	4.6
$Co\text{-}N_1$	1.74	1.70	0.04	$P_2\text{-}Co\text{-}P_3$	105.1	102.0	3.1
$N_1\text{-}N_2$	1.14	1.19	0.05	$P_2\text{-}Co\text{-}N_1$	115.6	120.2	4.6
				$P_3\text{-}Co\text{-}N_1$	113.6	118.3	4.7
				$Co\text{-}N_1\text{-}N_2$	180.0	177.5	2.5
Av. Error			0.05	Av. Error			3.8

Table 7.6: Comparison of experimental and calculated bond lengths (Å) and angles (°)for $[Co^{I}(PMe_3)_3N_2]^{-}$ (For experimental values see reference 10).

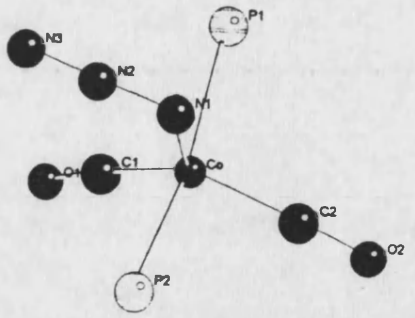

Figure 7.7: Definition of atom labels in $Co^{I}(PMe_3)_2(CO)_2N_3$.

Bond	Calculated	Expt.	Error	Bond	Calculated	Expt.	Error
$Co-P_1$	2.12	2.19	0.01	P_1-Co-P_2	156.6	173.5	16.9
$Co-P_2$	2.12	2.18	0.06	P_1-Co-C_1	95.7	94.2	1.5
$Co-C_1$	1.74	1.75	0.01	P_1-Co-C_2	97.3	90.7	6.6
$Co-C_2$	1.74	1.74	0.00	P_1-Co-N_1	77.2	87.5	10.3
$Co-N_1$	2.01	2.03	0.02	P_2-Co-C_1	93.5	90.2	3.3
C_1-O_1	1.16	1.13	0.03	P_2-Co-C_2	97.4	91.2	6.2
C_2-O_2	1.16	1.15	0.01	P_2-Co-N_1	79.3	86.2	6.9
N_1-N_2	1.21	1.18	0.03	C_1-Co-C_2	117.5	121.1	3.6
N_2-N_3	1.15	1.16	0.01	C_1-Co-N_1	124.4	117.4	7.0
				C_2-Co-N_1	118.1	121.4	3.3
				$Co-C_1-O_1$	174.1	172.6	1.5
				$Co-C_2-O_2$	174.3	172.7	1.6
				$Co-N_1-N_2$	116.6	127.9	11.3
				$N_1-N_2-N_3$	176.4	175.9	0.5
Av. Error			0.03	Av. Error			5.7

Table 7.7: Comparison of experimental and calculated bond lengths (Å) and angles (°)for $Co^{I}(PMe_3)_2(CO)_2N_3$ (For experimental values see reference 11).

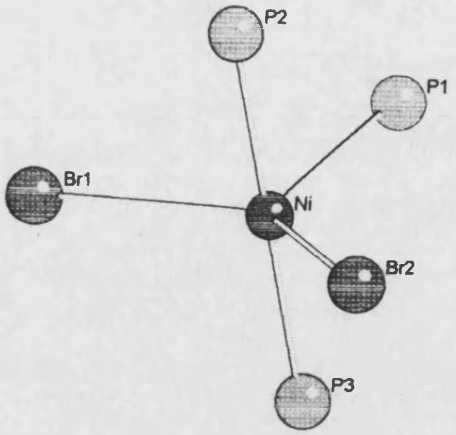

Figure 7.8: Definition of atom labels in $Ni^{II}(PMe_3)_3Br_2$.

Bond	Calculated	Expt.	Error	Bond	Calculated	Expt.	Error
$Ni\text{-}P_1$	2.20	2.20	0.00	$P_1\text{-}Ni\text{-}P_2$	88.8	96.3	7.5
$Ni\text{-}P_2$	2.13	2.21	0.08	$P_1\text{-}Ni\text{-}P_3$	91.2	96.3	5.1
$Ni\text{-}P_3$	2.18	2.21	0.03	$P_1\text{-}Ni\text{-}Br_1$	115.6	110.1	5.5
$Ni\text{-}Br_1$	2.38	2.58	0.20	$P_1\text{-}Ni\text{-}Br_2$	120.1	132.3	12.2
$Ni\text{-}Br_2$	2.37	2.43	0.06	$P_2\text{-}Ni\text{-}P_3$	179.6	167.3	12.3
				$P_2\text{-}Ni\text{-}Br_1$	81.6	87.7	6.1
				$P_2\text{-}Ni\text{-}Br_2$	81.6	86.6	5.0
				$P_3\text{-}Ni\text{-}Br_1$	98.0	86.3	11.7
				$P_3\text{-}Ni\text{-}Br_2$	98.8	86.2	12.6
				$Br_1\text{-}Ni\text{-}Br_2$	121.0	117.6	3.4
Av. Error			0.07	Av. Error			8.1

Table 7.8: Comparison of experimental and calculated bond lengths (Å) and angles (°)for $Ni^{II}(PMe_3)_3Br_2$ (For experimental values see reference 12).

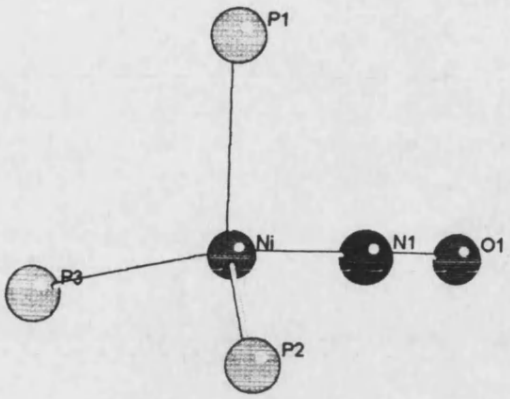

Figure 7.9: Definition of atom labels in $[Ni^0(PMe_3)_3NO]^+$.

Bond	Calculated	Expt.	Error	Bond	Calculated	Expt.	Error
$Ni-P_1$	2.22	2.23	0.01	P_1-Ni-P_2	105.6	105.0	0.6
$Ni-P_2$	2.22	2.24	0.02	P_1-Ni-P_3	104.9	105.0	0.1
$Ni-P_3$	2.22	2.24	0.02	P_1-Ni-N_1	113.9	110.0	3.9
$Ni-N_1$	1.66	1.65	0.01	P_2-Ni-P_3	106.1	107.1	1.0
$Ni-O_1$	1.15	1.14	0.01	P_2-Ni-N_1	110.7	114.6	3.9
				P_3-Ni-N_1	114.9	114.6	0.3
				$Ni-N_1-O_1$	178.8	175.4	3.4
Av. Error			0.01	Av. Error			1.9

Table 7.9: Comparison of experimental and calculated bond lengths (Å) and angles (°)for $[Ni^0(PMe_3)_3NO]^+$ (For experimental values see reference 13).

Comparing calculated and experimental bond lengths the first observation is that calculated values are, for the phosphine ligands, generally too short. The size of the underestimation ranges from 0.01-0.09Å, although in some cases there appears to

be an overestimation. It is expected that calculated phosphine-metal bond lengths will be too short due to the use of truncated hydrogen ligand mimics. The steric bulk of trimethylphosphines is apparently not well reproduced by the much smaller phosphine ligands. Although the methyl derivatives are not as bulky as the triphenylphosphine derivatives that are discussed below, they will still have sufficient bulk such that steric interactions will be considerable. The steric effects of phosphine ligands can be correlated with an easily measured parameter, the cone angle[14] ,θ, defined by a conical surface that can just enclose the van der Waals surface of all ligand atoms over all rotational functions about the M-P bond (see Figure 7.10). Typical values for cone angles are PH_3 87°, PMe_3 118° and PPh_3 145°. These values show that triphenylphosphine ligands are significantly more bulky than both the methyl and hydrogen derivatives.

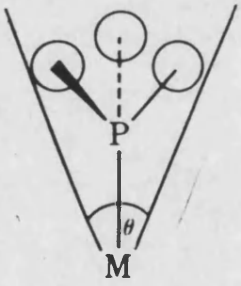

Figure 7.10: Definition of the cone angle, θ, for metal phosphine complexes.

It is not always possible to distinguish steric from electronic factors. However, in these studies some measure of the relative values can be made. In the previous chapter the one and two ligand systems investigated the electronic effects in various metal complexes. In this chapter the emphasis is towards the evaluation of steric

factors. The magnitude of electronic factors can be measured by comparing metal-ligand bond lengths calculated with a phosphine ligand (with the true PH_3 geometry) and the same bond with the trimethylphosphine ligand. In general these differences are found to be of the order of 0.01-0.04Å, although they can be as large as 0.07Å. In comparison, the magnitude of steric factors is, as discussed above, in the order of 0.01-0.09Å. However, this latter measure contains a number of assumptions. Firstly, that calculations based on the real molecule would reproduce experimental geometries exactly. Secondly, it ignores the errors introduced into these calculations by the errors inherent in the replacement of trimethylphosphine by phosphine. These errors have been shown in the previous chapter to be of the order of 0.02Å. These two approximations can have a significant effect on the perceived steric factors. Therefore, it is only possible to state that the magnitude of the steric and electronic factors appear to be approximately equal and that further investigation would be required in order to be confident in the relative effects of both steric and electronic factors.

Looking at the overall co-ordination number and the number of phosphine ligands in each complex reveals further evidence of the influence of steric factors. The nine complexes investigated can be broken down into three groups. The first group (group one) of four complexes contains systems that have a co-ordination number of four. The complexes in this group are; $[Co^{I}(PMe_3)_4]^{+}$, $Co^{I}(PMe_3)_3I$, $[Co^{I}(PMe_3)_3N_2]^{-}$ and $[Ni^{0}(PMe_3)_3NO]^{+}$. The second group (group two) contains two complexes with overall co-ordination of five but with only two phosphine ligands; $Co^{I}(PMe_3)_2(CO)_2Cl$ and $Co^{I}(PMe_3)_2(CO)_2N_3$. The final group (group three) of three

complexes have co-ordination numbers of five but contain three or more phosphine ligands; $[Co^{I}(PMe_3)_4CO]^+$, $[Co^{I}(PMe_3)_3(CO)_2]^+$ and $Ni^{II}(PMe_3)_3Br_2$. A comparison of the average errors between calculated and experimental values for the three groups reveals a number of points. The average errors in bond lengths and angles are respectively; 0.03Å and 3.8° for group one, 0.05Å and 5.4° for group two and 0.06Å and 8.4° for group three. Thus, the errors are seen to increase as the co-ordination number increases as well as the number of bulky phosphine ligands. This suggests that steric factors are an important consideration in complexes such as these. Therefore some increased account of steric interactions must be included to model complexes that have crowded co-ordination spheres as a result of either a high co-ordination number or the presence of a number of bulky ligands.

It is also noticeable that as well as there being a general trend for the phosphine-metal bond lengths to be too short, the remaining metal-ligand bonds are also generally too short. These complexes are of a more organometallic nature than the complexes studied in chapters 2-4, and so it might be expected that in order to calculate accurate geometries that it will be necessary to include gradient corrected functionals[15] to improve the LDA treatment. This point is discussed further in section 7.3.

7.2.4 Conclusions

Results of these calculations show that although the calculated geometries of these complexes are reasonably accurate, there is a general tendency to underestimate metal-ligand bond lengths. This is especially the case for the phosphine ligands

where there is an incomplete description of steric factors, although electronic factors should be well described. The size of steric effects has been shown to be relatively large, and would be expected to have adverse effects on calculated geometries of complexes similar to these if they are not accounted for. Therefore, it is necessary to include some treatment of steric factors in order to model such systems accurately and completely. This may be achieved, as proposed earlier, by the inclusion of a molecular mechanics term to account for the bulk of the ligand system without incurring increased computational costs that would result from a full DFT treatment.

7.3 Comparison of Real and Truncated Systems

7.3.1 Introduction

It has been shown above that it is possible to calculate reasonable molecular geometries of systems containing bulky alkylated ligands by replacing these groups with smaller hydrogen derivatives. However, geometries calculated using this method are not as accurate as has been shown previously with other transition metal systems (see chapters 2-4). It has been postulated above that one source of this error is due to the failure to include the true steric effects of the larger ligand. But, it is necessary to show that the LDA is capable of calculating accurate geometries for these molecules when the whole system is included. Therefore, in this section a full optimisation of the geometry of $Ni^0(PMe_3)_2(NO)(NO_2)$[16] is performed to investigate whether the LDA can give accurate geometries for such systems.

7.3.2 Computational Details

Computational details are as described in 7.2.2, with the exception that the only frozen parameters are the C-H bond lengths (1.05Å) and the H-C-H bond angles (109.5°).

7.3.3. Results and Discussion

Table 7.10 shows the results of geometry optimisation performed on the complex $Ni^0(PMe_3)_2(NO)(NO_2)$.

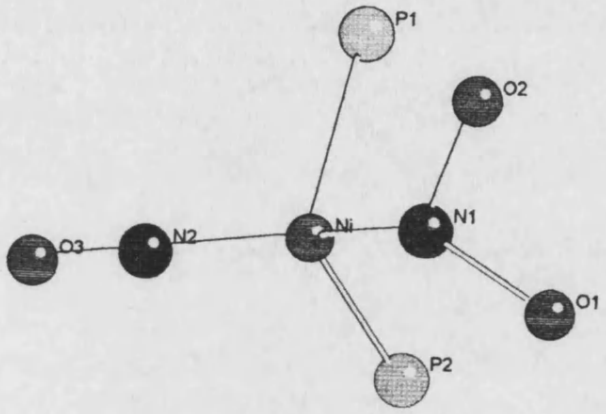

Figure 7.11: Definition of atom labels in $Ni^0(PMe_3)_2(NO)(NO_2)$.

Firstly, it can be seen that there is a general tendency for the calculated bond lengths to be shorter than the experimental values. The bonds to the phosphine ligands are found to be 0.04-0.05Å too short. This is a considerable error considering the accuracy that was found for other transition metal complexes earlier (see Chapters 2-4). However, this complex is of a more organometallic nature and as such involves more covalent bonding to a metal in a low oxidation state. It has been shown that the LDA is only a reasonable approximation to

complexes of this nature[17] and for a more accurate treatment the inclusion of gradient-corrected functionals is necessary The same behaviour is seen for the metal-nitrogen bond of the NO_2 ligand but not for NO and this suggests a more covalent picture of bonding with the former and much less so with the latter.

Bond	Expt.	Calculated	Error	Angle	Expt.	Calculated	Error
$Ni-P_1$	2.23	2.18	0.05	N_1-Ni-P_1	97.8	99.3	1.5
$Ni-P_2$	2.24	2.20	0.04	N_1-Ni-P_2	95.8	90.5	5.3
$Ni-N_1$	1.99	1.91	0.08	N_1-Ni-N_2	127.8	147.5	19.7
$Ni-N_2$	1.65	1.65	0.00	N_2-Ni-P_1	113.0	100.9	12.1
N_1-O_1	1.25	1.25	0.00	N_2-Ni-P_2	114.0	100.7	13.3
N_1-O_2	1.25	1.24	0.01	P_1-Ni-P_2	106.1	120.5	14.4
N_2-O_3	1.18	1.19	0.01	$O_1-N_1-O_2$	117.7	119.4	1.7
				$Ni-N_1-O_1$	123.4	121.4	2.0
				$Ni-N_1-O_2$	119.0	119.2	0.2
				O_3-N_2-Ni	166.7	147.8	18.9
Av. Error			0.03	Av. Error			8.9

Table 7.10: Comparison of experimental and calculated bond lengths (Å) and angles (°) for $Ni^0(PMe_3)_2(NO)(NO_2)$ (For experimental values see reference 16).

Angles at the metal centre are not accurate in all cases but in view of the need expressed above to include non-local gradient corrected functionals this is neither surprising nor disquieting. The inclusion of these corrections has been shown previously to have significant effects on the calculated potential energy surface and

can be expected to have similar effects here. So large distortions in bond angles are also possible to give more accurate calculated geometries.

7.3.4 Conclusions

From the results of the calculation performed on this complex it can be seen that when the whole of the ligand system is included there still appear to be errors in calculated geometries. Previously, the LDA was shown to give accurate geometries for transition metal complexes where the bonding was largely ionic. Complexes of this type exhibit more covalent bonding and therefore the LDA treatment is not as accurate. From other work on organometallic transition metal species the inclusion of gradient corrected functionals gives a much better treatment. It is also expected that such a result would be seen for this complex and other similar complexes. Future work may be required to validate that this is so.

7.4 Metal Triphenylphosphine Complexes

7.4.1 Introduction

Having demonstrated that it is possible to replace a methylated ligand with its truncated hydrogen derivative to represent electronic effects, the question remains as to whether a similar scheme can be adopted for larger ligands such as triphenylphosphine. In order to investigate this, a complex containing only the triphenylphosphine ligand was needed. An example of such a complex and the one used here, is $Ni^0(PPh_3)_3$[18]. Experimental bond lengths for the Ni-P bond in this molecule have an average bond length of 2.153Å.

Again, as above, the P-H bond lengths and the H-P-H angles were varied about the experimental value found for PH_3. In this case, however, bond angles are expressed in terms of a Ni-P-H angle, for which the equivalent angle for PH_3 is 118.83°. The geometry of the complex about the metal is idealised with a threefold rotation axis, close to the experimental geometry in $Ni(PPh_3)_3$ (bond angles 121.2°, 120.2° and 121.7° average 121.0°).

The P-H bond lengths were varied from 1.1 Å to 1.9 Å, and the H-P-H bond angles from 100° to 130°. This gives a suitable range of values at and around the experimental value. Ni-P bond lengths were then optimised and compared to the experimental values. This is a slightly different approach to the one outlined previously, in that there was no modelling of the full complex as this was considered a computationally expensive task, and in this case there was an experimental structure with which to compare calculated structures. The bond lengths of 36 structures were optimised. Of these, the four that reproduced the bond lengths most exactly were then used in the modelling of two further complexes $Ni^0(PPh_3)_2(SO_2)_2$[19] and $Ni^0(PPh_3)_2(CO)_2$[20] using PH_3 ligand mimics instead of PPh_3. This second set of calculations will establish whether or not the chosen parameters are capable of representing the electronic nature of the triphenylphosphine ligand in real systems.

7.4.2 Computational Details

For computational details see 7.2.2.

7.4.3 Results and Discussion

Calculations on $Ni(PPh_3)_3$ showed that of all the combinations of bond length and angle that were investigated the four presented in Table 7.11 reproduced the experimental value most closely.

As can be seen from Table 7.11 the average errors are in the region of 0.003-0.007Å which is well within acceptable error levels. Having shown that this degree of accuracy is possible for triphenylphosphine complexes using the phosphine mimic, the next stage is to investigate some other test cases and to determine which, if any, of these parameter sets is capable of reproducing complete geometries (bond lengths and angles) of more complex systems. Two suitable complexes were found, the first being bis(sulphur dioxide)bis(triphenylphosphine)nickel(0) and the second bis(carbonyl)bis(triphenylphosphine)nickel(0).

P-H Bond Length (Å)	H-P-H Bond Angle (°)	Calculated Bond Length (Å)			Av. Bond Length (Å)	Bond Length Error (Å)
		1	2	3		
1.5	100	2.162	2.165	2.154	2.160	0.007
1.6	100	2.164	2.125	2.148	2.146	0.007
1.2	110	2.150	2.154	2.146	2.150	0.003
1.1	110	2.156	2.161	2.152	2.156	0.003

Table 7.11: Comparison of calculated and experimental bond lengths (Å) for $Ni(PPh_3)_3$, calculated with various phosphine bond lengths and angles (For experimental values see reference 18).

Full geometry optimisations of the metal centre were carried out, the only fixed parameters were the P-H bond lengths and the H-P-H angles that were variously fixed at the values given above. No symmetry constraints were used to allow complete optimisation of all other degrees of freedom.

The calculated geometries and errors for each complex are presented in Tables 7.12-7.13 ($Ni^0(PPh_3)_2(SO_2)_2$) and Tables 7.14-7.15 ($Ni^0(PPh_3)_2(CO)_2$)) below. For the sulphur dioxide complex the average errors in bond lengths are very similar at 0.06-0.07Å for all the phosphine parameter sets. However, significant differences are observed in the calculated bond angles with average errors in the range of 3.2-14.0°. Errors of the magnitude of 14°, found with set 2, are too large to consider when modelling real complexes. However, the remaining errors are all less than 10° and this is certainly acceptable especially when the effect of the steric bulk of these ligands is ignored. Overall the fourth parameter set appears to give the best treatment of the system with average errors of 0.06Å and 3.2°.

Quite large errors are observed for the SO_2 group, and these errors significantly effect the overall average errors. Introducing gradient corrected functionals would be expected to reduce the size of these errors and hence the overall average errors. The fact that the phosphine parameters are obtained by reproducing experimental data indicates that both steric and electronic effects have been accounted for. However, the magnitude of the steric interactions will vary as a function of the total co-ordination number and the bulk of the ligands, so it will still be necessary to include the MM term to fully account for steric factors.

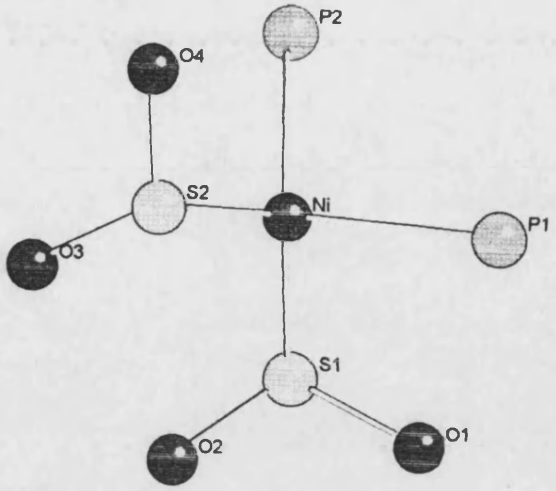

Figure 7.12: Definition of atom labels in $Ni^0(PPh_3)_2(SO_2)_2$.

Bond	Expt.	1	Error	2	Error	3	Error	4	Error
$Ni-P_1$	2.23	2.21	0.02	2.19	0.04	2.19	0.04	2.20	0.03
$Ni-P_2$	2.26	2.21	0.05	2.19	0.07	2.20	0.06	2.21	0.05
$Ni-S_1$	2.06	2.05	0.01	2.05	0.01	2.07	0.01	2.06	0.00
$Ni-S_2$	2.08	2.05	0.03	2.06	0.02	2.06	0.02	2.06	0.02
S_1-O_1	1.32	1.50	0.18	1.47	0.15	1.48	0.16	1.47	0.15
S_1-O_2	1.42	1.47	0.05	1.51	0.09	1.48	0.06	1.48	0.06
S_2-O_3	1.39	1.48	0.09	1.47	0.08	1.47	0.08	1.48	0.09
S_2-O_4	1.41	1.50	0.09	1.52	0.11	1.48	0.07	1.48	0.07
Av. Error			0.06		0.07		0.06		0.06

Table 7.12: Comparison of calculated and experimental bond lengths (Å) in $Ni^0(PPh_3)_2(SO_2)_2$ (For experimental values see reference 19).

Angle	Expt.	1	Error	2	Error	3	Error	4	Error
P_1-Ni-P_2	109.4	107.4	2.0	102.6	6.8	107.9	1.5	107.7	1.7
P_1-Ni-S_1	107.4	93.8	13.6	126.9	19.5	113.0	5.6	104.9	2.5
P_1-Ni-S_2	115.8	122.8	7.0	90.0	25.8	105.4	10.4	112.6	3.2
P_2-Ni-S_1	111.3	127.1	15.8	93.5	17.8	104.4	6.9	114.1	2.8
P_2-Ni-S_2	107.8	95.7	12.1	130.2	22.4	114.6	6.8	106.2	1.6
S_1-Ni-S_2	105.1	112.6	11.5	116.8	11.7	111.8	6.7	111.5	6.4
O_1-S_1-O_2	112	115.2	3.2	114.5	2.5	116.5	4.5	116.7	4.7
O_3-S_2-O_4	119	114.8	4.2	113.8	5.2	116.6	2.4	116.5	2.5
Av. Error			7.9		14.0		5.6		3.2

Table 7.13: Comparison of calculated and experimental bond angles (°) in $Ni^0(PPh_3)_2(SO_2)_2$ (For experimental values see reference 19).

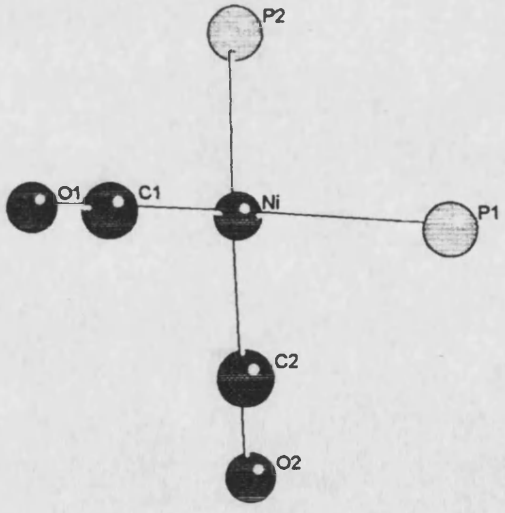

Figure 7.13: Definition of atom labels in $Ni^0(PPh_3)_2(CO)_2$.

Bond	Expt.	1	Error	2	Error	3	Error	4	Error
$Ni\text{-}P_1$	2.22	2.22	0.00	2.20	0.02	2.21	0.01	2.21	0.01
$Ni\text{-}P_2$	2.22	2.22	0.00	2.20	0.02	2.21	0.02	2.21	0.01
$Ni\text{-}C_1$	1.76	1.76	0.00	1.75	0.01	1.76	0.00	1.75	0.01
$Ni\text{-}C_2$	1.76	1.76	0.00	1.76	0.00	1.76	0.00	1.75	0.01
$C_1\text{-}O_1$	1.14	1.16	0.02	1.16	0.02	1.16	0.02	1.16	0.02
$C_2\text{-}O_2$	1.14	1.16	0.02	1.16	0.02	1.16	0.02	1.16	0.02
Av. Error			0.01		0.01		0.01		0.01

Table 7.14: Comparison of calculated and experimental bond lengths (Å) in $Ni^0(PPh_3)_2(CO)_2$ (For experimental values see reference 20).

Angle	Expt.	1	Error	2	Error	3	Error	4	Error
$P_1\text{-}Ni\text{-}P_2$	117.2	105.0	12.2	99.2	18.0	105.9	11.2	107.6	9.6
$P_1\text{-}Ni\text{-}C_1$	109.4	108.4	1.0	109.6	0.2	108.1	1.4	108.2	1.2
$P_1\text{-}Ni\text{-}C_2$	104.0	107.3	3.3	110.0	6.0	110.7	6.7	106.6	2.6
$P_2\text{-}Ni\text{-}C_1$	104.0	108.4	4.4	108.8	4.8	109.8	5.8	109.3	5.3
$P_2\text{-}Ni\text{-}C_2$	109.4	108.9	0.5	110.0	0.6	107.2	2.2	108.3	1.1
$C_1\text{-}Ni\text{-}C_2$	113.1	118.1	5.0	117.7	4.6	114.9	1.8	114.7	1.6
$O_1\text{-}C_1\text{-}Ni$	178.2	180.0	1.8	179.1	0.9	177.3	0.9	178.0	0.2
$O_1\text{-}C_2\text{-}Ni$	178.2	180.0	1.8	180.0	1.8	178.9	0.7	178.0	0.2
Av. Error			3.8		5.4		3.8		2.7

Table 7.15: Comparison of calculated and experimental bond angles (°) in $Ni^0(PPh_3)_2(CO)_2$ (For experimental values see reference 20).

The carbonyl complex gives calculated errors that are much reduced from the sulphur dioxide complex especially the average errors in bond length. However, it must be noted that a significant proportion of the average errors for the former complex are due to errors in the sulphur dioxide and not in the phosphines. The average bond length errors are 0.01Å and the average bond angle errors are 2.7-5.4°. Again, the best fit is found with parameter set 4 although, for this complex, all the parameters sets give accurate geometries.

Having established that the best set of parameter values for modelling nickel(0) triphenylphosphine complexes is to use a P-H bond length of 1.1Å and a H-P-H bond angle of 110°, the next stage is to test these values on a number of other triphenylphosphine complexes. A further three complexes were investigated; $Ni^0(PPh_3)_3(SO_2)_2$[19], $Ni^0(PPh_3)_2(N_3)(NO)$[21] and $Ni^{II}(PPh_3)_2(NO)Cl$[22] Again full geometry optimisations were carried out with no symmetry constraints and the only fixed parameters were those of the P-H bond lengths and H-P-H angles as described above. The results are presented in Tables 7.16-7.18 below.

Studying the results of calculations on these three triphenylphosphine complexes it is clear that the errors in bond lengths and angles are in some cases quite large. Even the average errors are generally of an unacceptable level. Bond lengths are in most cases calculated as being too short when compared to experimental values.

Although the phosphines have been parameterised empirically there still appears to be some significant errors in metal-phosphorus bond lengths. It was shown above that errors in bond lengths may also be due to the fact that the parameterisations were performed at the LDA level and this is not a good

approximation for these complexes. However, the parameterisation was performed by comparison with experimental structures and so this source of error should have been removed, for the phosphine ligands, and so these errors can be attributed to the neglect of steric interactions. Some treatment of steric effects is included in the parameterisation based on fitting of experimental data. However, the magnitude of steric effects will vary from complex to complex. Therefore, it will generally be necessary to include the MM term in order to obtain a full treatment of the steric effects in all complexes.

Bond angles are not affected in a uniform way, some are found to be too large others too small and this is to be expected as, for example, two phosphines will approach each other more closely than would be the case with the full ligand due to the decreased steric repulsion so it could be envisaged that the P-M-P angle would decrease and other angles would increase as a consequence of this. However, this will not be a straightforward relationship and will depend on the number and nature of all the ligands in the system.

By treating the complex $Ni^{II}(PPh_3)_2(NO)Cl$ with a nickel +2 oxidation state, the nitrosyl is forced into a bent geometry NO^- species. However, the experimental geometry suggests a more linear bonding mode which would be consistent with a NO^+ species and a nickel zero oxidation state. Therefore, using a nickel zero oxidation state may considerably reduce the error in the calculated metal-nitrosyl bond angle.

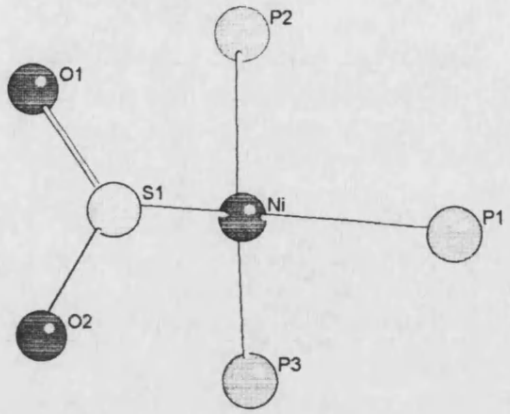

Figure 7.14: Definition of atom labels in $Ni(PPh_3)_3SO_2$.

Bond	Calculated	Expt.	Error	Angle	Calculated	Expt.	Error
$Ni-P_1$	2.21	2.28	0.07	P_1-Ni-P_2	114	113.4	0.6
$Ni-P_2$	2.19	2.23	0.04	P_1-Ni-P_3	111.5	111.7	0.2
$Ni-P_3$	2.19	2.27	0.08	P_1-Ni-S	102.8	100.5	2.3
Ni-S	2.03	2.04	0.01	P_2-Ni-P_3	106.2	114.3	8.1
$S-O_1$	1.49	1.45	0.04	P_2-Ni-S	111.3	109.5	1.8
$S-O_2$	1.49	1.45	0.04	P_3-Ni-S	111.2	106.3	4.9
				O_1-S-O_2	114.1	113.4	0.7
Av. Error			0.05				2.7

Table 7.16: Comparison of calculated and experimental bond lengths (Å) and bond angles (°) for $Ni(PPh_3)_3SO_2$ (For experimental values see reference 19).

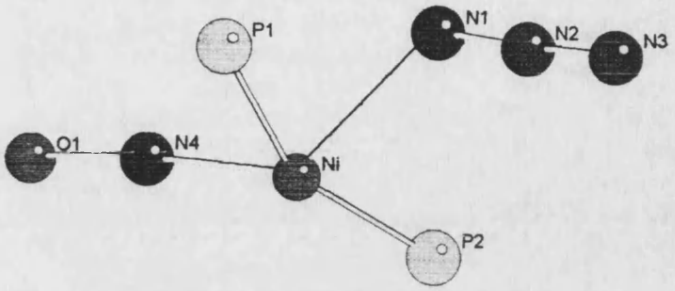

Figure 7.15: Definition of atom labels in $Ni(PPh_3)_2(N_3)(NO)$.

Bond	Calculated	Expt.	Error	Angle	Calculated	Expt.	Error
$Ni-P_1$	2.19	2.26	0.07	P_1-Ni-P_2	113.4	120.7	7.3
$Ni-P_2$	2.21	2.31	0.10	P_1-Ni-N_1	97.1	101.9	4.8
$Ni-N_4$	1.95	2.02	0.07	P_1-Ni-N_4	104.3	101.4	2.9
N_1-N_2	1.65	1.69	0.04	P_2-Ni-N_1	90.5	95.4	4.9
N_2-N_3	1.16	1.28	0.12	P_2-Ni-N_4	116.9	110.2	6.7
N_4-O_1	1.17	1.17	0.00	N_1-Ni-N_4	133.3	129.2	4.1
				$Ni-N_1-N_2$	117.4	128.2	10.8
				$N_1-N_2-N_3$	178.0	175.1	2.9
				$Ni-N_4-O_1$	154.9	152.9	2.0
Av. Error			0.09				4.8

Table 7.17: Comparison of calculated and experimental bond lengths (Å) and bond angles (°) for $Ni(PPh_3)_2(N_3)(NO)$ (For experimental values see reference 19).

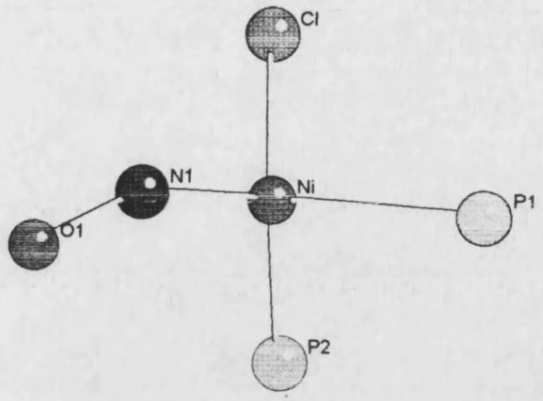

Figure 7.16: Definition of atom labels in $Ni^{II}(PPh_3)_2(NO)Cl$.

Bond	Calculated	Expt.	Error	Angle	Calculated	Expt.	Error
$Ni\text{-}P_1$	2.19	2.26	0.07	$P_1\text{-}Ni\text{-}P_2$	108.7	121.1	12.4
$Ni\text{-}P_2$	2.21	2.29	0.08	$P_1\text{-}Ni\text{-}N_1$	111.9	103.8	8.1
$Ni\text{-}N_1$	1.64	1.99	0.35	$P_1\text{-}Ni\text{-}Cl$	86.9	103.0	16.1
Ni-Cl	2.26	2.12	0.14	$P_2\text{-}Ni\text{-}N_1$	124.5	104.7	19.8
$N_1\text{-}O_1$	1.17	1.12	0.05	$P_2\text{-}Ni\text{-}Cl$	85.4	99.4	14.0
				$N_1\text{-}Ni\text{-}Cl$	132.1	126.9	5.2
				$Ni\text{-}N_1\text{-}O_1$	163.0	129.0	34.0
Av. Error			0.14				15.4

Table 7.18: Comparison of calculated and experimental bond lengths (Å) and bond angles (°) for $Ni^{II}(PPh_3)_2(NO)Cl$ (For experimental values see reference 22)

7.4.4 Conclusions

The use of ligand mimics has been shown to be a relatively accurate method for the calculations of molecular geometries of transition metal complexes containing triphenylphosphine ligands. A set of geometry parameters for phosphine ligands has been found so as to represent the electronic effects of the bulkier ligand. These parameters were initially found from studying a nickel tris(triphenylphosphine) complex, and further refined with two test molecules. The use of these parameters in other real molecules has shown that although reasonable accuracy is obtained, there is a need to account for not only electronic but also steric effects in order to calculate accurate geometries using this method.

7.5 Conclusions

Overall, it appears from all the results presented in this chapter that it is possible to calculate reasonable geometries using the truncated phosphines to replace more complex trimethyl- and triphenylphosphines. However, the neglect of steric interactions can introduce errors that are unacceptably large. In addition, the complexes that have been investigated here are generally organometallic and as such tend to exhibit covalent bonding. This introduces two possible sources of error in these calculations. Firstly, the parameterisation of the electronic effects was performed within the LDA and as such this may not be a complete and accurate treatment for these species. Secondly, the remainder of the complex not treated within the truncation scheme may be inaccurately represented by the use of the LDA and some form of gradient corrected functionals may be required.

Therefore, further work is required to investigate the effect on the parameter sets, calculated previously for the steric interactions, on the introduction of gradient corrected functionals. Also an investigation is required of the magnitude and effect of steric interactions by introducing a molecular mechanics term into the procedure.

Also, a further investigation of the $Ni^{II}(PPh_3)_2(NO)Cl$ species may be required with the nickel in a zero oxidation state in order to improve the treatment of the metal-nitrosyl bonding.

References

1. J.Elmsey and D.Hakk, "*The Chemistry of Phosphines*", Harper & Row, London, 1976, Chapter 2.

2. E. J. Baerends D. E. Ellis and P. Ros, *Chem. Phys.*, 1973, **2**, 41.

3. J.G.Snijders, P.Vernooijs and E.J.Baerends, *At. Data. Nucl. Data. Tables*, 1981, **26**, 483.

4. E. J. Baerends D. E. Ellis and P. Ros, *Theoret. Chim. Acta*, 1972, **27**, 339.

5. L.C.A.de Carvalho, M.Dartiguenave, Y.Dartiguenave and A.L.Beauchamp, *J. Am. Chem. Soc.*, 1984, **106**, 6848.

6. Y.Perez, M.Dartiguenave, Y.Dartiguenave, J.F.Britten and A.L.Beauchamp, *Organometallics*, 1990, **9**, 1041.

7. Y.Perez, A.Kerkeni, M.Dartiguenave, Y.Dartiguenave, F.Belanger-Gariepy and A.L.Beauchamp, *J. Orgamometallic. Chem.*, 1987, **323**, 397.

8. R.A.Jones, M.H.Seeberger, A.L.Stuart, B.R.Whittlesey and T.C.Wright, *Acta. Cryst.*, 1986, **C42**, 399.

9. J.A.Bandy, J.C.Green and O.N.Kirchner, *Acta. Cryst.*, 1985, **C41**, 1179.

10. H.F.Klein, R.Hammer, J.Wenninger, P.Freidrich and G.Huttner, *Z. Naturforsch. Teil. B*, 1978, **33**, 1267.

11. K.W.Chiu, G.Wilkinson, M.Thornton-Pett and M.B.Hutchinson, *Polyhedron*, 1984, **3**, 79.

12. J.W.Dawson, J.McLennan, W.Robinson, A.Merle, M.Dartiguenave, Y.Dartiguenave and H.B.Gray, *J. Am. Chem. Soc.*, 1974, **96**, 4428.

13. G.Elbaze, F.Dahan, M.Dartiguenave and Y.Dartiguenave, *Inorg. Chim. Acta*,

13. G.Elbaze, F.Dahan, M.Dartiguenave and Y.Dartiguenave, *Inorg. Chim. Acta*, 1984, **87**, 91.

14. C.A.Tolman, *Chem. Rev.*, 1977, **77**, 313.

15. (a) Becke, *Chem. Phys.*, 1986, **84**, 4524. (b) P. Perdew, *Phys. Rev.*, 1986, **B33**, 8822.

16. J.Kriege-Simondsen, G.Elbaze, M.Dartiguenave, R.D.Feltham and Y.Dartiguenave, *Inorg. Chem.*, 1982, **21**, 230.

17. T.Ziegler, Chem. Rev., 1991, **91**, 651.

18. D.Dick, D.Stephen and C.Campana, *Can. J. Chem.*, 1990, **68**, 628.

19. D.C.Moody and R.R.Ryan, *Inorg. Chem.*, 1979, **18**, 223.

20. C.Kruger and Y.-H.Tsay, *Cryst. Struct. Commun.*, 1974, **3**, 455.

21 L.R.Hanton and P.R.Raithby, *Inorg. Chem.*, 1971, **10**, 1952.

22 K.J.Haller and J.H.Enemark, *Inorg. Chem.*, 1978, **17**, 3552.

Chapter 8

A Combined Quantum Mechanical-Molecular Mechanical Method for the Study Of Transition Metal Systems

8.1 Introduction

The preceding chapters have shown variously that it is possible to reproduce the electronic effects of large alkyl and aryl substituted ligands by the use of the much smaller and hence computationally more expedient hydrogen derivatives. Studies of systems containing phosphine ligands have shown that the variation of ligand geometry can produce an accurate representation of these ligands with different transition metals in different oxidation sates. However, whilst these truncated ligands are capable of reproducing electronic factors they are less capable of treating steric factors, principally due to their reduced steric bulk.

In order to make a complete treatment of these complexes it is necessary to be able to include steric effects as well as the electronic effects. As has previously been stated this would be too expensive a task to carry out completely within *ab initio* methods for molecules of this size. Molecular mechanics is not capable of accurately treating transition metal complexes and certainly cannot be used model reaction mechanisms.

This problem can be overcome by the use of a combined Quantum Mechanical-Molecular Mechanical (QM/MM) method as has been described in Chapter 5. A

number of approaches have been taken to formulating these combined methods[1,2,3], and the application to which the method is to be used influences its nature. The method that is presented in this chapter is initially designed to calculate molecular geometries of transition metal complexes. Further work will lead to further applications in the calculation of transition states and the elucidation of reaction mechanisms.

8.2 Computational Details

The method presented here uses as its QM part the ADF program of Baerends et al.[4], in-house MM software is used for the MM part[5]. The software used uses a typical MM treatment[6]. The parameterisation of the QM part has been described previously but will be briefly outlined here. The MM part has not previously been explained and so this is outlined below.

The QM region is treated using Density Functional Theory (DFT). The division of the system into its respective QM and MM regions is discussed below. The atoms of the QM region are augmented by terminal hydrogen atoms to replace the bulk of the ligand system. The DFT calculations are performed with no symmetry constraints as few of these complexes will have symmetry of any kind. STO basis sets[7] are used at the triple-ζ level with polarisation functions added to all atoms including the terminal hydrogens. The frozen core approximation is employed[8], although in each case the core is only frozen to the minimum level. Spin-polarisation is included as many of the system will have a number of unpaired

electrons. The LDA[9] is used, although it has been stated previously that it may prove necessary to include some form of gradient corrected functionals.

The basic concepts of the MM method have been outlined in Chapter 1. The MM force field includes a number of terms; a bond stretch term, an angle bend term, a torsional term and a non-bonded term. Each of these terms needs to be parameterised for each specific molecule (additional terms may be included where necessary). Values for these terms have been determined by analysing a large number of molecules and determining average values for each particular parameter

A Morse potential is employed to describe the bond deformations rather than a harmonic term, more commonly used for traditional molecular mechanics force fields, this is in recognition that large distortions from equilibrium bond lengths may be encountered in these complexes. The parameters of the Morse potential expression, D_o, b_o and α, representing the heat of formation of the bond, the equilibrium bond length and the gradient of the Morse potential respectively. These and other parameter values are obtained from standard values calculated from a wide variety of organic complexes and averaged for each particular bond type (similarly for angles, torsions etc). A harmonic expression is employed for the angle term with the parameters of K_θ (force constant) and θ_o (ideal bond angle). Torsional terms are treated with a cosine function, the parameters are K (force constant), n (no. of minima/maxima in the torsion barrier) and S (sign applied to cosine function). Non-bonded terms are calculated using a Lennard-Jones potential with constants A and B for each atom type. See 8.4.2 for the form of these functions.

In all cases MM interactions involving distortion around the central metal term are set to zero, this includes all M-L bond terms, all L-M-L angle terms (X-L-M angle terms are non-zero) and all torsional terms involving the metal atom. Non-bonded terms are discounted for all interactions involving the central metal, in fact only 1,5 interactions and greater are included.

8.3 Methodology

The basis of this method is that it is possible to separate the electronic and steric effects present in transition metal complexes and to treat them separately. The electronic effects are treated by DFT using truncated ligand systems whereas the steric effects are treated using a MM approach. The implementation of this combined QM/MM method involves a number of separate steps. These steps, outlined below, are followed in strict sequence until the calculation is found to have converged.

The steps are:

1) Division of system into QM and MM regions

2) Generation of starting co-ordinates for QM atoms.

3) Addition of terminal hydrogens (according to pre-determined rules) to mimic electronic nature of bulkier ligand types.

4) One step geometry optimisation of QM atoms.

5) Calculation of Cartesian energy gradients for QM atoms.

6) Addition of MM atoms to give co-ordinates of whole system.

7) One cycle minimisation with QM atom gradients included.

8) Determine whether convergence has occurred (if so proceed to step 11).

9) Optimise geometry of MM atoms with QM atoms at fixed positions.

10) Calculate new co-ordinates.

11) Calculate finishing co-ordinates and stop.

Continue steps 2-10 until convergence has occurred.

Firstly, the system under investigation must be separated into its QM and MM regions. This is generally achieved by taking the metal and the first co-ordinated atoms to represent the QM region and the remainder as the MM region. The exception to this is that fairly small ligands such as CO, NO and SO_2 are treated entirely within the QM region. Figure 8.1 shows the partitioning of $[Co^{I}(PMe_3)_4CO]^+$ into its QM and MM regions and the subsequent addition of terminal hydrogens to the QM atoms to give the full QM region.

Starting co-ordinates of the QM atoms are derived according to typical bond lengths of similar complexes, with angles chosen to reflect regular geometries unless other information giving evidence to the contrary is available. Once the co-ordinates of the QM atoms have been defined it is necessary to add terminal hydrogens to all the truncated ligands so that the electronic effects of these ligands are well represented. The positions of these hydrogens are calculated by previously determined rules (see previous chapters). The bond length and angle parameters reflect the nature of the ligand, the metal and the metal oxidation state. Torsion angle values are initially set at regular values, such as 0°, 120° and 240° for three hydrogens attached to a single phosphorus (torsion angle defined with respect to the phosphorous, the metal and the same other ligand atom).

Once the co-ordinates of the QM atoms, including the terminal hydrogens, have been calculated, the QM input file can be generated. The details of the QM calculation have been described above. A single step geometry optimisation is performed. When the SCF calculation is converged, a set of Cartesian energy gradients is calculated. These gradients are extracted for use in the subsequent MM calculation, although the gradients for the terminal hydrogens are excluded as these atoms will not be present in the MM atom set.

To generate the MM co-ordinates, the QM atom co-ordinates are taken and then the remaining ligands are added by the use of idealised internal co-ordinate definitions for all MM atoms. Standard bond lengths and angles are used to determine these co-ordinates for the first cycle only. Subsequent cycles will use the co-ordinates of the previous minimised MM calculation, as the atoms are not allowed to move within the QM optimisation.

The MM program requires a number of defined parameters and these are contained in three input files (plus a separate file that contains the QM atom gradients). These consist of a co-ordinate file, a potential file and a run file. Firstly, the co-ordinate file simply contains a list of all the atoms involved in the MM calculation. The second file contains all the potential parameters for all the terms required to parameterise the system. These are all bond terms, all angle terms and all torsion terms. In addition a set of non-bonded parameters for all atoms is added except the central metal atom. No M-X bond stretch, X-M-X angle bend or torsional terms involving the metal centre are included in the potential file. These terms cannot be accurately parameterised empirically and are instead treated by the

QM atom energy gradients. The MM scheme calculates a set of gradients for each atom based on the MM force field as it applies to each atom. The routine that adjusts the MM atom co-ordinates after each cycle is intercepted and the QM atom gradients are added to those calculated by the MM scheme for these atoms.

The final file, the run file, defines the atom types that are involved in the MM calculation. Especially important are the weights of each atom type that are important to determine the movement of each atom within the force field. Also contained in this file is an explicit connectivity table which determines which atoms are bonded to each other and various parameters that determine exactly how the program runs. Once the MM input files are set up, with the exception of the co-ordinate file, they remain unchanged throughout the procedure.

The MM calculation contains two separate parts that are incorporated together. The first step is a single cycle of optimisation with the QM atom gradients included for all the QM atoms to represent distortion at the metal centre. Terms for all the MM atoms are also included. Since the gradients for the QM atoms were calculated at a single geometry, they cannot be applied once the geometry has changed from that at which they were calculated. Hence, the gradients for all the QM atoms are set to zero on all subsequent cycles. The MM geometry is then minimised whilst the QM atoms remain fixed.

The final co-ordinates of all the atoms are saved for use in subsequent cycles. The next step is to prepare the new input file for the QM calculation. This involves extracting the QM atom co-ordinates and adding the terminal hydrogens as before with the torsion angle values used are those of the atoms that the hydrogens

notionally replace so that this is a better approximation to the geometry of the real system.

This procedure is then continued with a sequence of QM and MM optimisations with co-ordinates updated on each MM cycle and new QM atom gradients generated on each QM cycle.

The final step is to determine when the calculation has converged. On the first cycle of each MM calculation the QM atom gradients are calculated as a sum of their QM and MM constituents. When the sum of these two terms is zero then the QM atoms will not move and so the calculation is deemed converged. In reality it is unlikely that the gradients on all QM atoms will ever all be zero. Therefore, by looking at the change in bond lengths of atoms in the QM region a convergence criterion can be applied. However, actual calculations are required to investigate the convergence properties of these calculations.

8.4 Calculations on $[Co^{I}(PMe_3)_4CO]^+$

8.4.1 Introduction

As a test of the combined method the complex $[Co^{I}(PMe_3)_4CO]^+$ was chosen. This complex had previously been treated by the simple truncated ligand only method and the results of that study had shown that although the overall errors in the calculated geometry were reasonable (av. bond length error 0.06Å, av. bond angle error 6.2°) they were certainly not of a comparable level to those calculated previously with other transition metal complexes. In particular the metal-phosphorus bond lengths were shown to be in error by as much as 0.09Å. It has

already been postulated that this is caused by the neglect of steric factors in these calculations. By carrying out the calculation with the inclusion of an MM term it is hoped the these errors will be significantly reduced.

8.4.2 Computational Details

The combined method has been described above, as well as general computational details. The separation of the system into its QM and MM regions is in this case a relatively straightforward decision. The QM region is determined as being the central cobalt atom, the four phosphorus donors and both the carbon and oxygen of the carbonyl group. These seven atoms are then augmented by a further twelve hydrogen atoms, three for each phosphine ligand, during the QM calculation. The positions of these hydrogens are determined by the results obtained previously. In this case the P-H bond length is 1.420Å and the H-P-H angle is 118.83°. For the MM calculations these hydrogens are removed and replaced by the methyl groups as found in the real system. The values of all the parameters used in the MM calculations are given in Tables 8.1-8.4. The atoms used in the QM and MM calculations are shown in Figure 8.1.

The form of the MM term is as given by (8.1) below:

$$E_{tot} = E_{str} + E_{bend} + E_{tor} + E_{vdw} \qquad (8.1)$$

where the terms are defined as:

Bond Stretch: $E_{str} = D_O[1-\exp(-e^{\alpha(b-bo)})]^2$

Angle Bend: $E_{bend} = (1/2)K_\theta(\theta - \theta_O)^2$

Torsion: $E_{tor} = K(1 + S(\cos n\omega))$

Van der Waals: $E_{vdw} = A/r^9 - B/r^6$

The following atom types are used in this calculation.

cl - cobalt

cz - carbonyl carbon

oz - carbonyl oxygen

cv - organic carbon

hz - organic hydrogen

pp - organic phosphorus

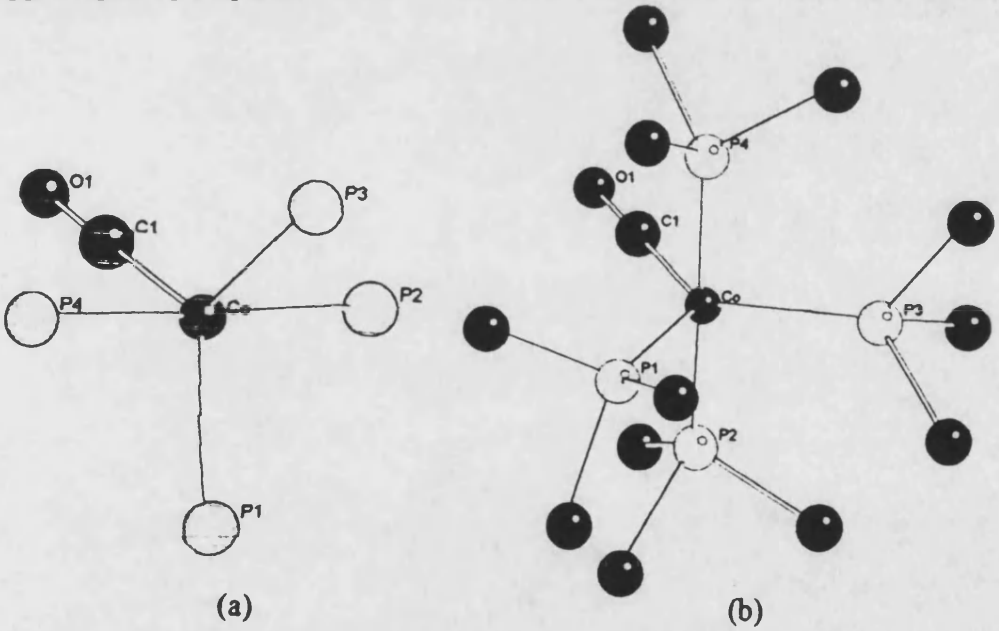

Figure 8.1 : Atom definition of $[Co(PMe_3)_4CO]^+$ for QM calculation (a) and MM calculation (b). (Hydrogens omitted for clarity)

Bond	D	b_o	α
cl - cz	0	0	0
cz - oz	0	0	0
cl - pp	0	0	0
pp - cv	68.0	1.85	2.0
hz - cv	68.0	1.05	2.0

Table 8.1: Bond stretch parameters for all bond interactions . D - force constant (kcal $mol^{-1}Å^{-2}$), b - ideal bond length (Å) and α - steepness of Morse potential well.

Angle	K_θ	θ_O
pp - cl - pp	0	0
pp - cl - cz	0	0
oz - cz - cl	0	0
hz - cv - hz	36.0	109.5
hz - cv - pp	57.3	109.5
cv - pp - cl	86.3	118.83
cv - pp - cv	86.3	99.00

Table 8.2: Angle bend parameters for all angle terms.
K_θ - force constant (kcal $mol^{-1}{}^{o-2}$) and θ_O - ideal bond angle (°).

Torsion Angle	K	n	S
oz - cz - cl - pp	0	0	0
cz - cl - pp - cv	0	0	0
cl - pp - cv - hz	0	0	0
pp - cl - pp - cv	0	0	0
cv - pp - cv - hz	0.8	3	1

Table 8.3 : Force constants, K (kcal mol^{-1}) n and S values for all torsion terms.

Atom type	A	B
hz	654.295	41.085
cv	14539.000	397.436
cz	14539.000	397.436
oz	16501.100	748.318
pp	13549.500	376.305
cl	0.000	0.000

Table 8.4: Non-bonded parameters for all atoms. A - constant, B - constant.

8.4.3 Results and Discussion

The optimisation of this complex has been carried out, as outlined above, with alternate DFT and MM steps. The results presented below (Figures 8.2 - 8.7) show

the calculated bond lengths of the bonds found in the QM region. Table 8.5 shows the experimental bond lengths.

Bond	Bond Length (Å)
Co - C_1	1.728
C_1 - O_1	1.167
Co - P_1	2.214
Co - P_2	2.219
Co - P_3	2.252
Co - P_4	2.246

Table 8.5: Experimental[10] bond lengths in $Co^{I}(PMe_3)_4CO$.

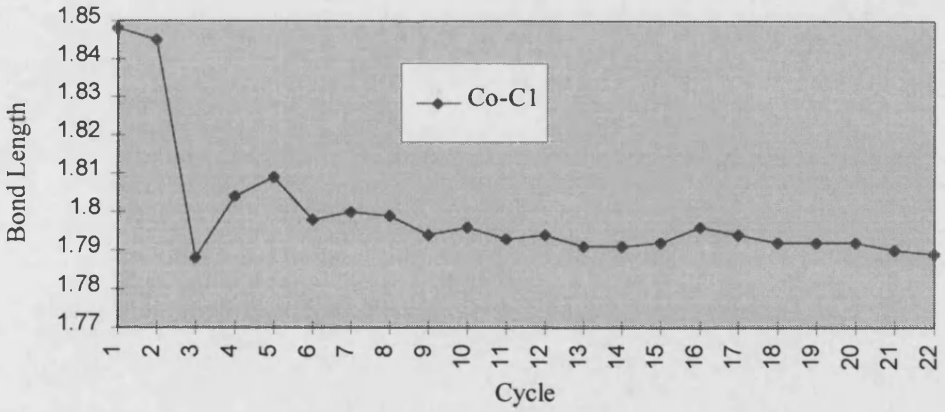

Figure 8.2: Change in bond length (Å) of bond Co-C_1.

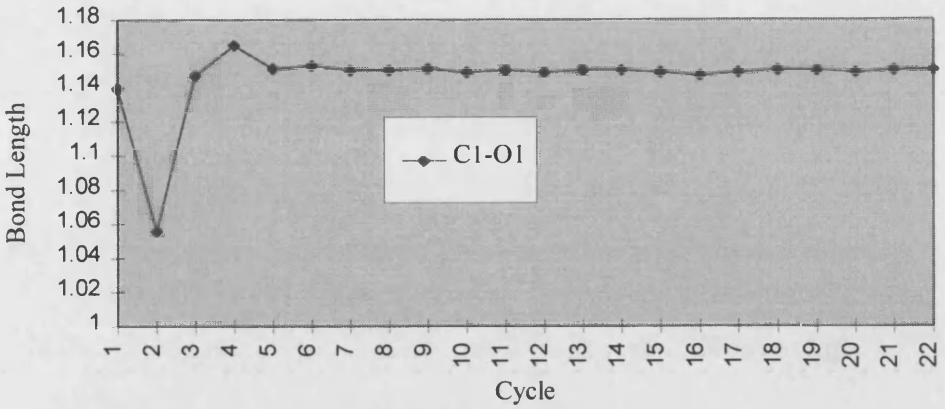

Figure 8.3: Change in bond length (Å) of bond C_1-O_1.

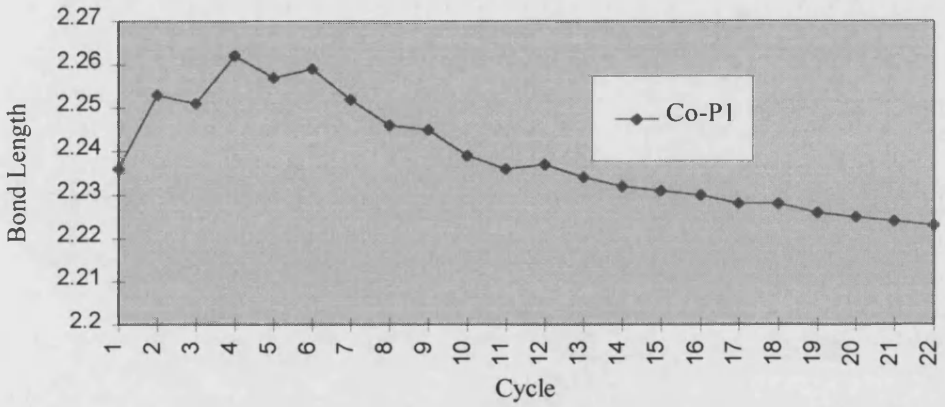

Figure 8.4: Change in bond length (Å) of bond Co-P_1.

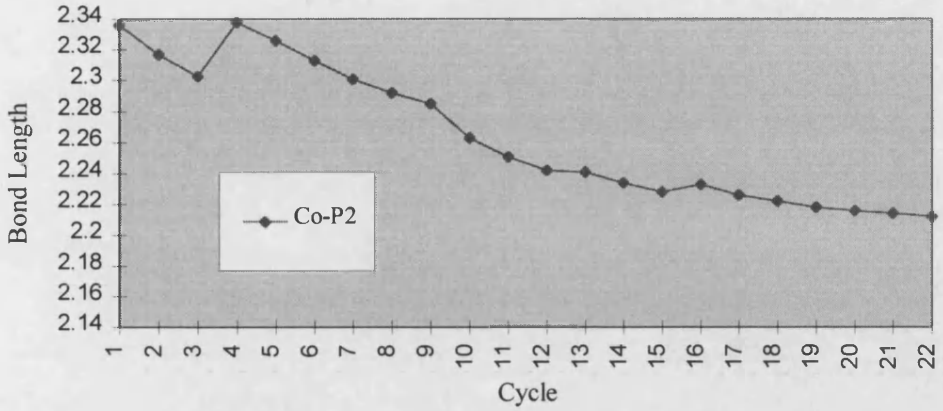

Figure 8.5: Change in bond length (Å) of bond Co-P_2.

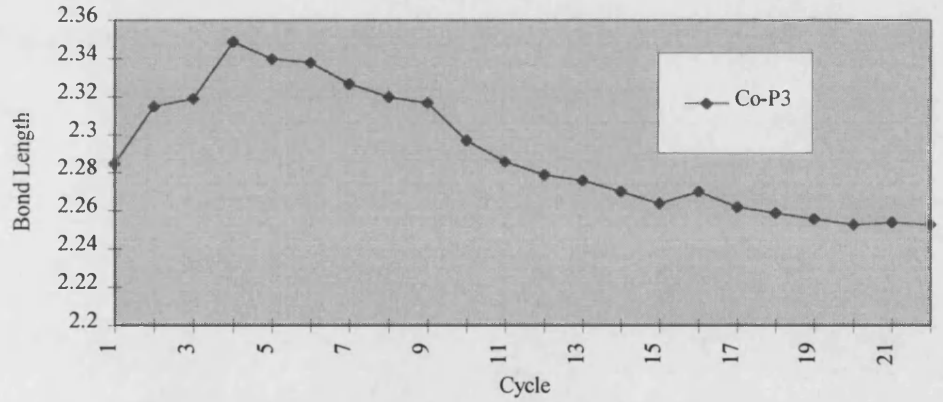

Figure 8.6: Change in bond length (Å) of bond Co-P_3.

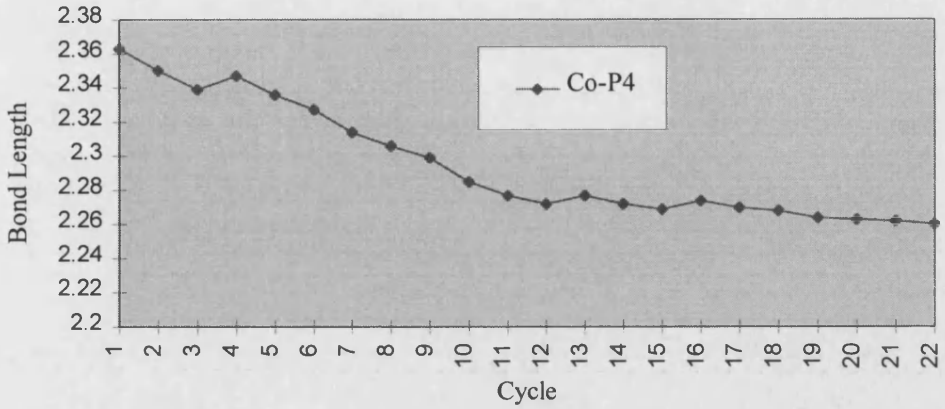

Figure 8.7: Change in bond length (Å) of bond Co-P_4.

Although the geometry has not converged it is quite clear that convergence is quite close as illustrated by the diminishing rate of change of the various bond lengths. After an initial period of a few cycles where the bond lengths oscillate somewhat there is a gradual decrease in the bond lengths, especially of the metal-phosphine bonds, towards the experimental value. The rate of change is constantly falling so that there is the expectation that calculated values will fall very close to the experimental value and certainly closer than the corresponding calculation where the MM term was excluded.

The calculated geometry of the metal centres illustrated in Table 8.6, and shows that in terms of bond angles there are quite large discrepancies between calculated and experimental values. The magnitude of these errors is certainly too large to be acceptable although this may be because convergence has not yet been reached in the calculation or because of inaccurate parameterisation. Both these possibilities need to be investigated further.

Bond	Expt.	Calculated	Error
P_1 -Co - P_2	92.0	87.7	4.3
P_1 -Co - P_3	109.6	139.5	29.9
P_1 -Co - P_4	95.9	87.4	8.5
P_1 -Co - C_1	134.0	109.7	24.3
P_2 -Co - P_3	95.6	86.5	9.1
P_2 -Co - P_4	163.6	174.6	11.0
P_2 -Co - C_1	81.6	97.3	15.7
P_3 -Co - P_4	95.3	95.8	0.5
P_3 -Co - C_1	116.4	110.8	5.6
P_4 -Co - C_1	82.6	86.5	3.9
Co -C_1 - O_1	177.3	167.5	9.8
Av. Error			11.1

Table 8.6: Comparison of calculated and experimental bond[10] angles (°) in $Co(PMe_3)_4CO$.

8.4.4 Conclusions

The results presented above for calculations made on $[Co^{I}(PMe_3)_4CO]^+$ using this combined DFT/MM method appear to illustrate that the inclusion of a MM term improves calculated bond lengths at the metal centre compared to simple DFT calculations using truncated ligands only. However, the actual geometry at the metal centre is not modelled as accurately and this could be caused by a number of points. Firstly, the calculation has not at this point been demonstrated to have

converged satisfactorily, and further cycles may improve the geometry significantly. Secondly, there may be an incorrect parameterisation of the molecular mechanics force field particularly through the non-bonded parameters. Finally, the inclusion of gradient corrected functionals may be necessary in the DFT calculations and also in the previous stages where the parameter values for the truncated ligands are determined.

Therefore, the is still much work to be carried out on this method before it can be used routinely to calculate molecular geometries, but the promise of this method has been illustrated and can be seen as a progression from other combined methods where the QM and MM regions are not allowed to interact.

References

1. (a) M.J.Field, P.A.Bash and M.Karplus, *J. Comp. Chem.*, 1990, **11**, 700. (b) J.Gao and L.Shao, *J. Phys. Chem.*, 1994, **98**, 13772. (c) R.V.Stanton, D.S.Hartsough and K.M.Merz Jr., *J. Comp. Chem.*, 1995, **16**, 113. (d) H.Liu and Y.Shi, *J. Comp. Chem.*, 1994, **15**, 1311. (E) J.Gao, *J. Phys. Chem.*, 1992, **96**, 537.

2. (a) F.Maseras, N.Koga and K.Morokuma, *Organometallics*, 1994, **13**, 4008. (b) W.Estelberger, D.Fuchs, C.Murr, H.Wachter and G.Reibnegger, *Biochim. Biophys. Acta*, 1995, 23.

3. I.H.Hillier, B.Waszkowycz, N.Gensmantel and D.W.Payling, *J. Chem. Soc. Perkin Trans. 2*, 1991, 225.

4. E. J. Baerends, D. E. Ellis and P. Ros, *Chem. Phys.*, 1973, **2**, 41.

5. In house MM software supplied by Dr. D.J.Osguthorpe, Molecular Graphics Unit, University Of Bath.

6. U.Burkett and N.L.Allinger, *Molecular Mechanics*, ACS Monograph, 177, American Chemical Society, Washington D.C., 1982.

7. (a) J.G.Snijders, P.Vernooijs and E.J.Baerends, *At. Data Nucl. Data Tables,* 1981, **26**, 483. (b) J.G.Snijders, P.Vernooijs and E.J.Baerends, *Slater Type Basis Functions for the Whole Periodic System.,* Internal Report, Free University, Amsterdam, 1981.

8. E. J. Baerends D. E. Ellis and P. Ros, *Theoret. Chim. Acta*, 1972, **27**, 339.

9. J.C.Slater, *Adv. Quantum. Chem.,* 1972, **6**, 1.

10. Y.Peres, M.Dartiguenave, Y.Dartiguenave, J.F.Britten and A.L.Beauchamp, *Organometallics*, 1990, **9**, 1041.

Chapter 9

Conclusions and Future Work

9.1 Conclusions

Density Functional Theory (DFT)[1] has been used to model various aspects of transition metal chemistry. It has been shown to be an accurate method for the calculation of molecular geometries, vibrational frequencies and electronic transition energies. Favourable comparisons are made with other computational methods, especially the Hartree-Fock (HF)[2] method. A number of conclusions can be drawn from this work with respect to the way that DFT performs for a variety of transition metal complexes.

In general, the species that have been studied are of an ionic nature. The Local Density Approximation (LDA)[3] has been shown to be able to reproduce experimental geometries to within 0.02Å without any treatment of the crystal environment.

The inclusion of gradient corrected functionals[4] leads to a significant bond lengthening which brings calculated values out of line with experiment. This is contrary to what has been shown previously for organometallic species[1]. Where a more covalent type of bonding is exhibited, the LDA tends to underestimate bond lengths (and overestimate bond energies) and the inclusion of gradient corrected functionals causes a lengthening of bonds and this leads to very good agreement with experimental values. The design of these gradient corrected functionals is such

that their form will always reduce the stability of bonds calculated when compared to those calculated with the LDA. The fact that the LDA is based on the homogeneous electron gas picture must introduce limitations in its application to real molecular systems where the electron density is far from constant. However, it appears that from the results presented in Chapters 2-4, that this is not the case. This suggests that either the LDA is not a poor approximation to systems that have a quite rapidly varying electron density (ionic bonding) and is a poor approximation to systems that have a relatively slowly varying electron density (covalent bonding), or that there is a further approximation in these calculations that has yet to be accounted for. This suggests that the crystal lattice may, in fact, have a significant influence on molecular geometries. This is emphasised by the observation of a steady improvement in calculated geometries of organometallic species from the LDA values (too short) to those where gradient corrections are included. This suggests that the methodology is correct; the LDA is a reasonable approximation to systems where electron density is slowly varying and including gradient corrections to account for the increased inhomogeneity brings about an improvement into line with experimental values. In addition the $CuCl_6^{4-}$ species is not found to be stable with respect to $CuCl_4^{2-}$ and $2Cl^-$ (both with the LDA and with gradient corrections included) but it is known as a stable structure in a crystal environment[5]. Analysis of atomic charges shows that this is in fact dissociation into a lower energy configuration and not the artifact of a poor treatment of long bonds. Therefore, there must be a significant part played by the crystal environment of this complex in stabilising the six co-ordinate structure. There does also appear to be a

difficulty with the treatment of $CuCl_5^{3-}$ which, unlike $CuCl_6^{4-}$ does not have an easy dissociation pathway to the more stable four co-ordinate system. The explicit exclusion of any treatment of the crystal environment may lead to a relatively poor treatment of this species and to the difficulties experienced with the tzp basis set. In addition to this, the $CuCl_4^{2-}$ species is found in a wide variety of geometries[6] ranging from square planar to distorted tetrahedral depending on the counter ion. This again suggests a significant influence from the crystal environment.

However, aside from these special cases, there is some evidence to suggest that lattice effects may not be significant in general. Calculations on the ionic species are seen to be affected by a number of factors such as basis set size, frozen core size, polarisation functions and spin polarisation. For the chlorocuprate series the evidence is not all conclusive due to the lack of an experimental structure for $CuCl_2$ and the large range of structures found for $CuCl_4^{2-}$. However, it is shown consistently that these factors can have a significant effect on calculated geometries, the bond length in $CuCl_2$ is seen to vary by as much as 0.1Å as a combination of these factors. Therefore, a careful choice of basis set etc. must be made in order to give accurate calculated values. Calculations on the geometries of tetrachloro species show that the best agreement with experimental values, using the LDA method, is found with the use of the larger basis set (triple-ζ as opposed to double-ζ) and with spin polarisation included (polarisation functions are included on all atoms). Therefore, the highest quality calculations give the most accurate results. If the LDA calculations were in good agreement with experiment as a

consequence of the fortuitous cancellation of errors then there would be no expectation that the highest quality calculations would be closest to experiment.

In light of these results it is unclear as to whether the inclusion of the crystal environment is important for the calculation of the molecular geometries of ionic species. Using the LDA method, excellent agreement with experimental results can be achieved. Inclusion of gradient corrected functionals leads to an overestimation of bond lengths, whereas for molecules with more covalent bonding they lead to accurate values. It is clear that further investigation is required to prove conclusively whether the inclusion of lattice effects is essential.

The chorocuprates have also been investigated using the DVXα method[7]. Transition energies have been calculated for both the ligand field (d-d) and charge transfer (c.t.) spectra. The calculations have attempted to show whether it is possible to calculate both the d-d and c.t. energies accurately and also if the method can be parameterised for the ligand and metal type. Each atom is embedded in a potential well, and by varying the parameters of this well it is shown that the d-d and c.t. transitions can be calculated accurately. The d-d orbital energies that are calculated with this method are seen to be in much better agreement than those calculated with other methods. The same parameters are used to calculate the energies for both the square planar and distorted tetrahedral species. This shows that there is a degree of transferability in these parameters. The c.t. spectra require a separate set of parameters from those used for the d-d spectra, but again good agreement is shown with experimental values. It does not seem possible to treat both the d-d and c.t. spectra simultaneously with the same parameters. This may be

a result of a lack of freedom in the d-orbital basis set or, probably, due to the neglect of the crystal environment. The electric field generated within the crystal lattice could have a significant impact on orbital energies. This field would have a larger effect on the ligand based orbitals than the relatively well shielded metal based orbitals. So the effect would not be a uniform shift of all orbital energies (and hence transition energies) and so significant changes in transition energies may occur. In effect, some empirical treatment of the crystal lattice has been introduced by the inclusion of well potentials. However, this scheme does not appear to yield an accurate treatment of the lattice. Hence, in order to calculate the whole electronic spectrum simultaneously it appears that the lattice effects must be included.

Other properties of transition metal complexes can also be calculated including Δ_{tet} values, d-orbital populations and atomic charges. Δ_{tet} values for the tetrachloro species are found to be in reasonable agreement with experiment and those calculated with gradient corrections (GC) give slightly better agreemnet than those calculated with the LDA. Where spin polarisation is allowed there is a significant increase in the errors between GC calculated and observed values over those shown for the LDA. Although the inclusion of spin polarisation does appear to increase the value of Δ_{tet} whether this is as a result of spin contamination is unclear. However, the value does appear to be relatively insensitive to geometry at or about the experimental bond length. Therefore, accurate values can be calculated with a spin restricted formalism at the experimental geometries or at the structure calculated by the LDA. Using the LDA calculated structure and then using GC to

calculate the Δ_{tet} value reduces the computational expense without significantly affecting the calculated value.

The vibrational frequencies of $[CrO_4]^{2-}$, $[MnO_4]^{2-}$ and $[FeO_4]^{2-}$ have been calculated using both the LDA and gradient corrected functionals. The frequencies have been shown to be accurately treated by DFT irrespective of whether gradient corrected functionals are included or not. There also does not appear to be a significant dependence on the size of the basis set used. However, inclusion of gradient corrected functionals with a triple-ζ basis set gives errors of 5% or less. In general, errors between calculated and experimental values are in the order of 10% or less. Again no account is taken of the crystal environment and this does not appear to have affected the calculated values.

Overall, the calculation of various molecular properties of ionic transition metal complexes by the DFT method appears to give good agreement with experimental values and within a reasonable time frame. The need to include some treatment of the crystal environment is suggested although whether it has a significant effect on these properties can only be resolved by further investigation.

DFT has also been used in conjunction with Molecular Mechanics (MM)[8] in order to develop a combined method that is capable of dealing with relatively large systems without incurring the high cost of a full DFT treatment. Initial studies into the effect of modeling simple transition metal complexes containing one and two ligands indicated that it is feasible to model a bulky ligand with a simpler derivative. Methylated ligands with oxygen, nitrogen, sulpur and phosphorous donors are treated by simpler hydrogen derivatives. Optimised metal-ligand bond

lengths with a variety of metals in different oxidation states show that by altering ligand geometry, the simpler ligands can be made to act electronically like the larger derivative. Reproduction of bond lengths is generally found to within 0.02Å. Those species that are not reproduced to this level of accuracy may require further alteration of ligand geometries. These results suggest that electronic effects of large and/or bulky ligands can be reproduced within a DFT treatment using ligand mimics.

The parameters that were obtained from the one and two ligand studies were used to treat some real complexes. Trimethylphosphine ligands were replaced with simple phosphine ligands and geometry optimisations performed using the LDA. The results show that, generally, the calculated geometries are in reasonable agreement with experimental values but two sources of error may exist. The first is that although this approach is capable of reproducing electronic effects, the bulkier ligands will have significantly increased steric interactions that cannot be modeled with the smaller ligands. There is shown to be some correlation between the total co-ordination number of these complexes, the number of phosphine ligands and the errors in calculated bond lengths and angles. Therefore, it appears that the reduced treatment of steric interactions causes significant errors in calculated geometries. Secondly, the calculations are performed with the LDA and, for complexes of a more covalent nature, the inclusion of gradient corrected functionals improves the calculated geometries. The electronic effects were parameterised from LDA calculations and so there may be some requirement to alter the parameterisation of electronic effects. Initial studies suggest that this may not be required as, although

absolute bond lengths are affected, the same parameters seem to give the best comparison with the methylated ligands.

A combined DFT and MM method has been produced. DFT is used to treat a small number of atoms at the metal center and MM to treat the bulk of the ligand system. The optimisation of the molecule is performed within MM but bond and angle terms for the metal center are calculated by DFT in a calculation where bulky ligands are replaced with simpler derivatives. Although only initial results are presented, it appears that by treating both electronic and steric effects, the calculated geometries of large transition metal complexes may be possible and with a much reduced computational cost.

9.2 Future Work

The work presented here has established that DFT is capable of accurately modeling the properties of transition metal complexes. However, it has not as yet been shown whether the neglect of the crystal environment for ionic species has a significant effect on calculated molecular properties. Therefore, more work needs to be carried out with the inclusion of some treatment of the environment. One possible method is to include a set of point charges. This would give a simplistic representation of the electric field, but would confirm whether there was any significant effect on the various molecular properties especially geometries. It is expected that transition energies and Δ_{tet} values will be affected by the crystal environment due to the effect on orbital energies of an electronic field.

Further the use of embedded clusters for the DVXα calculation of transition energies may enable the simultaneous calculation of both d-d and c.t. with the same set of well parameters. If it can be shown that each atom type can be parameterised with one set of parameters then it can be developed into a useful tool for calculating approximate molecular geometries for large systems. The transition energies can be calculated as the molecular geometry is varied and once a good match with experimental transitions is found then this will be a good first approximation to the geometry of the system.

The combined DFT and MM method needs further work to investigate the effect of gradient corrected functionals on both the parameters required to represent large ligands and also the calculation of molecular geometries of real molecules. Once it has been established whether this is required then further calculations can be made on optimising molecular geometries of real systems. Then further refinement of the method can be made so that geometries can be calculated reliably. It can then be used to investigate the chemical properties of such systems. Eventually it should be possible to use the method to study reaction mechanisms and energetics of large complexes in an accurate and computationally efficient way.

References

1. T.Ziegler, *Chem. Rev.*, 1991, **91**, 651.

2. (a) D.R.Hartree, *Proc. Camb. Phil. Soc.*, 1928, **24**, 89. (b) V.Fock, *Z. Physik.*, 1930, **61**, 126. (c) C.C.J.Roothan, *Rev. Mod. Phys.*, 1951, **23**, 69.

3. J.C.Slater, *Adv. Quantum. Chem.,* 1972, **6**, 1.

4. (a) A. J. Becke, *Chem. Phys.*, 1986, **84**, 4524. (b) J. P. Perdew, *Phys. Rev.*, 1986, **B33**, 8822. (c) J.P. Perdew, *Phys. Rev.*, 1987, **B34**, 7406 (erratum).

5. M.Studer, A.Riesen and T.A.Kaden, *Helv. Chim. Acta.*, 1989, **72**, 1253.

6. K.E.Halvorson, C.Patterson and R.D.Willett, *Acta. Cryst.*, 1990, **B46**, 508.

7. H.Johansen and N.K.Anderson, *Mol. Phys.*, 1986, **58**, 965.

8. V.Burkert and N.L.Allinger, "*Molecular Mechanics*", ACS monograph 177, Washington, 1982.